Escherichia coli SPFH membrane microdomain proteins HflKC contribute to aminoglycoside and oxidative stress tolerance

Aimee K Wessel, Yutaka Yoshii, Alexander Reder, Rym Boudjemaa, Magdalena Szczesna, Jean-Michel Betton, Joaquin Bernal-Bayard, Christophe Beloin, Daniel Lopez, Uwe Völker, et al.

Escherichia coli SPFH membrane microdomain proteins HflKC contribute to aminoglycoside and oxidative stress tolerance

Aimee K. WESSEL[1†], Yutaka YOSHII[1†], Alexander REDER[2], Rym BOUDJEMAA[3], Magdalena SZCZESNA[1,6], Jean-Michel BETTON[4], Joaquin BERNAL-BAYARD[1,7], Christophe BELOIN[1], Daniel LOPEZ[5], Uwe VÖLKER[2], Jean-Marc GHIGO[1*]

[1] *Institut Pasteur, Université de Paris-Cité, CNRS UMR6047, Genetics of Biofilms Laboratory F-75015 Paris, France.*

[2] *Department of Functional Genomics, Interfaculty Institute for Genetics and Functional Genomics, University Medicine Greifswald, 17487 Greifswald, Germany.*

3 Abbelight, 191 avenue Aristide Briand, 94230 Cachan

[4] *Institut Pasteur, Université de Paris-Cité, UMR UMR6047, Stress adaptation and metabolism in enterobacteria 75015 Paris, France.*

[5] *Universidad Autonoma de Madrid, Centro Nacional de Biotecnologia, Campus de Cantoblanco, Calle Darwin 3, 28049 Madrid, España*

[6] *Centre for Bacteriology Resistance Biology, Imperial College London, London, SW7 2AZ,UK*

[7] *Departamento de Genética, Facultad de Biología, Universidad de Sevilla, Apartado 1095, 41080 Sevilla, Spain*

† AW and YY equally contributed to this work. Author order was determined both alphabetically and in order of increasing seniority.

[*]**Corresponding author:** Jean-Marc Ghigo (jean-marc.ghigo@pasteur.fr)

Running Title: *E. coli* SPFH proteins contribute to stress tolerance

Keywords

Membrane microdomains; SPFH proteins; Flotillin; Lipid raft; Stress tolerance; *Escherichia coli*

ABSTRACT

Many eukaryotic membrane-dependent functions are often spatially and temporally regulated by membrane microdomains (FMMs) also known as lipid rafts. These domains are enriched in polyisoprenoid lipids and scaffolding proteins belonging to the Stomatin, Prohibitin, Flotillin, and HflK/C (SPFH) protein superfamily that was also identified in Gram-positive bacteria. By contrast, little is still known about FMMs in Gram-negative bacteria. In *Escherichia coli* K12, 4 SPFH proteins, YqiK, QmcA, HflK, and HflC, were shown to localize in discrete polar or lateral inner-membrane locations, raising the possibility that *E. coli* SPFH proteins could contribute to the assembly of inner-membrane FMMs and the regulation of cellular processes.

Here we studied the determinant of the localization of QmcA and HflC and showed that FMM-associated cardiolipin lipid biosynthesis is required for their native localization pattern. Using Biolog phenotypic arrays, we showed that a mutant lacking all SPFH genes displayed increased sensitivity to aminoglycosides and oxidative stress that is due to the absence of HflKC. Our study therefore provides further insights into the contribution of SPFH proteins to stress tolerance in *E. coli*.

IMPORTANCE

Eukaryotic cells often segregate physiological processes in cholesterol-rich functional membrane micro-domains. These domains are also called lipid rafts and contain proteins of the Stomatin, Prohibitin, Flotillin, and HflK/C (SPFH) superfamily, which are also present in prokaryotes but were mostly studied in Gram-positive bacteria. Here, we showed that the cell localization of the SPFH proteins QmcA and HflKC in the Gram-negative bacteria *E. coli* is altered in absence of cardiolipin lipid synthesis. This suggests that cardiolipins contribute to *E. coli* membrane microdomain assembly. Using a broad phenotypic analysis, we also showed that HflKC contribute to *E. coli* tolerance to aminoglycosides and oxidative stress. Our study, therefore, provides new insights into the cellular processes associated with SPFH proteins in *E. coli*.

INTRODUCTION

In addition to separating the intracellular content of cells from the environment, lipid bilayer membranes also contribute to specialized functions, including cross-membrane transport, enzymatic activity, signaling as well as anchoring of cytoskeletal and extracellular structures (1, 2). In eukaryotes, these membrane-dependent functions are often spatially and temporally regulated by functional membrane microdomains (FMMs) called lipid rafts (3-5). FMMs compartmentalize membrane cellular processes in cholesterol- and sphingolipid-enriched membrane regions formed upon lipid-lipid, lipid-protein and protein-protein interactions (5-7). A family of membrane proteins called SPFH proteins (for Stomatin/Prohibitin/Flotillin/HflK/C) has been shown to localize in eukaryotic lipid rafts and to recruit and provide a stabilizing scaffold to other raft-associated proteins (8-13).

Whereas most prokaryotes lack sphingolipids and cholesterol (14), the Gram-positive bacteria *Bacillus subtilis* and *Staphylococcus aureus* can also compartmentalize cellular processes in functional membrane microdomains (FMMs) (14-16). Although whether bacterial FMMs display a distinct lipidic composition still needs to be established, they have been reported to be potentially enriched in polyisoprenoid lipids as well as in cardiolipins at the cell poles (14-16)

FMMs also contain SPFH proteins, including flotillins, and a pool of proteins involved in diverse cellular processes (17) (14, 16). In *B. subtilis*, flotillins FloT and FloA colocalize in membrane foci and contribute to the assembly of membrane protein complexes (18) (15). Lack of flotillins impairs biofilm formation, sporulation, protease secretion, motility, and natural competence, indicating that the formation of FMMs also plays critical cellular roles in *B. subtilis* (15, 18-22).

SPFH proteins are also present in Gram-negative bacteria, and *Escherichia coli* K12 even possesses four genes, *yqiK*, *qmcA*, *hflK*, and *hflC*, which encode proteins with an SPFH domain and a N-terminal transmembrane segment (23). QmcA and YqiK are predicted to face the cytoplasmic compartment, while HflK and HflC are predicted to be exposed in the periplasm, forming the HflKC complex negatively regulating the protease activity of

FtsH against membrane proteins (24-27). HflC and QmcA are detected Fluorescent microscopy also showed that *E. coli* SPFH proteins HflC and QmcA are localized in discrete polar or lateral membrane foci (28), raising the possibility that *E. coli* SPFH proteins could localize in inner-membrane FMMs and regulate specific cellular processes (29). However, apart from the functional and structural description of HflKC as a regulator of the FtsH membrane protease (24, 27, 30) and a recent study suggesting that YqiK is involved in cell motility and resistance to ampicillin (31), the functions of FMM in *E. coli* and other Gram-negative bacteria are still poorly understood.

In this study, we used fluorescent and super-resolution microscopy to perform a detailed analysis of QmcA and HflC membrane localization signals. We then showed that the integrity of QmcA and HflC protein domains is required for their inner membrane localization, and that the lack of cardiolipin and isoprenoid lipids known to associate with FMMs alters their localization. Moreover, using single and multiple SPFH gene mutants, we showed that HflKC SPFH proteins contribute to aminoglycosides and oxidative stress resistance. Our study therefore provides new insights into the determinants of cellular localization and the function associated with *E. coli* SPFH proteins.

RESULTS

Chromosomal *E. coli* SPFH fluorescent fusion proteins show distinct localization patterns.

To investigate the determinant of cell localization of *E. coli* SPFH proteins, we first tagged YqiK and QmcA, which C-termini are predicted to be in the cytoplasm (26), with a C-terminal monomeric super folder green fluorescent protein (msfGFP). We then tagged HflC and HflK, which C-termini are predicted to be in the periplasm (26), with the C-terminal monomeric red fluorescent protein mCherry. All these fusions were expressed under their own promoter from their native chromosomal location (Sup. Fig. S1). Epifluorescence and super-resolution microscopy confirmed the previously reported polar localization of HflK and HflC (28), with 94% and 91% polar localization pattern for HflC-mCherry and HflK-mCherry, respectively (n=150) (Fig. 1B and Sup. Fig. S2). By contrast, C-terminally tagged QmcA-GFP showed punctate foci distributed throughout the cell body, with 96% of the cells harboring 5 foci or more (n=150) (Fig. 1A). However, we could not detect YqiK-GFP, possibly due to its low native chromosomal expression level. We then used anti-GFP or mCherry antibodies to perform immunodetection on cytoplasmic as well as inner and outer membrane fractions of *E. coli* strains expressing either HflC-mCherry or QmcA-GFP. In agreement with previous results (26, 29), both fusion proteins were detected in the inner membrane fraction and showed minimal degradation profile (Fig. 2 and Sup. Fig. S3 and S4). Moreover, the functionality of the HflKC fusion could be demonstrated (see result sections below).

Domain swap analysis shows that protein integrity is essential for QmcA-GFP and HflC-mCherry localization.

To identify HflC and QmcA membrane localization signals, we constructed multiple fluorescently tagged truncated versions of both proteins. We tagged with msfGFP a QmcA protein reduced to its transmembrane region and SPFH domain (QmcA-GFP is therefore now named TM^{QmcA}-$SPFH^{QmcA}$-GFP in Figure 3) and, separately, one reduced to the QmcA transmembrane region only (TM^{QmcA}-GFP) (Fig. 3A). To test the role of the QmcA transmembrane region, we also swapped TM^{QmcA} in the three constructs by the single-spanning TM domain of the phage coat protein Pf3 (TM^{Pf3}), which orients subsequent amino acids to the cytosol (38) (Fig. 3A). Similarly, in addition to the full

length HflC-mCherry, we tagged with mCherry the HflC transmembrane region and SPFH domain (HflC-mCherry is therefore now named TM^{HflC}-$SPFH^{HflC}$-mCherry in Figure 3) and, separately, only its TM region (TM^{HflC}-mCherry) (Fig. 3B). We also swapped the HflC TM region with the single-spanning TM region of colistin M immunity protein (TM^{Cmi}), which orients subsequent amino acids to the periplasm (39) (Fig. 3B). Epifluorescence microscopy of HflC and QmcA derivative fusions showed that in addition to native full-length constructs only full-length constructs with swapped TM (TM^{Pf3}-QmcA-GFP and TM^{Cmi}-HflC-mCherry) displayed significant punctate foci or polar localization, respectively (Fig. 3AB), although at reduced frequency compared to native QmcA-GFP and HflC-mCherry (Sup. Fig. S5). Finally, we prepared inner and outer membrane fractions of *E. coli* strains expressing each QmcA and HflC derivative, and we observed that all these constructs were still mainly located in the inner membrane fraction. This indicates that, while we observed that QmcA-GFP and HflC-mChery derivatives exhibit altered cell localization, they do not exhibit significant mis-localization and remain located in the inner membrane (Sup. Fig. S3 and Fig S4). These results therefore indicated that specific QmcA and HflC localization requires the combination of a transmembrane and full cytoplasmic (QmcA) or periplasmic (HflC) domain.

Lack of cardiolipin and isoprenoid lipid synthesis alters the cell localization of QmcA and HflC.

FMMs were proposed to be enriched with negatively charged cardiolipins and isoprenoids, which promote the localization of polar proteins and modulation of membrane lipid fluidity (15, 18, 32-37). We first tested whether alteration of cardiolipin synthesis could cause mis-localization of *E. coli* SPFH proteins QmcA or HflKC in a mutant lacking the major cardiolipin synthases *clsABC* (38). Whereas a super-resolution microscopy analysis only showed an alteration of the number of QmcA-GFP punctates (1-5 cluster per bacterium) compared to WT (10-15 cluster per bacterium) (Fig. 4A and Sup. Fig. S6), the localization of HflC-mCherry showed a drastic loss of polar localization pattern (Fig. 4B and Supp. Fig. S4). We then used an *idi* mutant with reduced isoprenoid lipid synthesis due to the lack of isomerization of isopentenyl diphosphate (IPP) into dimethylallyl diphosphate (DMAPP) (39, 40). Whereas QmcA-GFP punctate localization was not affected, HflC-mCherry polar localization was-abolished in the Δ*idi* mutant (Fig.

4A and Sup. Fig. S6). These results demonstrated that the alteration of cardiolipin and, in a lesser extent, isoprenoid lipid synthesis pathway affects HflC fusion protein localization in *E. coli*.

Phenotypic analysis of *E. coli* SPFH mutant shows that only the absence of HflKC increases *E. coli* sensitivity to aminoglycosides and oxidative stress.

To identify potential phenotypes and functions associated with the *E. coli* SPFH proteins YqiK, QmcA, HflK and HflC, we introduced single and multiple deletions of the corresponding SPFH genes. We observed that neither single mutants nor the quadruple Δ*hflK,* Δ*hflC,* Δ*qmcA*, and Δ*yqiK* (hereafter referred to Δ*SPFH* mutant) displayed any significant growth defects in rich or minimal media (Fig. 5A and Sup. Fig. S7A). Considering the role of SPFH proteins in the activation of inner-membrane kinases involved in *B. subtilis* biofilm formation (15), we tested adhesion and biofilm capacity of WT and ΔSPFH strains but could not detect any significant differences between these two strains. We then used Biolog™ phenotypic microarrays to perform a large-scale phenotypic assay comparing an *E. coli* WT and Δ*SPFH* mutant (Sup. Table S1). This analysis revealed that the Δ*SPFH* mutant is metabolically less active when grown in the presence of various aminoglycosides (tobramycin, capreomycin, sisomicin and paromomycin) or when exposed to paraquat (Fig. 5B and Sup. Fig. S7BC). Consistently, the minimal inhibitory concentration (MIC) for tobramycin of the Δ*SPFH* mutant was 3-fold lower than that of the WT MIC (Fig.5C), and the sensitivity of the Δ*SPFH* mutant to paraquat was increased compared to the WT (Fig. 5D and Sup. Fig. S7D). Test of individual SPFH-gene mutants for their sensitivity to tobramycin and paraquat showed that the HflKC complex is the sole responsible for both phenotypes, as both single *hflK* and *hflC* or a double *hflKC* mutants displayed increased sensitivity to tobramycin and oxidative stress (Fig. 5CD and Sup. Fig. S5E). This phenotype could be complemented upon the introduction of a plasmid expressing *hflKC* genes in the double *hflKC* mutant and C-terminally tagged HflC-mCherry and HflK-mCherry displayed wildtype MIC for tobramycin and paraquat, indicating that both fusions were functional and relevant proxies for the bacterial localization of the HflKC complex (Sup. Fig. S8).

Contribution of HflC localization to tobramycin and paraquat tolerance

Whereas the MIC determination for tobramycin and paraquat of an Δ*idi* mutant showed no significant difference compared to the WT, the MIC for tobramycin and paraquat of a ΔclsABC mutant was reduced by 2 to 3-fold (Fig.5CD). Considering the scaffolding role of HflKC and the importance of cell localization, we tested the localization and contribution to aminoglycoside and stress tolerance of AcrA, a protein previously identified in *E. coli* inner-membrane potentially associated with FMM (28). AcrA is an efflux pump involved in the transport of a wide range of substrates including aminoglycosides (41). However, while an *acrA* deletion did not altered *E. coli* MIC profile to tobramycin and paraquat as much as a Δ*hflC* mutant (Fig.5CD), the expression of AcrA-GFP from their native chromosomal context did not lead to any distinct polar co-localization with HflC in exponential or stationary phase conditions (Sup. Fig. S9).

Taken together, these results indicate that the HflKC SPFH protein complex contributes to oxidative and antibiotic stress resistance.

DISCUSSION

SPFH-domain proteins have been identified in most organisms (16, 42) and extensively studied in eukaryotes (3, 5, 43). By contrast, prokaryotic SPFH proteins and proteins associated with functional membrane microdomains (FMMs) are much less understood. This is particularly the case for Gram-negative bacteria, in which potential FMMs functions are mostly inferred from studies performed in *B. subtilis* and *S. aureus*. In this study, we investigated the functions and the localization determinants of *E. coli* SPFH proteins. Focusing on QmcA and HflKC SPFH proteins, we used a domain deletion and replacement approach and showed that most of the tested domain replacement variants correctly localized to the inner membrane but failed to display WT protein localization patterns. This indicates that inner-membrane localization alone is not sufficient for the correct subcellular distribution of HflC and QmcA, whose localization signals likely rely on oligomerization for focal flotillin cluster formation (44), which could be abolished in the domain deletion constructs, potentially explaining the observed localization defects.

QmcA and HflKC SPFH proteins display different localization patterns and could be part of different FMMs, potentially using different localization signals. The punctate localization pattern displayed by QmcA-GFP fusion was also observed in the case of *E. coli* YqiK expressed from plasmid and other Gram-positive bacteria flotillin homologues(15, 16, 36, 45, 46). Interestingly, *B. subtilis*, *B. anthracis* and *S. aureus* flotillin genes are physically associated with a gene encoding a NfeD protein, which could contribute to protein-protein interactions within flotillin assemblies (47, 48). Consistently, *E. coli qmcA* gene is located upstream of the NfeD-like *ybbJ* gene, like NfeD-like *yqiJ* gene is located upstream of *yqiK* (see Supplementary Figure S1). This further supports the notion that QmcA and YqiK could be considered as *E. coli* FloA/FloT homologs.

By contrast, the *hflKC* transcription unit is not closely associated with a *nfeD*-like gene, suggesting that HflKC may not be a flotillin. However, while QmcA and YqiK have an opposite orientation to HflK and HflC, they are structurally similar proteins and the four *E. coli* SPFH proteins could therefore share some degrees of functionalities. The topological similarity between HflK and HflC might contribute to HflKC complex

formation, and its interaction with FtsH protease, resulting in a large periplasmic FtsH-HflKC complex localized at the cell pole (24, 25, 49-52)

Along with phosphatidylethanolamine and phosphatidylglycerol, cardiolipins are the primary constituent components of *E. coli* membranes that concentrate into cell poles and dividing septum (53-56). It was indeed observed that the composition of *E. coli* membrane lipids at cell poles is altered in a *clsABC* cardiolipin deficient mutant, compensated by an increased amount of phosphatidylglycerol (32, 57). Several studies also reported that cardiolipin-enriched composition in membranes at cell poles influences both the localization and activity of inner membrane proteins, such as respiratory chain protein complexes and the osmosensory transporter ProP (33, 34, 58-60). We showed here that, similarly to ProP, HflC and QmcA localization patterns are affected in a *ΔclsABC* mutant, suggesting that HflKC and QmcA complexes could act as scaffolds for cardiolipin-enriched FMM cargo proteins. Isoprenoid lipids such as farnesol, carotenoids, and hopanoids have been proposed to be constituents of bacterial FMMs or to interact with SPFH proteins and FMM-associated proteins (14). Consistently, blocking the *S. aureus* carotenoid synthetic pathway by zaragozic acid leads to flotillin mis-localization (15), and the inactivation of farnesol synthesis in a *B. subtilis yisP* mutant impairs focal localization of the FMM-associated sensor kinase KinC (15). We showed that interfering with the *E. coli idi* isoprenoid biosynthesis pathway also strongly alters the localization of HflC. This further indicates that isoprenoid lipids contribute to the formation or integrity of FMMs, possibly by altering isoprenoid-dependent membrane fluidity, as shown in *S. aureus* and *B. subtilis* FMMs (14, 61).

Our investigation of the phenotypes displayed by an *E. coli* mutant lacking all SPFH protein genes showed that the absence of HflKC leads to an increased susceptibility to oxidative stress and aminoglycosides. The HflKC complex was previously shown to modulate the quality control proteolytic activity of FtsH by regulating the access of misfolded membrane protein products to FtsH (24, 25, 62). *E. coli* Δ*hflK* and Δ*hflC* mutant strains were also shown to accumulate increased amounts of hydroxyl radical, suggesting that HflK and HflC could influence tolerance to aminoglycosides and oxidative stress by suppressing excessive hydroxyl radical production. Alternatively, HflK and HflC could contribute to tobramycin resistance via FtsH-dependent proteolytic

activity (63) or favoring FMM formation and the assembly of membrane proteins and lipids, such as cardiolipin, involved in the transport and movement of aminoglycosides within cells and cell membranes. Consistently, several proteins associated with aminoglycosides transport potentially associated with FMMs composition, including transporters and several components of the AcrAB-TolC efflux pump (28), suggesting that deletion of *hflK* or *hflC* could reduce the activity of these proteins in FMMs and enhance entry of aminoglycosides. Whereas the susceptibility to aminoglycosides indeed partly relies on the AcrAB-TolC efflux pump (41, 64-66), we found that lack of the AcrA only moderately decreases the MIC to tobramycin, compared to a *hflKC* mutation. We also showed that the alteration of the cardiolipin pathway in a Δ*clsABC* mutant altered both the localization and sensitivity to tobramycin and paraquat of a HflC-GFP fusion. This suggests that cardiolipin could be required for the correct localization of HflKC to FMMs at cell poles. However, we observed that, although an *idi* isoprenoid pathway mutant affects HflC localization, it does not show altered sensitivity. We cannot rule out that that the effect of Δ*clsABC* mutant on resistance to aminoglycosides and oxidative stress could be unrelated to its impact on HflKC polar localization. Alternatively, the lack of effect of Δ*idi* mutant may be due to an uncomplete inactivation of the pathway since lycopene production in a Δ*idi* mutant is reduced by 1/3 but not totally abolished, due to the fact that the idi protein is a reversible isomerase.(39).

In conclusion, the present study provides new insights into the functions of *E. coli* SPFH proteins and some of their interacting partners and further experiments will be needed to fully uncover the roles played by this intriguing family of membrane proteins in Gram-negative bacteria.

MATERIALS & METHODS

Bacterial strains and growth conditions

Bacterial strains and plasmids used in this study are described in Sup. Table S2, and further explained in Sup. Fig. S1 and Figure 3. Unless stated otherwise, all experiments were performed in lysogeny broth (LB) or M63B1 minimal medium supplemented with 0.4% glucose (M63B1.G) at 37 °C. Antibiotics were used as follows: kanamycin (50 µg/mL); chloramphenicol (25 µg/mL); ampicillin (100 µg/mL); and zeocin (50 µg/mL). All compounds were purchased from Sigma-Aldrich (St Louis, MO, USA) except for Zeocin (InvivoGen, Santa Cruz, CA, USA).

Mutant construction

Generation of mutants in E. coli: Briefly, *E. coli* deletion or insertion mutants used in this study originated either from the *E. coli* Keio collection of mutants (67) or were generated by λ-red linear recombination using pKOBEG (Cm^R) or pKOBEGA (Amp^R) plasmids (68) using primers listed in Sup. Table S3. P1vir transduction was used to transfer mutations between different strains. When required, antibiotic resistance markers flanked by two FRT sites were removed using the Flp recombinase (69). Plasmids used in this study were constructed using an isothermal assembly method, Gibson assembly (New England Biolabs, Ipswich, MA, USA) using primers listed in Sup. Table S3. The integrity of all cloned fragments, mutations, and plasmids was verified by PCR with specific primers and DNA sequencing

Construction of deletion mutants

Δ*yqiK*, Δ*qmcA*, Δ*hflK*, Δ*hflC*, Δ*clsA*, Δ*clsB*, Δ*clsC*, Δ*idi*, Δ*acrA*, deletions were transferred into *E. coli* MG1655*strep* by P1vir phage transduction from the corresponding mutants in the *E. coli* BW25113 background of the Keio collection (67). The associated kanamycin marker was then removed using the Flp recombinase expressed from the plasmid pCP20 (69). (Details regarding the construction of all other strains used in this study are presented in Sup.Table S2).

Construction of GFP and mCherry fusions

See Supplementary Methods section in Supplementary Materials

Construction of complemented strains

The *hflKC* genes were amplified from MG1655*strep* using primers listed in Supplementary Table S3 and cloned at the downstream of the IPTG-inducible promoter of a pZS*12 vector using the Gibson assembly to generate plasmids pZS*12-HflKC Then, these plasmids were introduced into Δ*hflKC* mutants, respectively, to construct complemented mutants (Sup. Table S2). A pZS*12 empty vector was also introduced into wildtype and Δ*hflKC* mutants. Mutants harbouring these pZS*12 plasmids were incubated and used for the below experiments in the presence of IPTG (1 mM) and ampicillin.

Epifluorescence microscopy

Bacteria were incubated into 5 mL of fresh LB medium and harvested at OD_{600} 0.4 for samples in exponential phase or OD_{600} 2.0 for stationary phase. After washing twice with M63B1 medium, cells corresponding to 1 mL of the bacterial culture were pelleted by centrifugation and resuspended into 0.1 mL of M63B1 medium for exponential samples, or 1 mL of the medium for stationary samples. Ten µL aliquots of the cell suspension were immobilized on glass slides previously covered with freshly made M63B1 medium 0.8% agarose pads. Cells were observed using a ZEISS Definite focus fluorescent microscope (Carl Zeiss, Oberkochen, Germany), equipped with an oil-immersion objective lens microscope (Pln-Apo 63X/1.4 oil Ph3). GFP or mCherry fluorescence was exited with a ZEISS Colibri LED illumination system and the fluorescence signal was detected with Zeiss FS38 HE (Carl Zeiss) or Semrock HcRed filters (Semrock, Rochester, NY, USA). GFP, and mCherry fluorescence images were taken at 1000, and 2000 msec. exposure, respectively. Image processing was performed using ImageJ and Adobe Photoshop. For each tested strain, the subcellular localization patterns of 50 randomly selected bacteria were evaluated four times (a total of 200 cells), and each frequency was expressed as percentiles.

Super-resolution microscopy

Bacteria were imaged using single-molecule localization microscopy and stochastic

391 optical reconstruction microscopy (SMLM-STORM), using a previously described
392 method (70). Overnight cultures were fixed with PFA 4%, permeabilized with Triton
393 0,05%, and labeled with either GFP monoclonal FluoTag®-Q — Sulfo-Cyanine 5 (Cy5),
394 or RFP monoclonal FluoTag®-Q – Cy5, which are single-domain antibodies (sdAb)
395 conjugated to Cy5. Labeling was performed at 1:250 (concentration), and washing steps
396 were carried out three times using Abbelight's SMART kit buffer. For imaging,
397 Abbelight's imaging system was used with NEO software. Abbelight's module was added
398 to an Olympus IX83 with 100x TIRF objective, N.A. 1.49. We used Hamamatsu's
399 sCMOS Flash 4 camera and a 647nm 500mW Oxxius laser, with an astigmatic lens, to
400 allow for 3D imaging of the sample (71).
401
402 **Inner membrane separation**
403 *E. coli* overnight cultures were diluted into 1 L of fresh LB medium to OD_{600} of 0.02 and
404 incubated at 37°C and 180 rpm until reaching OD_{600} 0.4. Cells were harvested and washed
405 once with 10 mM HEPES (pH 7.4) and stored at -20°C for at least 1 h. Bacteria were then
406 resuspended in 10 mL of 10 mM HEPES (pH 7.4) containing 100 µL of Benzonase (3.10^4
407 U/mL) and were passed through a FRENCH press (Thermo) at 20,000 psi. The lysate was
408 centrifugated at 15,000 *g* for 15 min at 4 °C to remove cell debris, and aliquots of the
409 suspension were stored at 4 °C as the whole extract. Then, the suspension was centrifuged
410 at 100,000 *g* for 45 min at 4 °C to separate supernatant and pellets, and aliquots of the
411 supernatant were stored at 4 °C as the cytosolic and periplasmic fractions. The pellets
412 were suspended into 600 µL of cold 10 mM HEPES (pH 7.4) and homogenized by using
413 2 mL tissue grinder (Kontes Glass, Vineland, NJ, USA). Discontinuous sucrose gradients
414 with the following composition were placed into ultracentrifugation tube: bottom to top
415 0.5 mL of 2 M sucrose, 2.0 mL of 1.5 M sucrose, and 1.0 mL of 0.8 M sucrose, and 500
416 µL of the homogenized samples were placed on the top of sucrose gradients. The
417 gradients were centrifuged at 100,000 *g* for 17.5 h at 4 °C. Subsequently, 400 µL of
418 aliquots were collected into 11 microtubes from top to bottom, and the samples were
419 proceeded to the immunodetection method, as described below.
420
421 **Immunodetection of inner membrane proteins**

Aliquots of samples were suspended in 4× Laemmli buffer (BioRad) with 2-Mercaptoethanol (Sigma) and incubated for 5 min at 98 °C. The protein samples (10 µL each) were run on 4-20 % Mini-PROTEAN TGX Stain-FreeTM precast Gels (BioRad) in 1× TGX buffer and then transferred to nitrocellulose membrane using a Trans-Blot® Turbo™ Transfer System (BioRad). Subsequently, the membranes were blocked using blocking buffer consisting of 5% skim milk in PBS with 0.05% Tween 20 (PBST) for 2 h at 4 °C with agitation. The membranes were then incubated in PBST containing 1% skim milk with first antibodies, polyclonal rabbit antiserum raised against ExbB and TolC (kindly given by Dr. Philippe Delepelaire), GFP (Invitrogen, A6455, Thermo Fisher Scientific, Indianapolis, IN, USA) and mCherry (Invitrogen, PA5-34974) at 1:20,000 overnight at 4 °C with agitation. The membranes were washed in PBST and incubated in PBST containing 1% skim milk with a secondary antibody, anti-rabbit IgG conjugated with horseradish peroxidase (Cell signaling, 7074S), at 1:10,000 for 2 h at 25 °C with agitation. After washing the excess secondary antibody, specific bands were visualized using the ECL prime detection method (GE Healthcare) and imaged with an imaging system, iBright^{TM} CL1500 (Invitrogen).

Microbial growth phenotypic analysis

A high-throughput analysis for microbial growth phenotypes using a colorimetric reaction, Phenotype MicroArrays (Biolog Inc., Hayward, CA, USA), was performed in accordance with the manufacturer's protocol. Briefly, several colonies of *E. coli* grown on LB agar were transferred in 10 mL of a mixture of Biolog IF-0a media (BioLog) and sterilized water into a sterile capped test tube. The suspension was mixed gently, and the turbidity was adjusted to achieve the appropriate transmittance using the Biolog turbidimeter (BioLog). The cell suspension was diluted with the IF-0a plus dye mix, as mentioned in the manufacturer's protocol. 100 µL of the mixture suspension was inoculated into PM plates 1-3 and 9-20 and incubated for 72 h at 37 °C. The absorbance of each well was taken every 15 min. The OmniLog software (BioLog) was used to view and edit data, to compare data lists, and to generate reports.

Monitoring of bacterial growth

An overnight culture of *E. coli* was diluted into fresh LB and M63B1 supplemented with 0.4% glucose medium to OD_{600} of 0.05, and 200 µL aliquots were cultured in the presence or absence of paraquat (Methyl viologen dichloride hydrate, Sigma-Aldrich) in 96-well microplates at 37 °C for 24 h with shaking. The absorbance of each culture at 600 nm was measured every 15 min for 24 h using a microplate reader (Tecan Infinite, Mannedorf, Switzerland).

Susceptibility of *E. coli* against Tobramycin and Paraquat

The broth microdilution method was used to determine the MIC (minimum inhibitory concentration) values of Tobramycin (Sigma-Aldrich) and Paraquat (Sigma-Aldrich) in 96-well microtiter plates. Briefly, 100 µL of LB medium was distributed into each well of the microtiter plates. Tobramycin was 2-fold serially diluted in each well. Five µL of approximately 1×10^7 CFU/mL of *E. coli* was inoculated into each well, and the plates were incubated at 37°C for 24 h. The lowest concentration that visibly inhibited bacterial growth was defined as the MIC. All strains were evaluated in biological and technical triplicates.

The spot assay was performed to evaluate the susceptibility of *E. coli* against paraquat. Briefly, an overnight culture of *E. coli* was diluted into fresh LB medium to OD_{600} of 0.05. Ten µL of the diluted culture was spotted on LB plates containing either no or 100 µM paraquat. The plates were incubated at 37°C for 24 h, and the photographs were taken. All strains were evaluated in triplicate.

Statistical analysis

Data analysis was performed using GraphPad Prism 9.5 software (GraphPad, La Jolla, CA, USA). All data are expressed as mean (± standard deviation, SD) in figures. Statistical analysis was performed using unpaired non-parametric Mann-Whitney test. Differences were considered statistically significant for *P* values of <0.05.

ACKNOWLEDGMENTS

We thank Philippe Delepelaire for insightful comments and material support. We thank Uwe Sauer and Philip Warmer for initial assessment of lipid composition of some of the strains used in this study. We are grateful to Eva Wolrab and Sven van Teeffelen for their initial interest in the project and for providing the strains for msfGFP and mCherry constructions. This work was supported by EU Horizon 2020 Rafts4Biotech grant 720776 (to JMG, DL, AKW, YY, AR, UV and MS), the French government's Investissement d'Avenir Program, Laboratoire d'Excellence "Integrative Biology of Emerging Infectious Diseases" (grant n°ANR-10-LABX-62-IBEID) and the *Fondation pour la Recherche Médicale* (grant no. DEQ20180339185). This work benefited from the facilities and expertise of Add Photonic BioImaging platform (UTechS PBI, Institut Pasteur). A.K.W. was supported by a Pasteur-Roux-Cantarini postdoctoral and a grant from the Philippe Foundation.

AUTHOR CONTRIBUTIONS:

A.K.W., Y.Y., and J.-M.G. designed the experiments. A.K.W., Y.Y., A.R., R.B.; M.S., J.B-B. performed the experiments. A.K.W., Y.Y., A.R., U.V. M.S., R.B., J.-M.B., C.B., D.L. and J.-M.G. analyzed the data. Y.Y., A.K.W. and J.-M.G. wrote the paper with significant contribution from all authors.

DATA AVAILABILITY

The data that support the findings of this study are presented in the paper and/or the Supplementary Materials. Strains and plasmids are available from the corresponding author, JMG, upon reasonable request.

COMPETING INTERESTS

The authors declare no competing financial or non-financial interests.

REFERENCES

1. Alberts B, Johnson A, Lewis J, Raff M, Roberts K, Walter P. 2002. Molecular biology of the cell 6th edition ed. Garland Science., New York.
2. Cho W, Stahelin RV. 2005. Membrane-protein interactions in cell signaling and membrane trafficking. Annu Rev Biophys Biomol Struct 34:119-51.
3. Simons K, Ikonen E. 1997. Functional rafts in cell membranes. Nature 387:569-72.
4. Rajendran L, Simons K. 2005. Lipid rafts and membrane dynamics. J Cell Sci 118:1099-102.
5. Simons K, Sampaio JL. 2011. Membrane organization and lipid rafts. Cold Spring Harb Perspect Biol 3:a004697.
6. Pike LJ. 2006. Rafts defined: a report on the Keystone Symposium on Lipid Rafts and Cell Function. J Lipid Res 47:1597-8.
7. Sezgin E, Levental I, Mayor S, Eggeling C. 2017. The mystery of membrane organization: composition, regulation and roles of lipid rafts. Nat Rev Mol Cell Biol 18:361-374.
8. Langhorst MF, Reuter A, Stuermer CA. 2005. Scaffolding microdomains and beyond: the function of reggie/flotillin proteins. Cell Mol Life Sci 62:2228-40.
9. Morrow IC, Parton RG. 2005. Flotillins and the PHB domain protein family: rafts, worms and anaesthetics. Traffic 6:725-40.
10. Stuermer CA, Plattner H. 2005. The 'lipid raft' microdomain proteins reggie-1 and reggie-2 (flotillins) are scaffolds for protein interaction and signalling. Biochem Soc Symp doi:10.1042/bss0720109:109-18.
11. Browman DT, Hoegg MB, Robbins SM. 2007. The SPFH domain-containing proteins: more than lipid raft markers. Trends Cell Biol 17:394-402.
12. Zeke A, Lukács M, Lim WA, Reményi A. 2009. Scaffolds: interaction platforms for cellular signalling circuits. Trends Cell Biol 19:364-74.
13. Zhao F, Zhang J, Liu YS, Li L, He YL. 2011. Research advances on flotillins. Virol J 8:479.
14. Lopez D, Koch G. 2017. Exploring functional membrane microdomains in bacteria: an overview. Curr Opin Microbiol 36:76-84.
15. Lopez D, Kolter R. 2010. Functional microdomains in bacterial membranes. Genes Dev 24:1893-902.
16. Bramkamp M, Lopez D. 2015. Exploring the existence of lipid rafts in bacteria. Microbiol Mol Biol Rev 79:81-100.
17. Bach JN, Bramkamp M. 2013. Flotillins functionally organize the bacterial membrane. Mol Microbiol 88:1205-17.
18. Donovan C, Bramkamp M. 2009. Characterization and subcellular localization of a bacterial flotillin homologue. Microbiology 155:1786-1799.
19. Dempwolff F, Möller HM, Graumann PL. 2012. Synthetic motility and cell shape defects associated with deletions of flotillin/reggie paralogs in Bacillus subtilis and interplay of these proteins with NfeD proteins. J Bacteriol 194:4652-61.
20. Yepes A, Schneider J, Mielich B, Koch G, García-Betancur JC, Ramamurthi KS, Vlamakis H, López D. 2012. The biofilm formation defect of a Bacillus subtilis flotillin-defective mutant involves the protease FtsH. Mol Microbiol 86:457-71.

21. Mielich-Süss B, Schneider J, Lopez D. 2013. Overproduction of flotillin influences cell differentiation and shape in Bacillus subtilis. mBio 4:e00719-13.
22. Schneider J, Mielich-Süss B, Böhme R, Lopez D. 2015. In vivo characterization of the scaffold activity of flotillin on the membrane kinase KinC of Bacillus subtilis. Microbiology 161:1871-1887.
23. Hinderhofer M, Walker CA, Friemel A, Stuermer CA, Möller HM, Reuter A. 2009. Evolution of prokaryotic SPFH proteins. BMC Evol Biol 9:10.
24. Kihara A, Akiyama Y, Ito K. 1996. A protease complex in the Escherichia coli plasma membrane: HflKC (HflA) forms a complex with FtsH (HflB), regulating its proteolytic activity against SecY. Embo j 15:6122-31.
25. Saikawa N, Akiyama Y, Ito K. 2004. FtsH exists as an exceptionally large complex containing HflKC in the plasma membrane of Escherichia coli. J Struct Biol 146:123-9.
26. Chiba S, Ito K, Akiyama Y. 2006. The Escherichia coli plasma membrane contains two PHB (prohibitin homology) domain protein complexes of opposite orientations. Mol Microbiol 60:448-57.
27. Ma C, Wang C, Luo D, Yan L, Yang W, Li N, Gao N. 2022. Structural insights into the membrane microdomain organization by SPFH family proteins. Cell Res 32:176-189.
28. Guzmán-Flores JE, Steinemann-Hernández L, González de la Vara LE, Gavilanes-Ruiz M, Romeo T, Alvarez AF, Georgellis D. 2019. Proteomic analysis of Escherichia coli detergent-resistant membranes (DRM). PLoS One 14:e0223794.
29. Guzman-Flores JE, Alvarez AF, Poggio S, Gavilanes-Ruiz M, Georgellis D. 2017. Isolation of detergent-resistant membranes (DRMs) from Escherichia coli. Anal Biochem 518:1-8.
30. Ito K, Akiyama Y. 2005. Cellular functions, mechanism of action, and regulation of FtsH protease. Annu Rev Microbiol 59:211-31.
31. Padilla-Vaca F, Vargas-Maya NI, Elizarrarás-Vargas NU, Rangel-Serrano Á, Cardoso-Reyes LR, Razo-Soria T, Membrillo-Hernández J, Franco B. 2019. Flotillin homologue is involved in the swimming behavior of Escherichia coli. Arch Microbiol 201:999-1008.
32. Koppelman CM, Den Blaauwen T, Duursma MC, Heeren RM, Nanninga N. 2001. Escherichia coli minicell membranes are enriched in cardiolipin. J Bacteriol 183:6144-7.
33. Romantsov T, Helbig S, Culham DE, Gill C, Stalker L, Wood JM. 2007. Cardiolipin promotes polar localization of osmosensory transporter ProP in Escherichia coli. Mol Microbiol 64:1455-65.
34. Mileykovskaya E, Dowhan W. 2009. Cardiolipin membrane domains in prokaryotes and eukaryotes. Biochim Biophys Acta 1788:2084-91.
35. Feng X, Hu Y, Zheng Y, Zhu W, Li K, Huang CH, Ko TP, Ren F, Chan HC, Nega M, Bogue S, López D, Kolter R, Götz F, Guo RT, Oldfield E. 2014. Structural and functional analysis of Bacillus subtilis YisP reveals a role of its product in biofilm production. Chem Biol 21:1557-63.
36. García-Fernández E, Koch G, Wagner RM, Fekete A, Stengel ST, Schneider J, Mielich-Süss B, Geibel S, Markert SM, Stigloher C, Lopez D. 2017. Membrane Microdomain Disassembly Inhibits MRSA Antibiotic Resistance. Cell 171:1354-1367.e20.

603 37. Zielińska A, Savietto A, de Sousa Borges A, Martinez D, Berbon M, Roelofsen
604 JR, Hartman AM, de Boer R, van der Klei IJ, Hirsch AKH, Habenstein B,
605 Bramkamp M, Scheffers D-J. 2020. Flotillin mediated membrane fluidity
606 controls peptidoglycan synthesis and MreB movement. bioRxiv
607 doi:10.1101/736819:736819.
608 38. Nishijima S, Asami Y, Uetake N, Yamagoe S, Ohta A, Shibuya I. 1988.
609 Disruption of the Escherichia coli cls gene responsible for cardiolipin synthesis.
610 J Bacteriol 170:775-80.
611 39. Hemmi H, Ohnuma S, Nagaoka K, Nishino T. 1998. Identification of genes
612 affecting lycopene formation in Escherichia coli transformed with carotenoid
613 biosynthetic genes: candidates for early genes in isoprenoid biosynthesis. J
614 Biochem 123:1088-96.
615 40. Hahn FM, Hurlburt AP, Poulter CD. 1999. Escherichia coli open reading frame
616 696 is idi, a nonessential gene encoding isopentenyl diphosphate isomerase. J
617 Bacteriol 181:4499-504.
618 41. Aires JR, Nikaido H. 2005. Aminoglycosides are captured from both periplasm
619 and cytoplasm by the AcrD multidrug efflux transporter of Escherichia coli. J
620 Bacteriol 187:1923-9.
621 42. Tavernarakis N, Driscoll M, Kyrpides NC. 1999. The SPFH domain: implicated
622 in regulating targeted protein turnover in stomatins and other membrane-
623 associated proteins. Trends Biochem Sci 24:425-7.
624 43. Morrow IC, Rea S, Martin S, Prior IA, Prohaska R, Hancock JF, James DE,
625 Parton RG. 2002. Flotillin-1/reggie-2 traffics to surface raft domains via a novel
626 golgi-independent pathway. Identification of a novel membrane targeting
627 domain and a role for palmitoylation. J Biol Chem 277:48834-41.
628 44. Bach JN, Bramkamp M. 2015. Dissecting the molecular properties of
629 prokaryotic flotillins. PLoS One 10:e0116750.
630 45. Dempwolff F, Schmidt FK, Hervás AB, Stroh A, Rösch TC, Riese CN, Dersch
631 S, Heimerl T, Lucena D, Hülsbusch N, Stuermer CA, Takeshita N, Fischer R,
632 Eckhardt B, Graumann PL. 2016. Super Resolution Fluorescence Microscopy
633 and Tracking of Bacterial Flotillin (Reggie) Paralogs Provide Evidence for
634 Defined-Sized Protein Microdomains within the Bacterial Membrane but
635 Absence of Clusters Containing Detergent-Resistant Proteins. PLoS Genet
636 12:e1006116.
637 46. Somani VK, Aggarwal S, Singh D, Prasad T, Bhatnagar R. 2016. Identification
638 of Novel Raft Marker Protein, FlotP in Bacillus anthracis. Front Microbiol
639 7:169.
640 47. Dempwolff F, Wischhusen HM, Specht M, Graumann PL. 2012. The deletion of
641 bacterial dynamin and flotillin genes results in pleiotrophic effects on cell
642 division, cell growth and in cell shape maintenance. BMC Microbiol 12:298.
643 48. Yokoyama H, Matsui I. 2020. The lipid raft markers stomatin, prohibitin,
644 flotillin, and HflK/C (SPFH)-domain proteins form an operon with NfeD
645 proteins and function with apolar polyisoprenoid lipids. Crit Rev Microbiol
646 46:38-48.
647 49. Kihara A, Ito K. 1998. Translocation, folding, and stability of the HflKC
648 complex with signal anchor topogenic sequences. J Biol Chem 273:29770-5.

649 50. Edgar R, Rokney A, Feeney M, Semsey S, Kessel M, Goldberg MB, Adhya S,
650 Oppenheim AB. 2008. Bacteriophage infection is targeted to cellular poles. Mol
651 Microbiol 68:1107-16.
652 51. Bandyopadhyay K, Parua PK, Datta AB, Parrack P. 2010. Escherichia coli HflK
653 and HflC can individually inhibit the HflB (FtsH)-mediated proteolysis of
654 lambdaCII in vitro. Arch Biochem Biophys 501:239-43.
655 52. Qiao Z, Yokoyama T, Yan XF, Beh IT, Shi J, Basak S, Akiyama Y, Gao YG.
656 2022. Cryo-EM structure of the entire FtsH-HflKC AAA protease complex. Cell
657 Rep 39:110890.
658 53. Raetz CR, Dowhan W. 1990. Biosynthesis and function of phospholipids in
659 Escherichia coli. J Biol Chem 265:1235-8.
660 54. Lin TY, Weibel DB. 2016. Organization and function of anionic phospholipids
661 in bacteria. Appl Microbiol Biotechnol 100:4255-67.
662 55. Sohlenkamp C, Geiger O. 2016. Bacterial membrane lipids: diversity in
663 structures and pathways. FEMS Microbiol Rev 40:133-59.
664 56. El Khoury M, Swain J, Sautrey G, Zimmermann L, Van Der Smissen P, Décout
665 JL, Mingeot-Leclercq MP. 2017. Targeting Bacterial Cardiolipin Enriched
666 Microdomains: An Antimicrobial Strategy Used by Amphiphilic
667 Aminoglycoside Antibiotics. Sci Rep 7:10697.
668 57. Oliver PM, Crooks JA, Leidl M, Yoon EJ, Saghatelian A, Weibel DB. 2014.
669 Localization of anionic phospholipids in Escherichia coli cells. J Bacteriol
670 196:3386-98.
671 58. Romantsov T, Stalker L, Culham DE, Wood JM. 2008. Cardiolipin controls the
672 osmotic stress response and the subcellular location of transporter ProP in
673 Escherichia coli. J Biol Chem 283:12314-23.
674 59. Arias-Cartin R, Grimaldi S, Arnoux P, Guigliarelli B, Magalon A. 2012.
675 Cardiolipin binding in bacterial respiratory complexes: structural and functional
676 implications. Biochim Biophys Acta 1817:1937-49.
677 60. Romantsov T, Gonzalez K, Sahtout N, Culham DE, Coumoundouros C, Garner
678 J, Kerr CH, Chang L, Turner RJ, Wood JM. 2018. Cardiolipin synthase A
679 colocalizes with cardiolipin and osmosensing transporter ProP at the poles of
680 Escherichia coli cells. Mol Microbiol 107:623-638.
681 61. van Tilburg AY, Warmer P, van Heel AJ, Sauer U, Kuipers OP. 2022.
682 Membrane composition and organization of Bacillus subtilis 168 and its
683 genome-reduced derivative miniBacillus PG10. Microb Biotechnol 15:1633-
684 1651.
685 62. Akiyama Y. 2009. Quality control of cytoplasmic membrane proteins in
686 Escherichia coli. J Biochem 146:449-54.
687 63. Hinz A, Lee S, Jacoby K, Manoil C. 2011. Membrane proteases and
688 aminoglycoside antibiotic resistance. J Bacteriol 193:4790-7.
689 64. Venter H, Mowla R, Ohene-Agyei T, Ma S. 2015. RND-type drug efflux pumps
690 from Gram-negative bacteria: molecular mechanism and inhibition. Front
691 Microbiol 6:377.
692 65. Nikaido E, Shirosaka I, Yamaguchi A, Nishino K. 2011. Regulation of the
693 AcrAB multidrug efflux pump in Salmonella enterica serovar Typhimurium in
694 response to indole and paraquat. Microbiology 157:648-655.

66. Garneau-Tsodikova S, Labby KJ. 2016. Mechanisms of Resistance to Aminoglycoside Antibiotics: Overview and Perspectives. Medchemcomm 7:11-27.
67. Baba T, Ara T, Hasegawa M, Takai Y, Okumura Y, Baba M, Datsenko KA, Tomita M, Wanner BL, Mori H. 2006. Construction of Escherichia coli K-12 in-frame, single-gene knockout mutants: the Keio collection. Mol Syst Biol 2:2006.0008.
68. Chaveroche MK, Ghigo JM, d'Enfert C. 2000. A rapid method for efficient gene replacement in the filamentous fungus Aspergillus nidulans. Nucleic Acids Res 28:E97.
69. Cherepanov PP, Wackernagel W. 1995. Gene disruption in Escherichia coli: TcR and KmR cassettes with the option of Flp-catalyzed excision of the antibiotic-resistance determinant. Gene 158:9-14.
70. Boudjemaa R, Cabriel C, Dubois-Brissonnet F, Bourg N, Dupuis G, Gruss A, Leveque-Fort S, Briandet R, Fontaine-Aupart MP, Steenkeste K. 2018. Impact of Bacterial Membrane Fatty Acid Composition on the Failure of Daptomycin To Kill Staphylococcus aureus. Antimicrob Agents Chemother 62.
71. Cabriel C, Bourg N, Dupuis G, Leveque-Fort S. 2018. Aberration-accounting calibration for 3D single-molecule localization microscopy. Opt Lett 43:174-177.

716 **FIGURE LEGENDS**
717
718 **Figure 1. Cell localization patterns of HflC and QmcA.** Epifluorescence microscopy
719 of cells expressing QmcA-GFP (A) and HflC-mCherry (B). Representative images are
720 shown. Percentages indicate the frequencies of cells showing localization foci.
721 Arrowheads indicate polar or punctate localization foci. Scales are indicated as white bars.
722
723 **Figure 2. QmcA and HflC localize to the inner membrane.** SDS-PAGE and
724 immunodetection analyses of whole-cell extracts, cytosolic fractions, and inner (IM) or
725 outer membrane (OM) fractions prepared from cells expressing QmcA-GFP (**A**) and
726 HflC-mCherry (**B**). Anti-GFP and anti-mCherry antibodies were used to detect the
727 presence of QmcA-GFP and HflC-mCherry, respectively. An anti-ExbB antibody were
728 used to detect the inner membrane- (IM) marker ExbB and anti-TolC antibodies to detect
729 the outer membrane- (OM) marker TolC.
730
731 **Figure 3. The localization pattern and membrane topology of full-length, domain**
732 **swapped or truncated versions of QmcA and HflC.** (**A**) GFP fusion derivatives of
733 QmcA and (**B**) mCherry fusion derivatives of HflC. The representative images are shown
734 in each strain with the frequencies of cells showing punctate (**A**) or polar localization (**B**).
735 In figure 3A, first panel, the control WT QmcA-GFP is re-named TM^{QmcA}-$SPFH^{QmcA}$-
736 GFP and the fluorescence microscopy image corresponding to its localization is therefore
737 a duplicate of the one presented in Figure 1A. Similarly, In figure 3B, first panel, the
738 control WT HflC-mCherry is re-named TM^{HflC}-$SPFH^{HflC}$-mCherry and the fluorescence
739 microscopy image corresponding to its localization is therefore a duplicate of the one
740 presented in Figure 1B. In membrane topology, helical structures represent
741 transmembrane (TM) domains; silver, native TM domain of QmcA; pink, Pf3 domain;
742 green, native TM domain of HflC; black, Cmi domain. Scale bars are 2 μm.
743
744 **Figure 4. Alteration of QmcA and HflC cell localization in *E. coli* cardiolipin and**
745 **isoprenoid pathway mutants.** Two-dimensional super-resolution microscopy images of
746 WT, Δ*clsABC*, and Δ*idi* strains expressing QmcA-GFP (**A**) and HflC-mCherry (**B**) in
747 stationary phase. Number or nature of detected cluster is indicated. Scales are indicated
748 as white bars.
749
750 **Figure 5. Phenotypic analysis of *E. coli* SPFH mutants**. **A**: Bacterial growth curve of
751 WT and SPFH gene deletion mutants in LB medium. **B**: Biolog bacterial growth curve of
752 WT and ΔSPFH in the presence of tobramycin and paraquat. **C**: Minimum inhibitory
753 concentration (MIC) for tobramycin of *E. coli* WT and indicated mutants. **D**: Minimum
754 inhibitory concentration (MIC) for paraquat of *E. coli* WT and indicated mutants. *$p <$
755 0.05, **$p < 0.01$, ***$p < 0.001$, ****$p < 0.0001$compared with WT.
756
757

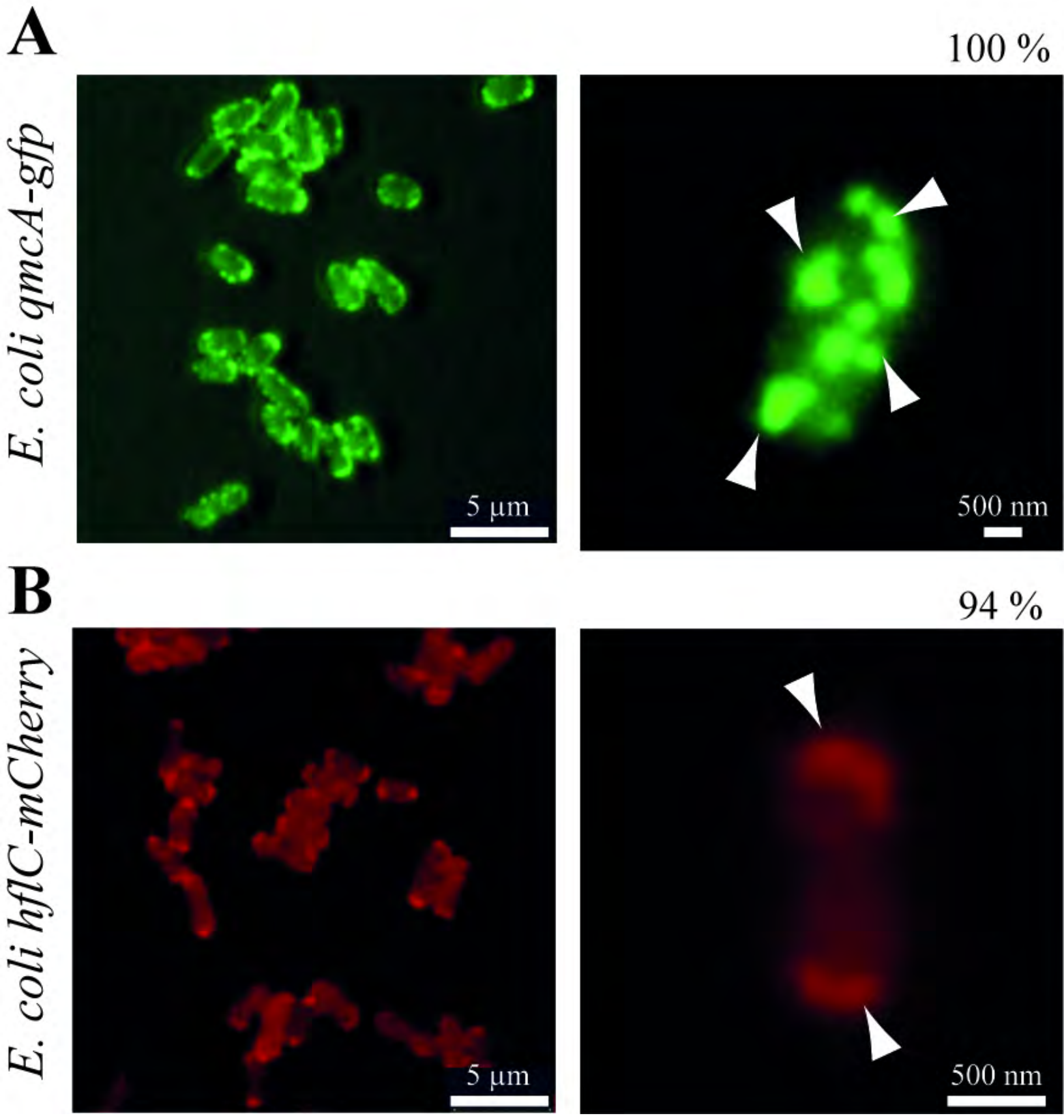
A
E. coli qmcA-gfp
100 %
5 µm
500 nm
B
E. coli hflC-mCherry
94 %
5 µm
500 nm

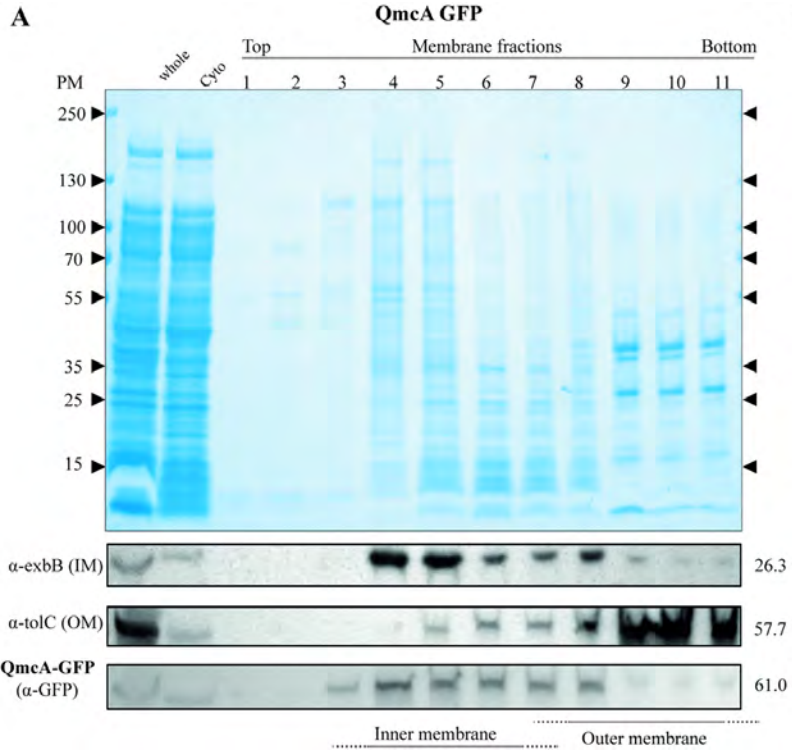
A
QmcA GFP
whole
Cyto
Top
Membrane fractions
Bottom
PM
1 2 3 4 5 6 7 8 9 10 11
250
130
100
70
55
35
25
15
α-exbB (IM)
26.3
α-tolC (OM)
57.7
QmcA-GFP
(α-GFP)
61.0
Inner membrane
Outer membrane

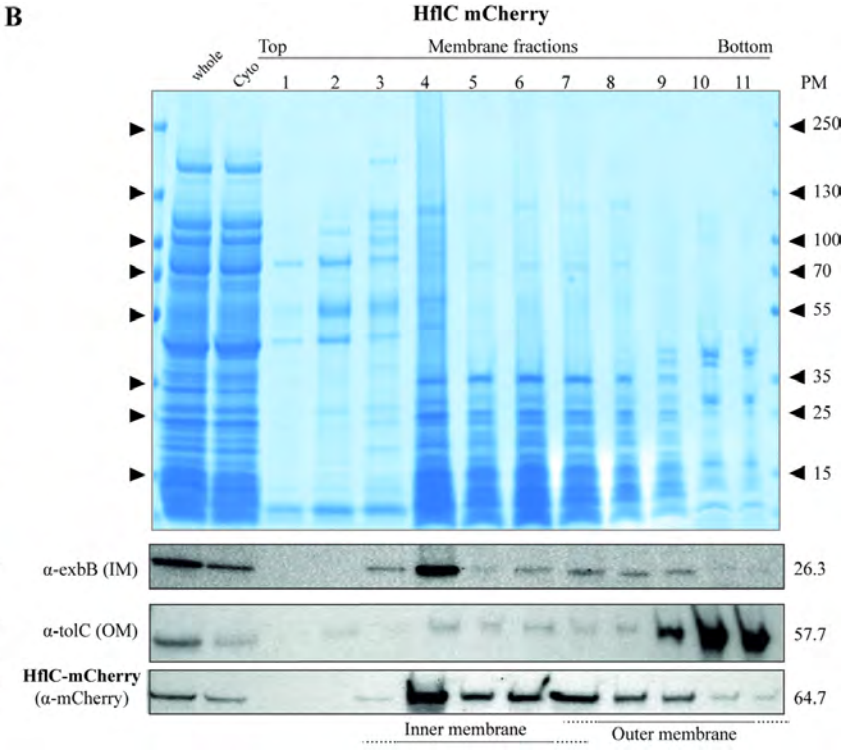
B
HflC mCherry
whole
Cyto
Top
Membrane fractions
Bottom
1 2 3 4 5 6 7 8 9 10 11
PM
250
130
100
70
55
35
25
15
α-exbB (IM)
26.3
α-tolC (OM)
57.7
HflC-mCherry
(α-mCherry)
64.7
Inner membrane
Outer membrane

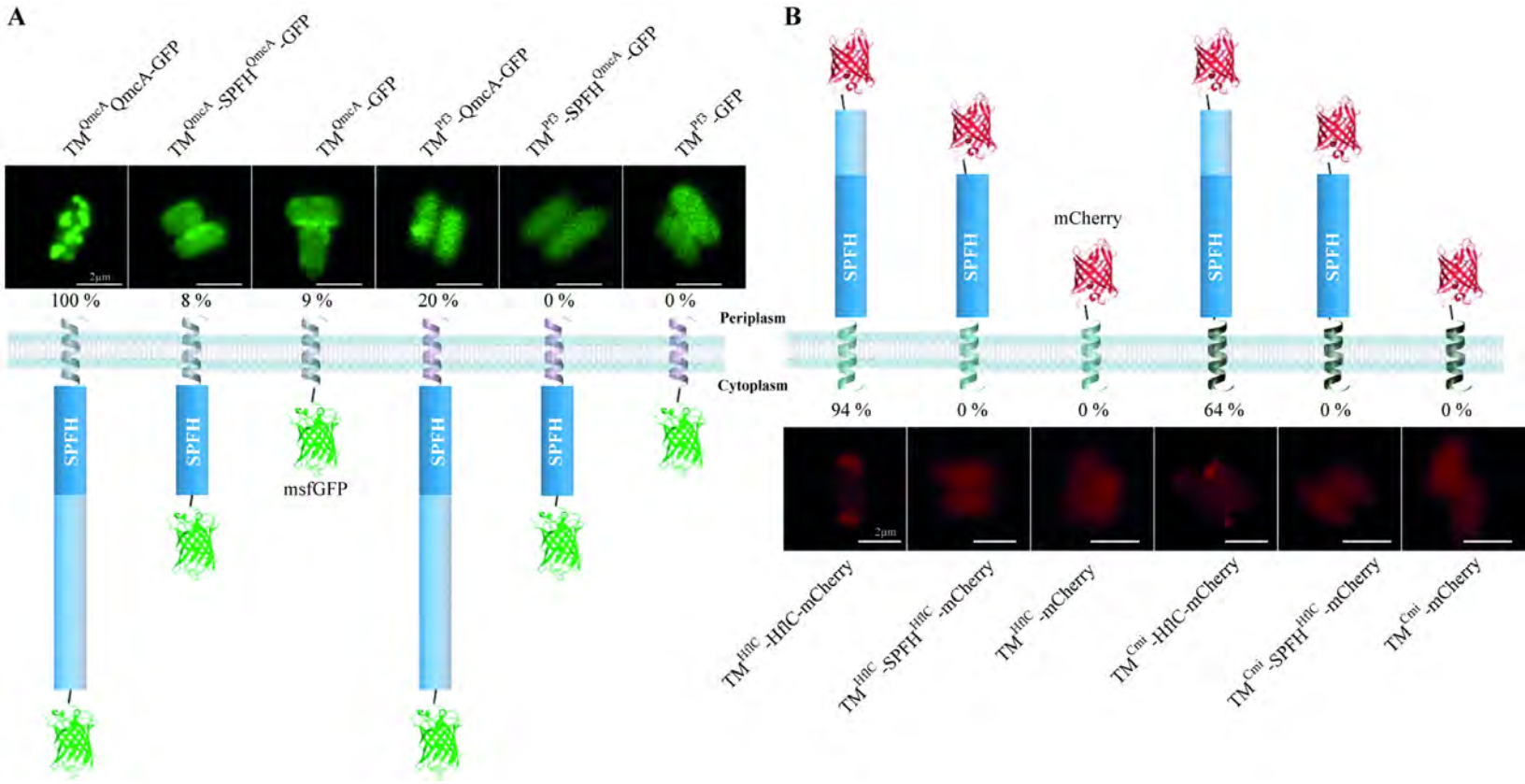
A
TM QmcA QmcA-GFP
TM QmcA -SPFH QmcA -GFP
TM QmcA -GFP
TM P3 -QmcA-GFP
TM P3 -SPFH QmcA -GFP
TM P3 -GFP
2μm
100 %
8 %
9 %
20 %
0 %
0 %
Periplasm
Cytoplasm
SPFH
msfGFP
B
mCherry
94 %
0 %
0 %
64 %
0 %
0 %
2μm
TM HflC -HflC-mCherry
TM HflC -SPFH HflC -mCherry
TM HflC -mCherry
TM Cmi -HflC-mCherry
TM Cmi -SPFH HflC -mCherry
TM Cmi -mCherry

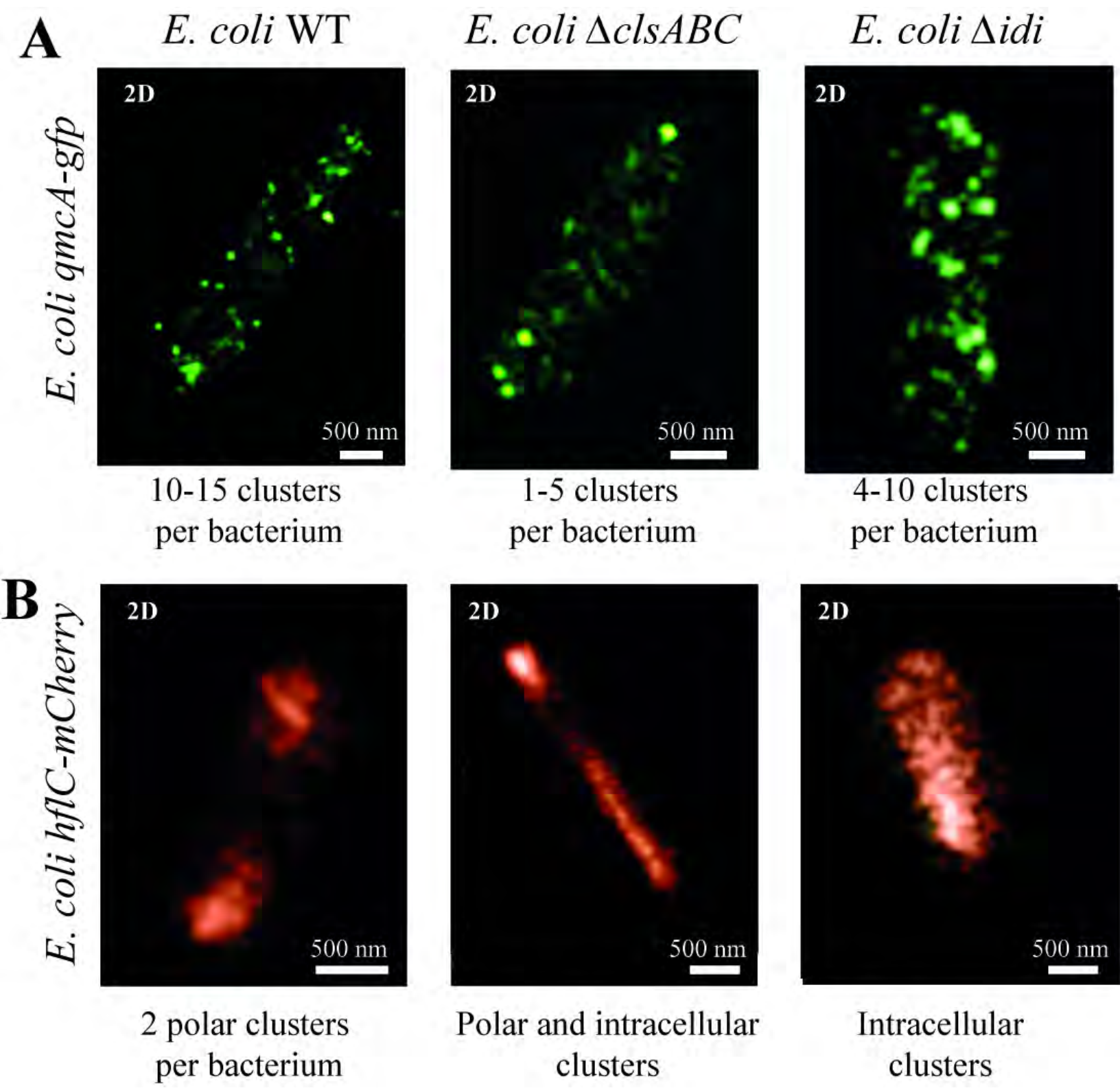
A
E. coli WT
E. coli ΔclsABC
E. coli Δidi
E. coli qmcA-gfp
2D
500 nm
10-15 clusters per bacterium
1-5 clusters per bacterium
4-10 clusters per bacterium
B
E. coli hflC-mCherry
2D
500 nm
2 polar clusters per bacterium
Polar and intracellular clusters
Intracellular clusters

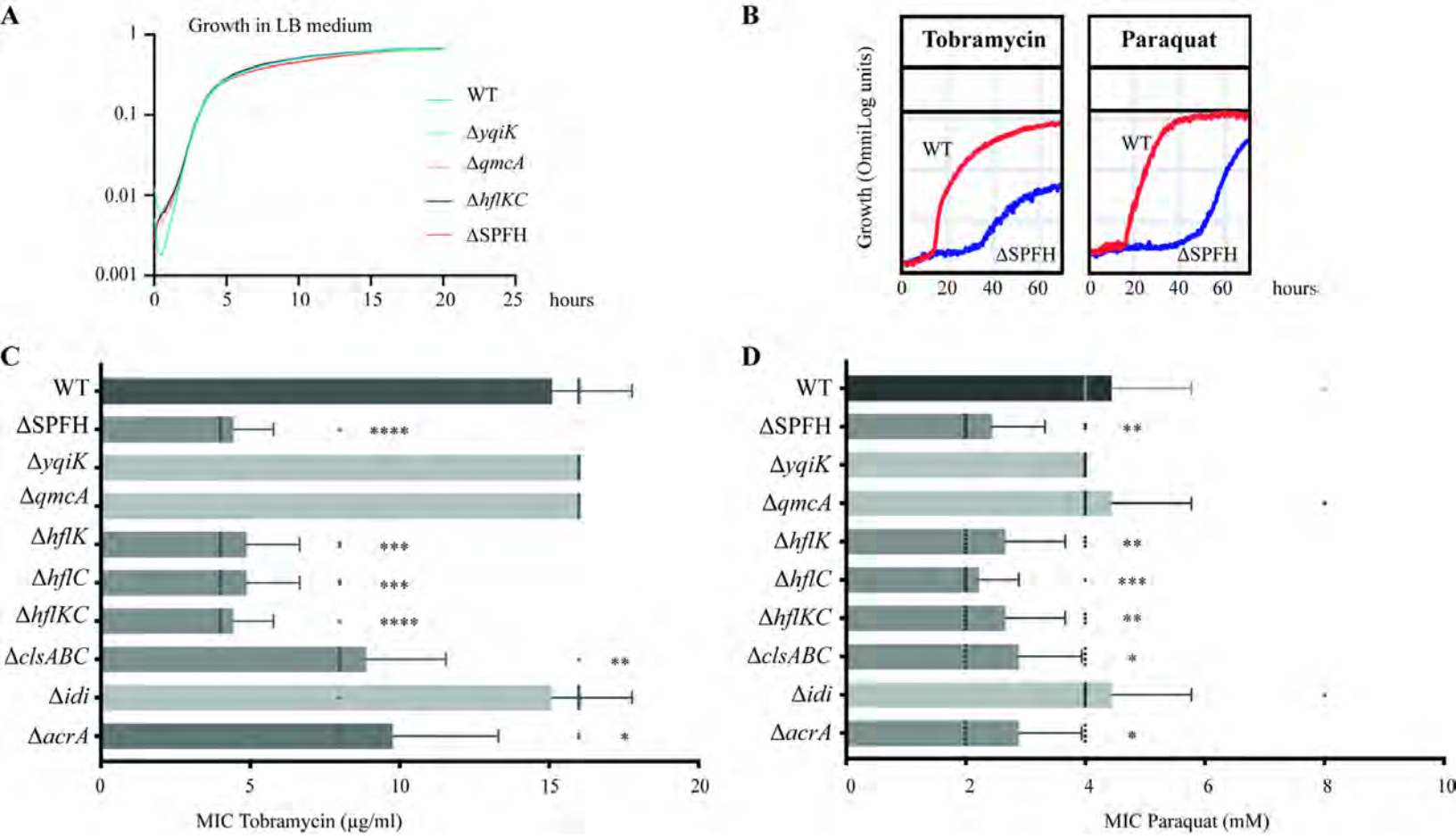
A
Growth in LB medium
1
0.1
0.01
0.001
0
5
10
15
20
25
hours
WT
ΔyqiK
ΔqmcA
ΔhflKC
ΔSPFH
B
Tobramycin
Paraquat
Growth (OmniLog units)
WT
ΔSPFH
0
20
40
60
hours
C
WT
ΔSPFH
ΔyqiK
ΔqmcA
ΔhflK
ΔhflC
ΔhflKC
ΔclsABC
Δidi
ΔacrA
****
***
***
****
**
*
0
5
10
15
20
MIC Tobramycin (µg/ml)
D
WT
ΔSPFH
ΔyqiK
ΔqmcA
ΔhflK
ΔhflC
ΔhflKC
ΔclsABC
Δidi
ΔacrA
**
**
***
**
*
*
0
2
4
6
8
10
MIC Paraquat (mM)

SUPPLEMENTARY MATERIALS

Escherichia coli SPFH membrane microdomain proteins HflKC contributes to aminoglycoside and oxidative stress tolerance

Wessel AK, Yoshii Y *et al.*

This pdf file includes supplementary methods, supplementary figures S1 to S9 and supplementaryTables S2 and S3. Supplementary Table S1 is provided separately as a dataset.

SUPPLEMENTARY METHODS

Construction of YqiK tagged with GFP and HflK tagged with mCherry

YqiK-GFP chromosomal construct

The *yqiK* (except for the stop codon), msf*gfp,* and *aphAIII* genes encoding YqiK, msfGFP, and KmFRT cassette were amplified from MG1655 *strep*, MG1655mreB-GFP (1), and MG1655Δ*cpxP*::KmFRT (2) chromosomes, respectively. Then, the intermediate plasmid pUC18 *yqiK-gfp-aphAIII* was constructed by combining these three DNA fragments with the linearized backbone vector pUC18, using Gibson assembly (New England Biolabs, Ipswich, MA, USA) and primers described in Table S3. Next, the DNA fragment encoding YqiK-GFP-KmFRT was amplified from the plasmid pUC18*yqiK-gfp-aphAIII* using the long recombining primers described in Table S3. The resulting PCR product was introduced on its native location under the *yqiK* promoter in strain MG1655 *strep* using pKOBEG plasmid by λ-red recombination to produce YqiK-GFP.

HflK-mCherry chromosomal construct

The DNA gene block corresponding to the entire *hflK* gene except for the stop codon, mCherry, and KmFRT with 40 bp-long homology regions of upstream of the *hflK* start codon and downstream of the *aphAIII* last codon was designed from the DNA sequence of MG1655 *strep*, MG1655mreB-mCherry (3), and MG1655Δ*cpxP*::KmFRT (2) chromosomes, respectively, and purchased from Eurofins Genomics (France). Then, the DNA oligonucleotide was introduced on its native location under the *hflK* promoter in *MG1655 strep* using pKOBEG plasmid by λ-red recombination to produce HflK-mCherry.

Construction of QmcA-GFP and QmcA-derivatives tagged with GFP

The *qmcA and ybbJ*, msf*gfp,* and *aphAIII* genes encoding QmcA and YbbJ, msfGFP and KmFRT cassette, respectively, were amplified from MG1655 *strep*, MG1655mreB-GFP, and MG1655Δ*cpxP*::KmFRT (2) chromosomes. The sequence of information on the *pf3* gene was obtained from (4).

• ***TM^{QmcA}-QmcA-GFP chromosomal construct***

The intermediate plasmid pUC18*qmcA-gfp-aphAIII* was constructed by combining DNA fragments of the entire *qmcA* gene except for the stop codon, msfGFP, the entire *ybbJ* gene followed by 20 bp upstream regions of the start codon, and KmFRT, with the linearized backbone vector pUC18 using Gibson assembly (New England Biolabs). The DNA fragment encoding QmcA-GFP-KmFRT was amplified from the plasmid pUC18*qmcA-gfp-aphAIII* using the long recombining primers described in Table S3, and introduced on its native location under the *qmcA* promoter in strain MG1655 *strep* using pKOBEG plasmid by λ-red recombination to produce TM^{qmcA}-QmcA-GFP.

TM^{QmcA}-SPFH^{QmcA}-GFP chromosomal construct

The DNA fragment encoding msfGFP-KmFRT with 40 bp-long upstream and downstream homology regions was amplified from the TM^{pf3}-SPFH^{QmcA}-GFP chromosomal construct using the long recombining primers described in Table S3. Then, the resulting PCR product was introduced on the chromosome at the downstream position of the *qmcA* SPFH domain region in strain MG1655 *strep* by λ-red recombination to produce TM^{QmcA}-SPFH^{QmcA}-GFP.

• ***TM^{QmcA} -GFP chromosomal construct***

The DNA fragment encoding to msfGFP-KmFRT with 40 bp-long upstream and downstream homology regions was amplified from the TM^{QmcA}-QmcA-GFP chromosomal construct using long recombining primers described in Table S3. Then, the resulting PCR product was introduced on the chromosome at the downstream position of the *qmcA* TM domain region in strain MG1655 *strep* by λ-red recombination to produce TM^{QmcA}-GFP.

• **Δ*qmcA::zeo* chromosomal construct**

The *zeo* gene with 40 bp-long upstream and downstream homology regions was amplified from

the MG1655_ λATT:*amp_GFPmut3_*Δ*fimAICDFGH::zeo* Δ*yadyadNecpDhtrEyadMLKC::cat* (5) using long recombining primers described in Table S3. Then, the resulting PCR product was introduced on the native location under the *qmcA* promoter in strain MG1655 strep by λ-red recombination to generate *ΔqmcA*::zeo.

• ***TM^{pf3}-QmcA-GFP chromosomal construct***

The plasmid pZS*12*TM^{pf3}-gfp-aphAIII* was constructed via pZS*12*TM^{pf3}-gfp,* by combining DNA fragments of *pf3*, msfGFP, and KmFRT, with the linearized backbone vector pZS*12 using Gibson assembly (New England Biolabs) and primers described in Table S3. Then, the intermediate plasmid pZS*12*TM^{pf3}-qmcA-gfp-aphAIII* was constructed by combining the DNA fragment of *qmcA* gene except for the native TM domain region with the linearized vector pZS*12*TM^{pf3}-gfp* using Gibson assembly (New England Biolabs). Next, the DNA fragment encoding TM^{pf3}-QmcA-GFP-KmFRT with 40 bp-long upstream and downstream homology regions was amplified from the intermediate plasmid using the long recombining primers described in Table S3. The resulting PCR product was introduced on its native location under *qmcA* promoter by λ-red recombination into strain Δ*qmcA*::*zeo* using pKOBEG plasmid to produce TM^{pf3}-QmcA-GFP.

• ***TM^{pf3}-SPFH^{QmcA}-GFP chromosomal construct***

The intermediate plasmid pZS*12*TM^{pf3}-SPFH^{QmcA}-gfp-aphAIII* was constructed by combining the SPFH domain region of *qmcA* gene with the linearized vector PZ*12 *TM^{pf3}-gfp-aphAIII* using Gibson assembly (New England Biolabs). Then, the DNA fragment encoding TM^{pf3}-SPFH^{QmcA}-GFP-KmFRT with 40 bp-long upstream and downstream homology regions was amplified from the plasmid pZS*12 *TM^{pf3}-SPFH^{QmcA}-GFP-aphAIII* using the long recombining primers described in Table S3. The resulting PCR product was introduced on its native location under *qmcA* promoter by λ-red recombination into Δ*qmcA*::*zeo* strain using pKOBEG plasmid to produce TM^{pf3}-SPFH^{QmcA}-GFP.

• ***TM^{pf3}-GFP chromosomal construct***

The DNA fragment encoding *TM^{pf3}*-GFP-KmFRT with 40 bp-long upstream and downstream homology regions was amplified from pZS*12*TM^{pf3}-gfp-aphAIII* using the long recombining primers described in Table S3. The resulting PCR product was introduced on its native location under *qmcA* promoter by λ-red recombination into Δ*qmcA*::*zeo* strain using pKOBEG plasmid to produce TM^{pf3}-GFP.

Construction of HflC derivatives tagged with mCherry

The *hflC*, *mCherry,* and *cat* genes encoding HflC, mCherry, and CmFRT cassette, respectively, were amplified from MG1655 *strep*, MG1655mreB-mCherry, and MG1655ΔyfcV-P::CmFRT (6) chromosomes. The sequence of information on *cmi* gene was obtained from (4).

• ***TM^{HflC}-HflC-mCherry chromosomal construct***

The intermediate plasmid pUC18*TM^{hflC}-HflC-mCherry-aphAIII* was constructed by combining DNA fragments of the *hflC* gene except for the stop codon, mCherry, and KmFRT, with the linearized backbone vector pUC18 using Gibson assembly (New England Biolabs) and primers described in Table S3. The DNA fragment encoding HflC-mCherry-KmFRT with 40 bp-long upstream and downstream homology regions was amplified from the plasmid pUC18*TM^{hflC}-HflC-mCherry-aphAIII* using the long recombining primers described in Table S3 and introduced on its native location under the *hflC* promoter in strain *MG1655 strep* using pKOBEG plasmid by λ-red recombination to TM^{hflC}-HflC-mCherry.

• ***TM^{HflC}- SPFH^{HflC} -mCherry chromosomal construct***

The DNA fragment encoding mCherry-CmFRT with 40 bp-long upstream and downstream homology regions was amplified from the TM^{cmi}-SPFH^{HflC}-mCherry chromosomal construct, using the long recombining primers described in Table S3. The resulting PCR product was introduced on the chromosome at the downstream position of the *hflC* SPFH domain region by λ-red recombination into *MG1655 strep* strain using pKOBEGA plasmid to produce TM^{hflC}-SPFH^{HflC}-mCherry.

• ***TM^{HflC}-mCherry chromosomal construct***

The DNA fragment encoding mCherry-KmFRT with 40 bp-long upstream and downstream homology regions was amplified form the plasmid pUC18*TM^{hflC}-HflC-mCherry-aphAIII* using the long recombining primers described in Table S3. The resulting PCR product was introduced on the chromosome at the downstream position of the *hflC* TM domain region by λ-red recombination into *MG1655 strep* strain using pKOBEGA plasmid to produce TM^{hflC}-mCherry.

• ***TM^{cmi}-HflC-mCherry chromosomal construct***

The plasmid pZS*12*TM^{cmi}-mCherry-cat* was constructed, via pZS*12*TM^{cmi}-mCherry,* by combining DNA fragments encoding *TM^{cmi}*, mCherry, and CmFRT, with the linearized backbone vector pZS*12 using Gibson assembly (New England Biolabs) and the primers described in Table S3. Then, the intermediate plasmid pZS*12*TM^{cmi}-hflC-mCherry-cat* was constructed by combining the DNA fragment of *hflC* gene except for the native TM domain region with the linearized vector pZS*12*TM^{cmi}-mCherry-cat* using Gibson assembly (New England Biolabs). Then, the DNA fragment encoding TM^{cmi}-HflC-mCherry-CmFRT with 40 bp-long upstream and downstream homology regions was amplified from the intermediated plasmid using the long recombining primers described in Table S3. The resulting PCR product was introduced on its native location under *hflC* promoter by λ-red recombination into Δ*hflC*::KmFRT strain using pKOBEGA plasmid to produce TM^{cmi}-HflC-mCherry.

• *TM^{cmi}- SPFH^{HflC} -mCherry chromosomal construct*

The intermediated plasmid pZS*12*TM^{cmi}-SPFH^{HflC}-mCherry-cat* was constructed by combining the *hflC* SPFH domain region with the linearized initial plasmid pZS*12*TM^{cmi}-mCherry-cat*, which was used for generating TM^{cmi}-HflC-mCherry chromosomal construct, using Gibson assembly (New England Biolabs). Then, the DNA fragment encoding TM^{cmi}-SPFH^{HflC}-mCherry-CmFRT with 40 bp-long upstream and downstream homology regions was amplified from the intermediated plasmid using the long recombining primers described in Table S3. The resulting PCR product was introduced on its native location under *hflC* promoter by λ-red recombination into Δ*hflC*::KmFRT strain using pKOBEGA plasmid to produce TM^{cmi}-SPFH^{HflC}-mCherry.

• *TM^{cmi}- mCherry chromosomal construct*

The DNA fragment encoding TM^{cmi}-GFP-CmFRT with 40 bp-long upstream and downstream homology regions was amplified from the plasmid pZS*12*TM^{cmi}-mCherry-cat* using the long recombining primers described in Table S3. The resulting PCR product was introduced on its native location under *hflC* promoter by λ-red recombination into Δ*hflC*::KmFRT strain using pKOBEGA plasmid to produce TM^{cmi}-mCherry.

Construction of QmcA-GFP and HflC-mCherry in the ΔclsABC and Δidi mutants

• *QmcA-GFP chromosomal construct* in the Δ*clsABC* strain

TM^{QmcA}-QmcA-GFP-KmFRT mutation from TM^{QmcA}-QmcA-GFP chromosomal construct

was introduced into strain Δ*clsABC* by P1vir phage transduction (Δ*clsABC* QmcA-GFP).

• ***TM^{QmcA}-QmcA-GFP chromosomal construct*** **in the Δ*idi* strain**

TM^{QmcA}-QmcA-GFP-KmFRT mutation from TM^{QmcA}-QmcA-GFP chromosomal construct was introduced into strain Δ*idi* by P1vir phage transduction (Δ*idi* QmcA-GFP).

• ***TM^{HflC}-HflC-mCherry chromosomal construct*** **in the *ΔclsABC* strain**

TM^{HflC}-HflC-mCherry-KmFRT mutation from TM^{HflC}-HflC-mCherry chromosomal construct was introduced into strain Δ*clsABC* by P1vir phage transduction (Δ*clsABC* HflC-mCherry).

• ***TM^{HflC}-HflC-mCherry chromosomal construct*** **in the Δ*idi* strain**

TM^{HflC}-HflC-mCherry-KmFRT mutation from TM^{HflC}-HflC-mCherry chromosomal construct was introduced into strain Δ*idi* by P1vir phage transduction (Δ*idi* HflC-mCherry).

• ***AcrA-GFP***

The DNA fragment encoding GFP-KmFRT region with 40 bp-long upstream and downstream homology regions was amplified from the TM^{pf3}-SPFH^{QmcA}-GFP chromosomal construct using the long recombining primers described in Table S3. The resulting PCR product was introduced on chromosome at the downstream position of the *acrA* gene (without stop codons) in *MG1655 strep* by λ-red recombination, to produce a GFP fusion. The mutation harboring KmFRT was introduced into a MG1655 *strep* strain having clean background by P1vir phage transduction (AcrA-GFP).

REFERENCES

1. **Pédelacq JD, Cabantous S, Tran T, Terwilliger TC, Waldo GS.** 2006. Engineering and characterization of a superfolder green fluorescent protein. Nat Biotechnol **24:**79-88.10.1038/nbt1172: 10.1038/nbt1172

2. **Beloin C, Valle J, Latour-Lambert P, Faure P, Kzreminski M, Balestrino D, Haagensen JA, Molin S, Prensier G, Arbeille B, Ghigo JM.** 2004. Global impact of mature biofilm lifestyle on *Escherichia coli* K-12 gene expression. Mol Microbiol **51:**659-674.10.1046/j.1365-2958.2003.03865.x: 10.1046/j.1365-2958.2003.03865.x

3. **Bendezú FO, Hale CA, Bernhardt TG, de Boer PA.** 2009. RodZ (YfgA) is required for proper assembly of the MreB actin cytoskeleton and cell shape in *E. coli*. Embo j **28:**193-204.10.1038/emboj.2008.264: 10.1038/emboj.2008.264

4. **Luiten RG, Putterman DG, Schoenmakers JG, Konings RN, Day LA.** 1985. Nucleotide sequence of the genome of Pf3, an IncP-1 plasmid-specific filamentous bacteriophage of Pseudomonas aeruginosa. J Virol **56:**268-276

5. **Larsonneur F, Martin FA, Mallet A, Martinez-Gil M, Semetey V, Ghigo JM, Beloin C.** 2016. Functional analysis of Escherichia coli Yad fimbriae reveals their potential role in environmental persistence. Environmental microbiology 18:5228-5248.

6. **Korea CG, Badouraly R, Prevost MC, Ghigo JM, Beloin C.** 2010. *Escherichia coli* K-12 possesses multiple cryptic but functional chaperone-usher fimbriae with distinct surface specificities. Environ Microbiol **12**: 1957–1977. https://doi.org/10.1111/j.1462-2920.2010.02202.x

SUPPLENTARY FIGURES

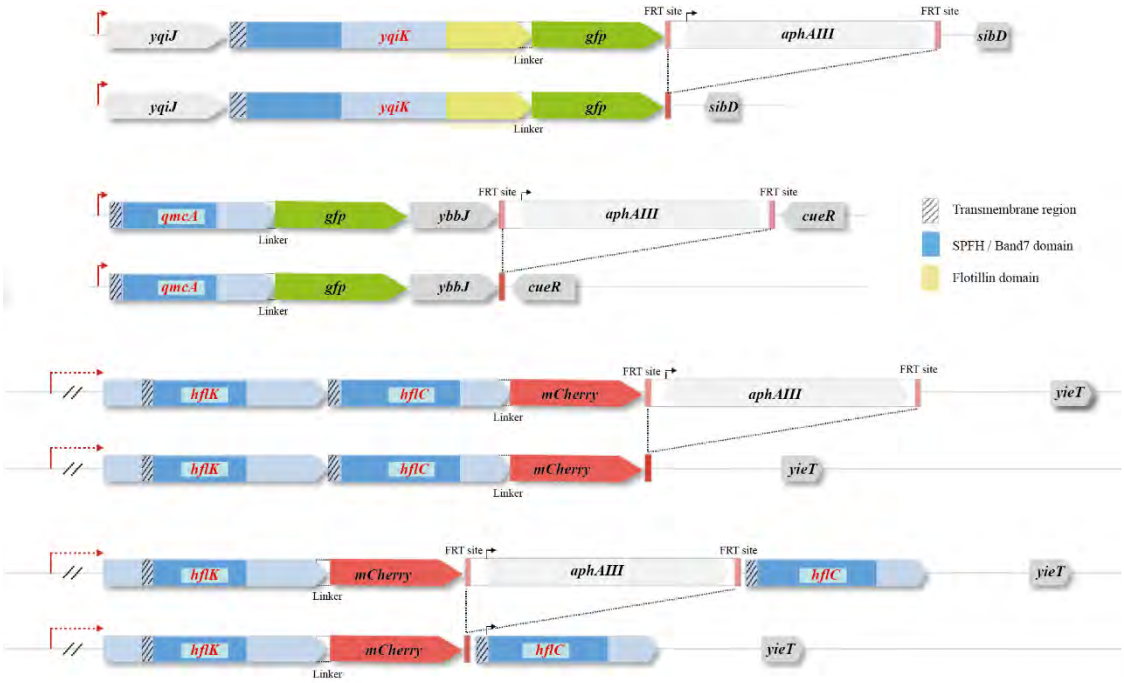

Supplementary Figure S1. Schematic representation of chromosomal GFP or mCherry fusions to genes encoding *E. coli* SPFH proteins. SPFH protein-encoding genes, *yqiK*, *qmcA*, are fused with monomeric super folder green fluorescent protein GFP (msfGFP) and *hflK*, and *hflC* to monomeric red fluorescent protein mCherry, respectively. Fusions were constructed as described in the Materials and Method section and the associated kanamycin antibiotic resistance marker (*aphAIII)* was inserted downstream of the fusion genes and removed using pCP20 plasmid, encoding the *flp* flippase.

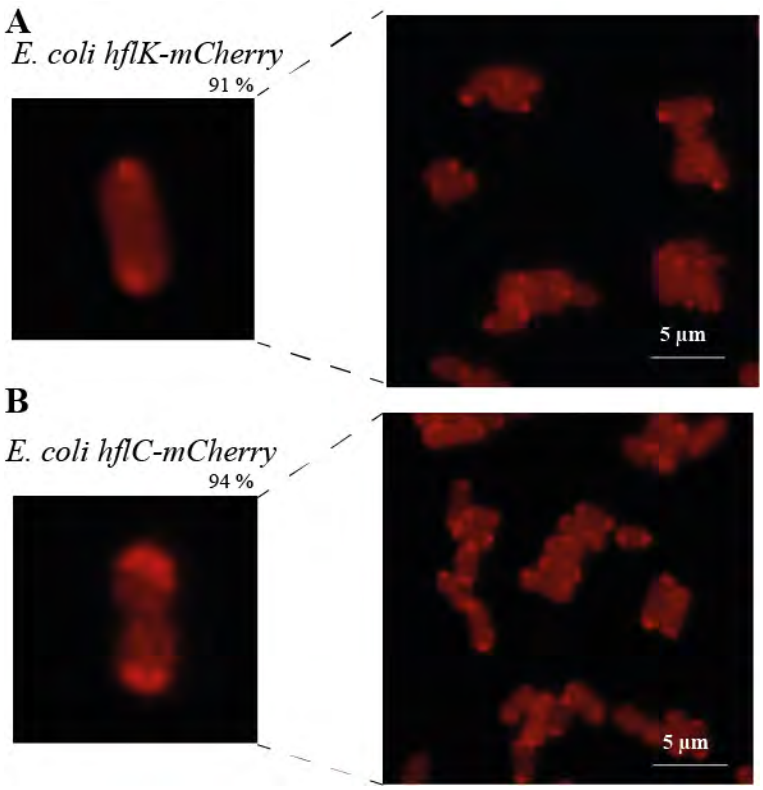

Supplementary Figure S2. Localization pattern of HflK and HflC. Epifluorescence microscopic images of cells expressing HflK-mCherry (A) and HflC-mCherry (B) in exponential phase with high and low magnifications.

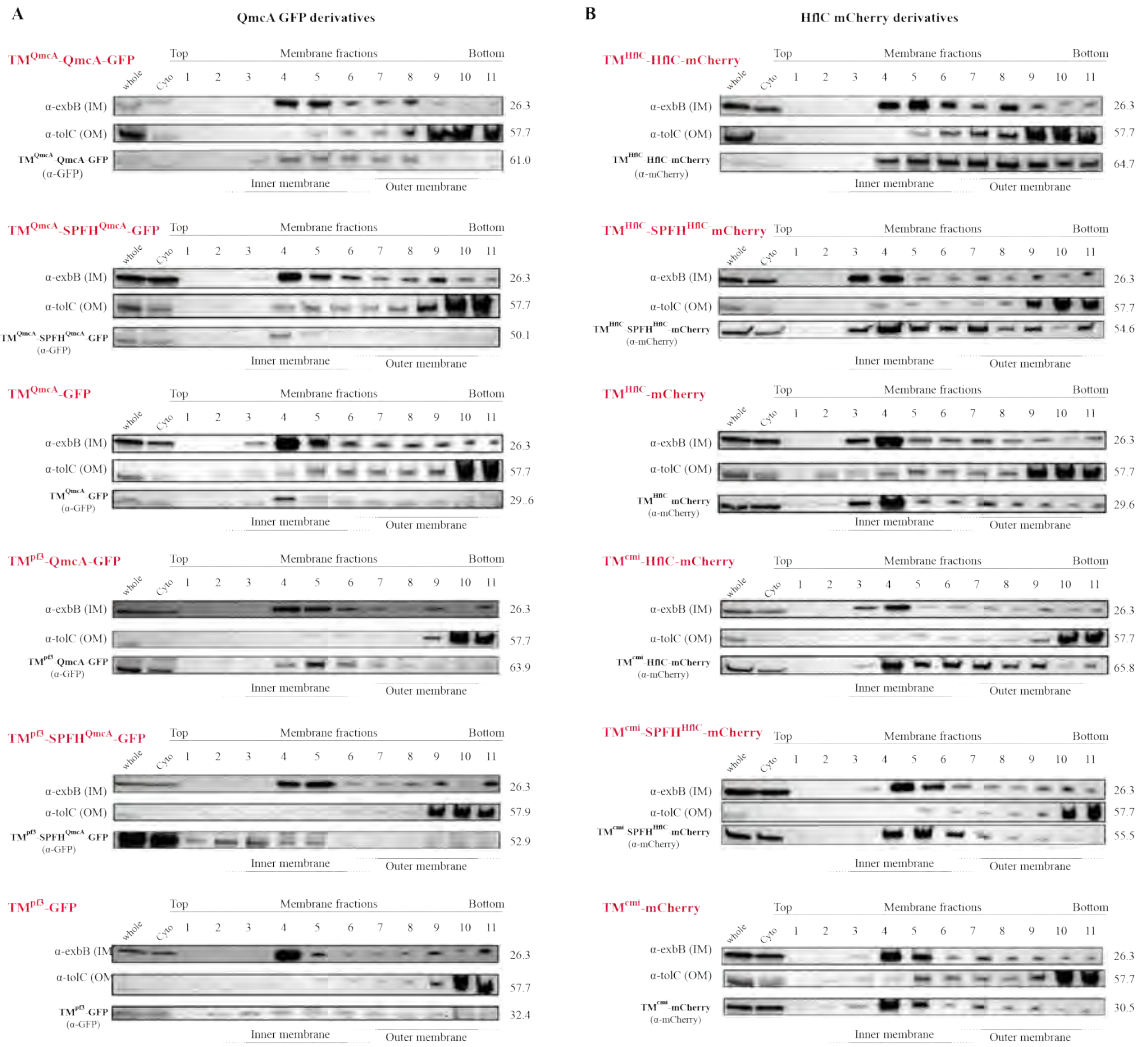

Supplementary Figure S3. Inner membrane localization of QmcA and HflC in domain swap constructs. SDS-PAGE and immunodetection analyses using proteins of whole-cell extract, cytosolic fraction, and membrane fractions prepared from cells expressing GFP fusion derivatives of QmcA (**A**) or mCherry fusion derivatives of HflC. (**B**). In immunodetection analysis, anti-ExbB antibodies were used to detect the inner membrane- (IM) marker ExbB and anti-TolC antibodies to detect the outer membrane- (OM) marker TolC. Anti-GFP and anti-mCherry antibodies were used to detect the expressions of GFP and mCherry fused proteins, respectively.

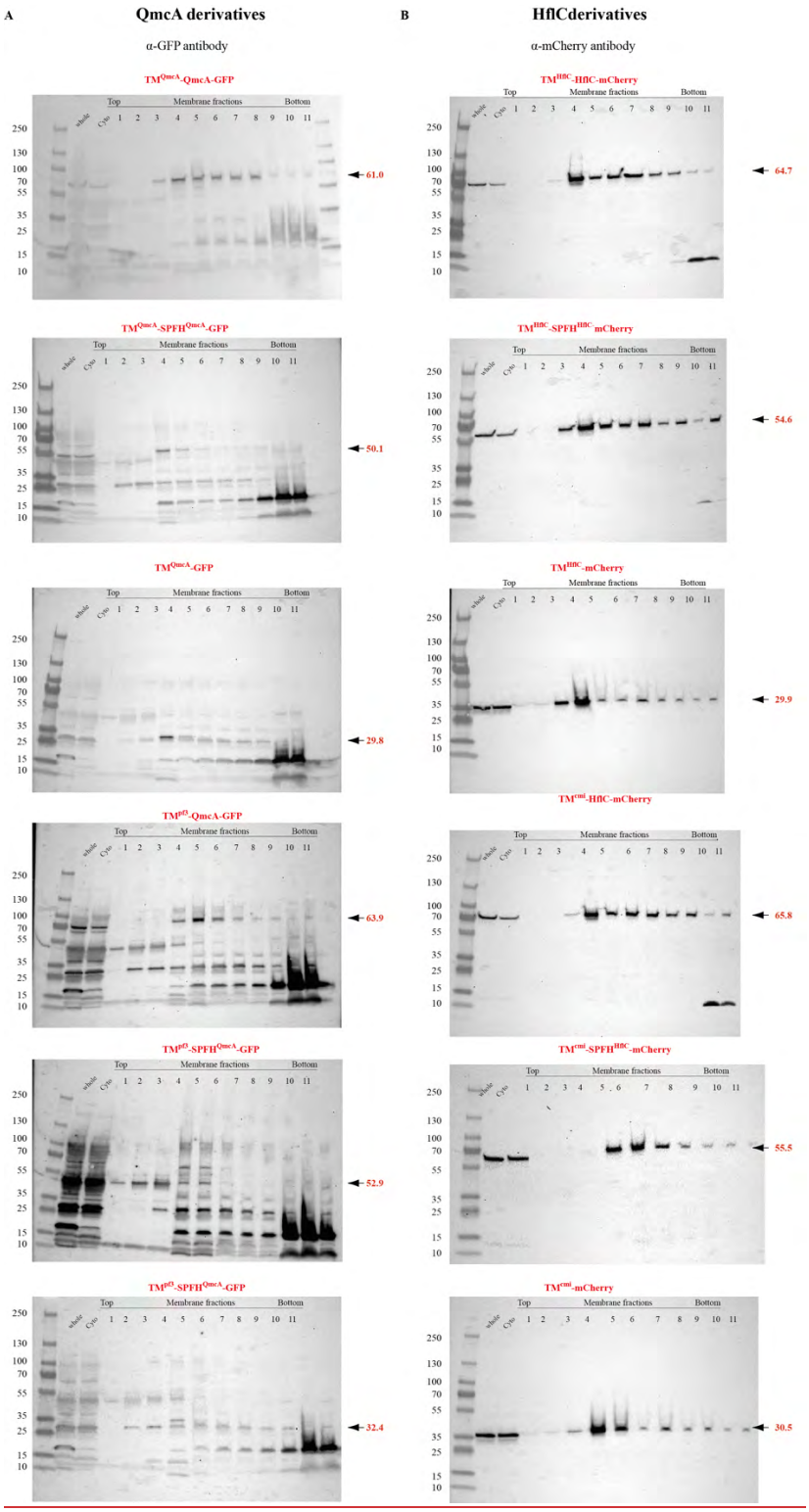

Supplementary Figure S4. Detection of QmcA and HflC fusion derivatives in domain swap constructs. A: immunodetection of GFP fusion derivatives of QmcA using anti-GFP antibody. **B:** immunodetection of mCherry fusion derivatives of HflC using anti-mCherry antibody.

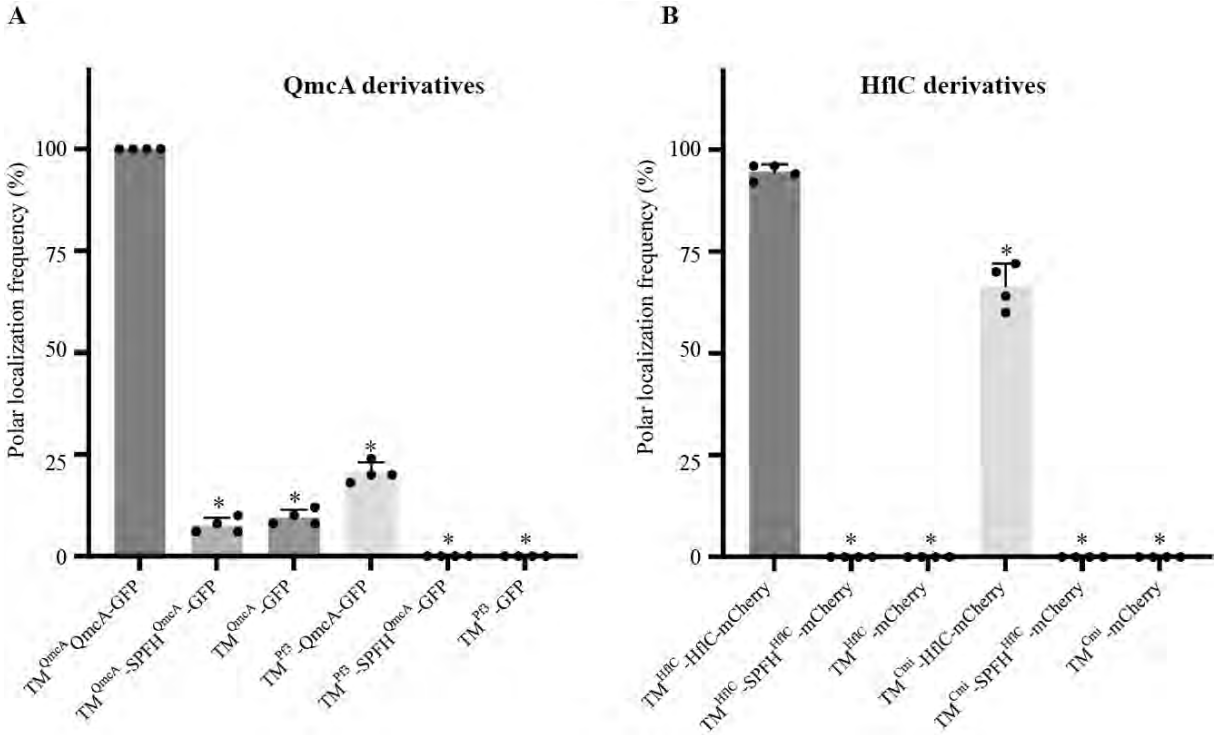

Supplementary Figure S5. Quantification data for punctate or polar localizations in QmcA and HflC derivatives,. **A:** QmcA derivatives. **B:** HflC derivatives. *$p < 0.05$ compared with TM^{QmcA}-QmcA-GFP or TM^{HflC}-HflC-mCherry.

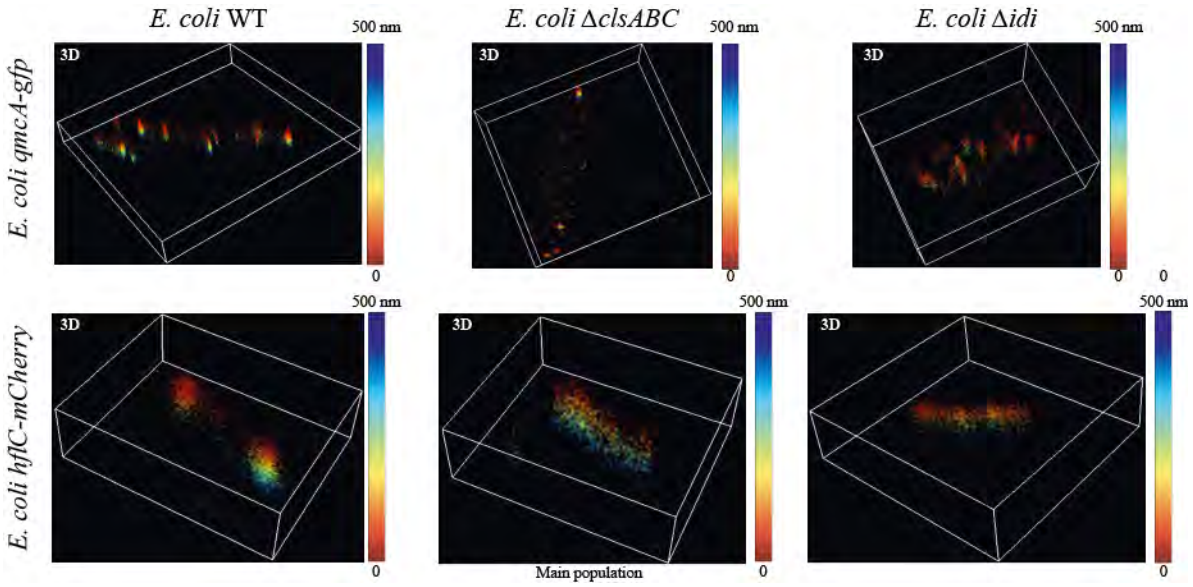

Supplementary Figure S6. The subcellular localization of QmcA and HflC in mutants with the alteration of cardiolipin or isoprenoid synthetic pathway. Three-dimensional super-resolution microscopy images of WT, Δ*clsABC*, and Δ*idi* strains expressing QmcA-GFP and HflC-mCherry in stationary phase, with colors corresponding to depth location along the Z axis, 0-500 nm, with 0 nm expressed in red, and 500 nm expressed in deep blue.

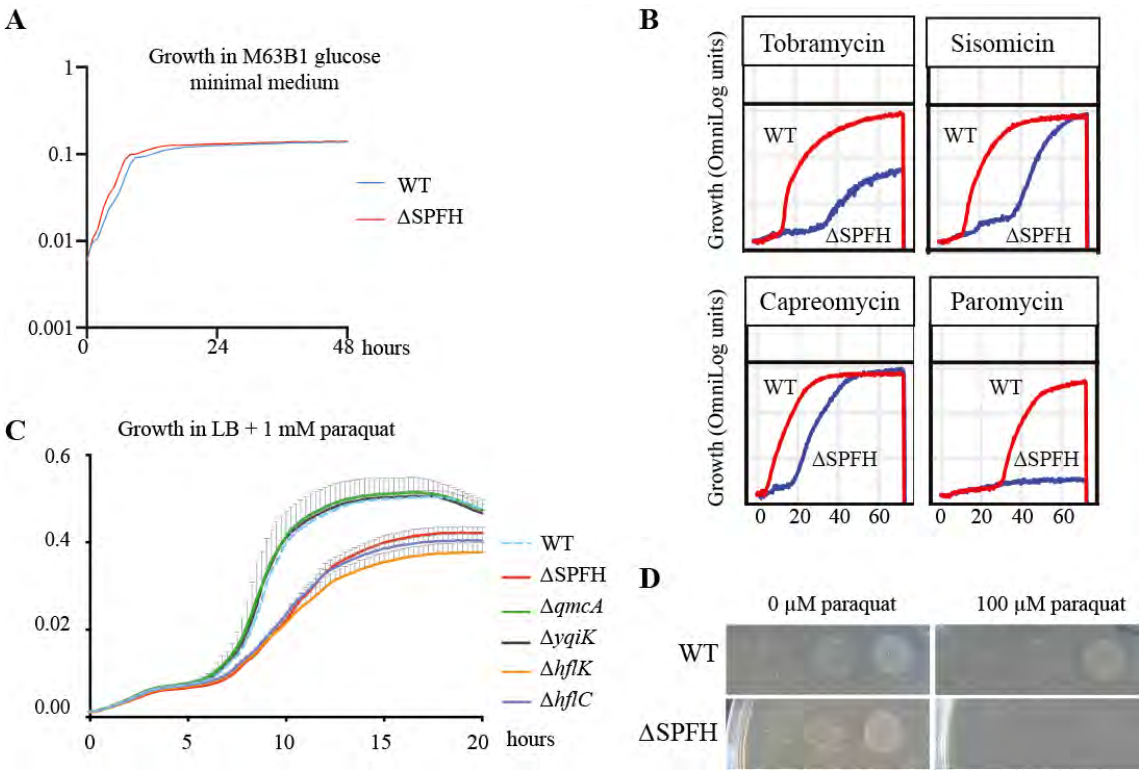

Supplementary Figure S7. Phenotypic analysis of *E. coli* SPFH mutant

(**A**) Growth curve of *E. coli* WT and ΔSPFH mutant in M63B1glucose minimal medium. (**B**) Biolog metabolic activity curve of WT and ΔSPFH in presence of tobramycin, capreomycin, sisomicin, and paromycin. (**C**) Bacterial growth curve of WT and ΔSPFH in the presence of 0.8 mM paraquat. (**D**) Paraquat susceptibility assay of WT and ΔSPFH spotted on M63B1glucose agar containing 100 μM paraquat. (**E**) Growth curve of WT and indicated SPFH gene mutants in the presence of 0.8 mM paraquat.

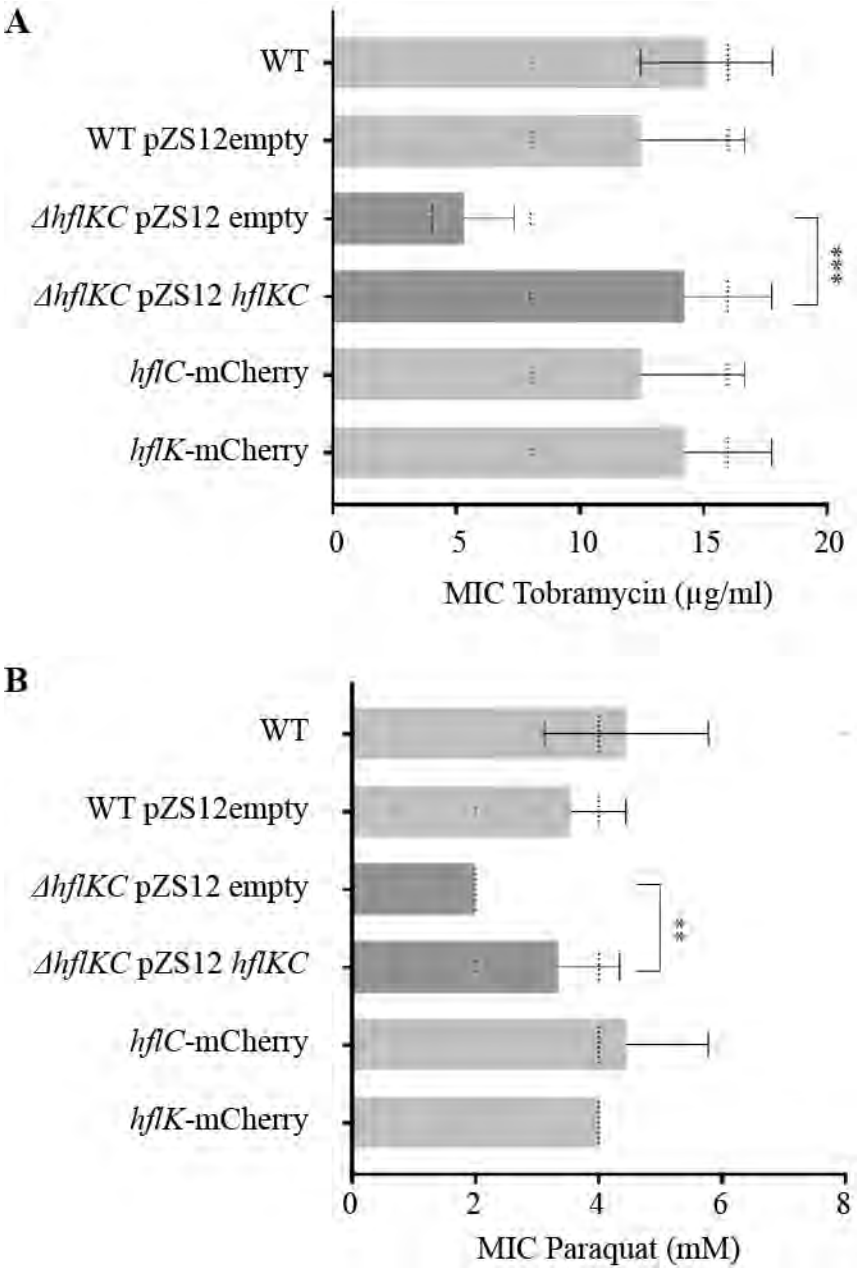

Supplementary Figure S8. Susceptibility to tobramycin and paraquat of complemented mutants. Minimum inhibitory concentrations (MICs) for tobramycin (**A**) and paraquat (**B**) of *E. coli* Wt, Δ*hflKC* strains harboring empty vector and *hflKC*- complemented strains or strain expressing *hflC or hflK-mCherry constructs* from their native chromosomal context. $^{**}p < 0.01$, $^{***}p < 0.001$.

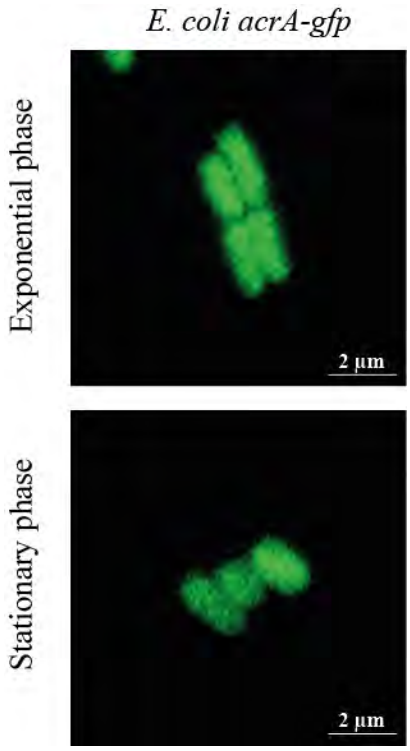

Supplementary Figure S9. Localization of AcrA-GFP fusion protein does not show polar localization pattern when expressed from native chromosomal context. Epifluorescence microscopic images of cells expressing AcrA-GFP in exponential and stationary phases.

Supplementary Table S2. Bacterial strains and plasmids used in this study

E. coli strains and plasmids	Genotype or description	Antibiotic resistance(s)	Reference
Strains			
BW25113Δ*yqiK*::Kmfrt	Keio collection	Km^R	(1)
BW25113Δ*qmcA*::Kmfrt	Keio collection	Km^R	(1)
BW25113Δ*hflK*::Kmfrt	Keio collection	Km^R	(1)
BW25113Δ*hflC*::Kmfrt	Keio collection	Km^R	(1)
BW25113Δ*clsA*::Kmfrt	Keio collection	Km^R	(1)
BW25113Δ*clsB*::Kmfrt	Keio collection	Km^R	(1)
BW25113Δ*clsC*::Kmfrt	Keio collection	Km^R	(1)
BW25113Δ*idi*::Kmfrt	Keio collection	Km^R	(1)
BW25113Δ*acrA*::Kmfrt	Keio collection	Km^R	(1)
MG1655 *strep*	Spontaneous streptomycin-resistant mutant of K-12 wild-type strain	$Strep^R$	(2)
MG1655mreB-GFP	Source of msf*gfp* gene	No resistance	Gift from Dr. Sven van Teeffelen
MG1655mreB-mCherry	Source of *mCherry* gene	No resistance	Gift from Dr. Sven van Teeffelen
MG1655Δ*cpxP*::KmFRT	Source of kanamycine resistance cassette	Km^R	(3)
MG1655ΔyfcV-P::CmFRT	Source of chloramphenicol resistance cassette	Cm^R	(4)
DH5alpir pSW25 ptetAccdB	Source of spectinomycin resistance cassette	$Spec^R$	(5)

MG1655_λATT:*amp_GFPmut3_*Δ*fimAICDFGH*::zeo Δ*yadyadNecpDhtrEyadMLKC*::*cat*	Source of zeocin resistance cassette	Zeo^R	(6)
Δ*yqiK*	P1 vir transduction from BW25113Δ*yqiK*::Kmfrt into MG1655 *strep*	$Strep^R$	This study
Δ*qmcA*	P1 vir transduction from BW25113Δ*qmcA*::Kmfrt into MG1655 *strep*	$Strep^R$	This study
Δ*hflK*	P1 vir transduction from BW25113Δ*hflK*::Kmfrt into MG1655 *strep*	$Strep^R$	This study
Δ*hflC*	P1 vir transduction from BW25113Δ*hflC*::Kmfrt into MG1655 *strep*	$Strep^R$	This study
Δ*hflKC*	Double mutant of Δ*hflK* and Δ*hflC*. MG1655*strepR*, Δ*hlfKC*::Cmfrt	$Strep^R$	This study
Δ*yqiJK*	Double mutant of Δ*yqiJ* and Δ*yqiK*. MG1655*strepR*, Δ*yqiJK*::Spec	$Strep^R$, $Spec^R$	This study
Δ*qmcA*, Δ*yqiJK*	Triple mutant of Δ*qmcA* and Δ*yqiJK*. MG1655*strepR*, Δ*qmcA,* Δ*yqiJK*::Spec	$Strep^R$, $Spec^R$	This study
Δ*SPFH*	Quintuple mutant of Δ*yqiK*, Δ*qmcA*, Δ*hflK*, and Δ*hflC*. MG1655*strepR*, Δ*qmcA*, Δ*yqiJK*::Spec, Δ*hlfKC*::Cmfrt	$Strep^R$, $Spec^R$	This study
Δ*clsA*	P1 vir transduction from BW25113Δ*clsA*::Kmfrt into MG1655 *strep*	$Strep^R$	This study
Δ*clsB*	P1 vir transduction from BW25113Δ*clsB*::Kmfrt into MG1655 *strep*	$Strep^R$	This study
Δ*clsC*	P1 vir transduction from BW25113Δ*clsC*::Kmfrt into MG1655 *strep*	$Strep^R$	This study

Δ*clsAB*	Double mutant of Δ*clsA* and Δ*clsB*. P1 vir transduction from BW25113Δ*clsA*::Kmfrt into Δ*clsB*	$Strep^R$	This study
Δ*clsABC*	Triple mutant of Δ*clsA*, Δ*clsB*, and Δ*clsC*. P1 vir transduction from BW25113Δ*clsC*::Kmfrt into Δ*clsAB*	$Strep^R$	This study
Δ*idi*	P1 vir transduction from BW25113Δ*idi*::Kmfrt into MG1655 *strep*	$Strep^R$	This study
Δ*acrA*	P1 vir transduction from BW25113Δ*acrA*::Kmfrt into MG1655 *strep*	$Strep^R$	This study
Δ*qmcA*::*zeo*	MG1655 *strep,* Δ*qmcA*::*zeo*	$Strep^R$, Zeo^R	This study
yqiK-gfp	MG1655 *strep, yqiK*::*gfp* Kmfrt	$Strep^R$, Km^R	This study
qmcA-gfp	MG1655 *strep, qmcA*::*gfp* Kmfrt	$Strep^R$, Km^R	This study
hflK-mCherry	MG1655 *strep, hflK*::*mCherry* Kmfrt	$Strep^R$, Km^R	This study
hflC-mCherry	MG1655 *strep, hflC*::*mCherry* Kmfrt	$Strep^R$, Km^R	This study
TM^{qmcA}-$SPFH^{qmcA}$-*gfp*	MG1655 *strep,* Δ*qmcA*::TM^{qmcA}-$SPFH^{qmcA}$-*gfp* Kmfrt	$Strep^R$, Km^R	This study
TM^{qmcA}-*gfp*	MG1655 *strep,* Δ*qmcA*::TM^{qmcA}-*gfp* Kmfrt	$Strep^R$, Km^R	This study
TM^{Pf3}-*qmcA-gfp*	MG1655 *strep,* Δ*qmcA*::TM^{pf3}-*qmcA-gfp* Kmfrt	$Strep^R$, Km^R	This study
TM^{Pf3}-$SPFH^{qmcA}$-*gfp*	MG1655 *strep,* Δ*qmcA*::TM^{pf3}-$SPFH^{qmcA}$-*gfp* Kmfrt	$Strep^R$, Km^R	This study
TM^{Pf3}-*gfp*	MG1655 *strep,* Δ*qmcA*::TM^{pf3}-*gfp* Kmfrt	$Strep^R$, Km^R	This study
TM^{hflC}-$SPFH^{hflC}$-*mCherry*	MG1655 *strep,* ΔhflC*::*TM^{hflC}-$SPFH^{hflC}$-*mCherry* Cmfrt	$Strep^R$, Cm^R	This study
TM^{hflC}-*mCherry*	MG1655 *strep,* ΔhflC*::*TM^{hflC}-*mCherry* Kmfrt	$Strep^R$, Km^R	This study
TM^{cmi}-*hflC-mCherry*	MG1655 *strep,* Δ*hflC*::TM^{cmi}-*hflC- mCherry* Cmfrt	$Strep^R$, Cm^R	This study
TM^{cmi}-$SPFH^{hflC}$-*mCherry*	MG1655 *strep,* Δ*hflC::*TM^{Cmi} -$SPFH^{hflC}$-*mCherry* Cmfrt	$Strep^R$, Cm^R	This study
TM^{cmi}-*mCherry*	MG1655 *strep,* Δ*hflC::*TM^{Cmi}-*mCherry* Cmfrt	$Strep^R$, Cm^R	This study

Δ*clsABC qmcA-gfp*	P1 vir transduction from *qmcA-gfp* into Δ*clsABC*	$Strep^R$, Km^R	This study
Δ*idi qmcA-gfp*	P1 vir transduction from *qmcA-gfp* into Δ*idi*	$Strep^R$, Km^R	This study
Δ*clsABC hflC-mCherry*	P1 vir transduction from *hflC-mCherry* into Δ*clsABC*	$Strep^R$, Km^R	This study
Δ*idi hflC-mCherry*	P1 vir transduction from *hflC-mCherry* into Δ*idi*	$Strep^R$, Km^R	This study
acrA-gfp	MG1655 *strep, acrA*::*gfp* Kmfrt	$Strep^R$, Km^R	This study
Plasmids			
pKOBEG	*ori*R101*ts araC* arabinose-inducible λred γβα operon	Cm^R	(7)
pKOBEGA	pKOBEG derivative	Amp^R	(7)
pCP20	Rep(Ts) Flp^+	Cm^R, Amp^R	(8)
pUC18	High-copy-number, lac promoter cloning vector, ampicillin resistant (AmpR)	Amp^R	(9)
pZS*12	Tightly regulated $P_{LtetO-1}$ Low copy-number vector ampicillin resistant (AmpR)	Amp^R	(10)
pUC18y*qiK-gfp-aphAIII*	Assembly of *YqiK-mCherry-aphAIII* into pUC18	Amp^R, Km^R	This study
pUC18TM^{QmcA}-*QmcA-gfp-aphAIII*	Assembly of TM^{QmcA}-*QmcA-gfp-aphAIII* into pUC18	Amp^R, Km^R	This study
pZS*12TM^{pf3}-*gfp*	Assembly of TM^{pf3}-*gfp* into pZS*12	Amp^R	This study
pZS*12TM^{pf3}-*gfp-aphAIII*	Assembly of *aphAIII* into PZ*12TM^{pf3}-*gfp*	Amp^R, Km^R	This study
pZS*12TM^{pf3}-*QmcA-gfp-aphAIII*	Assembly of *qmcA* into PZ*12TM^{pf3}-*gfp-aphAIII*	Amp^R, Km^R	This study
pZS*12 TM^{pf3}-$SPFH^{QmcA}$-*gfp-aphAIII*	Assembly of $SPFH^{qmcA}$ into PZ*12TM^{pf3}-*gfp-aphAIII*	Amp^R, Km^R	This study
pUC18TM^{HflC}-*HflC-mCherry-aphAIII*	Assembly of TM^{HflC}-*HflC-mCherry-aphAIII* into pUC18	Amp^R, Km^R	This study
pZS*12TM^{cmi}-*mCherry*	Assembly of *cmi-mCherry* into pZS*12	Amp^R	This study
pZS*12TM^{cmi}-*mCherry-cat*	Assembly of *Cmfrt* into PZ*12 *cmi-mCherry*	Amp^R, Cm^R	This study

pZS*12*TM*^{cmi}-*hflC-mCherry-cat*	Assembly of *hflC* into PZ*12 *cmi-mCherry-Cmfrt*	Amp^{R}, Cm^{R}	This study
pZS*12*TM*^{cmi}-*SPFH*^{HflC}-*mCherry-cat*	Assembly of *SPFH*^{HflC} into PZ*12 *cmi-mCherry-Cmfrt*	Amp^{R}, Cm^{R}	This study
pZS*12-*HflKC*	Assembly of *hflKC* into pZS*12	Amp^{R}	This study

REFERENCES

1. **Baba T, Ara T, Hasegawa M, Takai Y, Okumura Y, Baba M, Datsenko KA, Tomita M, Wanner BL, Mori H.** 2006. Construction of Escherichia coli K-12 in-frame, single-gene knockout mutants: the Keio collection. Molecular systems biology **2:**2006.0008. https://doi.org/10.1038/msb4100050

2. **Ferrières L, Hémery G, Nham T, Guérout AM, Mazel D, Beloin C, Ghigo JM.** 2010. Silent mischief: bacteriophage Mu insertions contaminate products of Escherichia coli random mutagenesis performed using suicidal transposon delivery plasmids mobilized by broad-host-range RP4 conjugative machinery. Journal of bacteriology **192:** 6418–6427. https://doi.org/10.1128/JB.00621-10

3. **Beloin C, Valle J, Latour-Lambert P, Faure P, Kzreminski M, Balestrino D, Haagensen JA, Molin S, Prensier G, Arbeille B, Ghigo JM.** 2004. Global impact of mature biofilm lifestyle on Escherichia coli K-12 gene expression. Molecular microbiology **51:**659–674. https://doi.org/10.1046/j.1365-2958.2003.03865.x

4. **Korea CG, Badouraly R, Prevost MC, Ghigo JM, Beloin C.** 2010. *Escherichia coli* K-12 possesses multiple cryptic but functional chaperone-usher fimbriae with distinct surface specificities. Environmental microbiology **12:**1957–1977. https://doi.org/10.1111/j.1462-2920.2010.02202.x

5. **Létoffé S, Audrain B, Bernier SP, Delepierre M, Ghigo JM**. 2014. Aerial exposure to the bacterial volatile compound trimethylamine modifies antibiotic resistance of physically separated bacteria by raising culture medium pH. mBio 5:e00944-00913.10.1128/mBio.00944-13: 10.1128/mBio.00944-13

6. **Larsonneur F, Martin FA, Mallet A, Martinez-Gil M, Semetey V, Ghigo JM, Beloin C.** 2016. Functional analysis of *Escherichia coli* Yad fimbriae reveals their potential role in environmental persistence. Environmental microbiology **18:**5228-5248. doi: 10.1111/1462-2920.13559. Epub 2016 Oct 24. PMID: 27696649.

7. **Chaveroche MK, Ghigo JM, d'Enfert C.** 2000. A rapid method for efficient gene replacement in the filamentous fungus Aspergillus nidulans. Nucleic acids research **28:** E97. https://doi.org/10.1093/nar/28.22.e97

8. **Cherepanov PP, Wackernagel W**. 1995. Gene disruption in Escherichia coli: TcR and KmR cassettes with the option of Flp-catalyzed excision of the antibiotic-resistance determinant. Gene **158:**9–14. https://doi.org/10.1016/0378-1119(95)00193-a

9. **Norrander J, Kempe T, Messing J.** 1983. Construction of improved M13 vectors using oligodeoxynucleotide-directed mutagenesis. Gene. 26:101-6. doi: 10.1016/0378-1119(83)90040-9.

10. **Lutz R, Bujard H.** 1997. Independent and tight regulation of transcriptional units in Escherichia coli via the LacR/O, the TetR/O and AraC/I1-I2 regulatory elements. Nucleic Acids Res **25:**1203-1210.10.1093/nar/25.6.1203: 10.1093/nar/25.6.1203

Supplementary Table S3. Primers used for generating chromosomal mutants or assembling plasmids in this study

Purpose	**Name**	**Sequence (5'-3')**
For amplifying the DNA fragment to generate Δ*hflKC* strain	Up.ΔhflKC-CmFRT-5	gacaacagggatcaccgcataacaaatatggagcacaaacgtgtaggctggagctgcttcgaag
	Down.ΔhflKC-CmFRT-3	ggatgcggtggctttattgacctgtaccgcagtcgttatacatatgaatatcctccttagttcc
For amplifying the DNA fragment to generate Δ*yqiJK* strain	Up.ΔyqiJK-Spec-5	caaagtaaatattgcgtcactaaatggacattggagtgatatgcgtcaattgcgccgaataaatac
	Down.ΔyqiJK-Spec-3	ccccggctttttgggccagggattattcctggaagagggttcattggctggcaccaagcagttt
For amplifying the DNA fragment to generate Δ*qmcA*::*zeo* strain	Up.ΔqmcA-Zeo-5	caattttgctgattatggacggtacaacaggaggtttttccgttctggatccgagcacgtgttgac
	Down.ΔqmcA-Zeo-3	gactgagccagaaaatatgtggatgaacgaccattaactccatctcagtcctgctcctcggccacg
For assembling the pUC18y*qiK-gfp-aphAIII* plasmid	Up.GFP_pUC18yqiK-gfp-5	cacccttaacctcaacaactcccgtcgaagaaaaagcagagggcggcggcggcagcatgagtaaaggtgaagaac
	Down.GFP_pUC18yqiK-gfp-3	caaaatctttctgtcgttatttgtagagttcatccatg
	Up.KmFRT_pUC18yqiK-gfp-5	cgacagaaagattttgggagcaaatgatgtgtgtaggc
	Down.KmFRT_pUC18yqiK-gfp-3	ccccggctttttgggccagggattattcctggaagagggtcagggtttactcatatgaatatc
	Up.linearized pUC18_pUC18yqiK-gfp-5	gcccaaaaagccgggggaattcgtaatcatggtcatag
	Down.linearized pUC18_pUC18yqiK-gfp-5	gttgaggttaagggtgggatcctctagagtcgacctg
For amplifying the DNA fragment to generate YqiK-GFP strain	Up.yqiK_YqiK-GFP-KmFRT-5	Same as Up.GFP_pUC18yqiK-gfp-5
	Down.KmFRT_YqiK-GFP-KmFRT-3	Same as Down.KmFRT_pUC18yqiK-gfp-3
For assembling the pUC18TM^{QmcA}-*QmcA-gfp-aphAIII* plasmid	Up.qmcA-gfp_pUC18qmcA-gfp-5	ccgagctggtgaaagacagcgccaacaaacggactcagccaggcggcggcggcagcatgagtaaaggtgaagaactgttc
	Down.qmcA-gfp_pUC18qmcA-gfp-3	ggctgagtccgtttgttggcttatttgtagagttcatccatgccgtgcgtgatacctgctg
	Up.ybbJ_pUC18qmcA-gfp-5	cagcaggtatcacgcacggcatggatgaactctacaaataagccaacaaacggactcagcc
	Down.ybbJ_pUC18qmcA-gfp-3	caaaatctttctgtcgttaagacgagacggctcggatatg
	Up.KmFRT_pUC18qmcA-gfp-5	cgacagaaagattttgggagcaaatgatgtgtgtaggc

	Down.KmFRT_pUC18qmcA-gfp-3	gaaaatctctccggctgctgtcatcatcgggcagggtgatcagggtttactcatatgaatatc
	Up.linearized pUC18_pUC18qmcA-gfp-5	cagccggagagattttcgaattcgtaatcatggtcatag
	Down.linearized pUC18_pUC18qmcA-gfp-5	ctttcaccagctcggggatcctctagagtcgacctg
For amplifying the DNA fragment to generate TM^{qmcA}-QmcA-GFP strain	Up.qmcA_QmcA-GFP-KmFRT-5	Same as Up.qmcA-gfp_pUC18qmcA-gfp-5
	Down.KmFRT_QmcA-GFP-KmFRT-3	Down.KmFRT_pUC18qmcA-gfp-3
For amplifying the DNA fragment to generate TM^{qmcA}-$SPFH^{qmcA}$-GFP strain	UP.SPFHqmcA_SPFHqmcA-GFP-KmFRT-5	gcggaagggatccgtcaggcggaaatcctcaaagccgaaggtgaatttaacaacaacatgag taaagg
	Down.KmFRT_SPFHqmcA-GFP-KmFRT-3	gaaaatctctccggctgctgtcatcatcgggcagggtgatcagggtttactcatatgaatatc
For amplifying the DNA fragment to generate TM^{qmcA}-GFP strain	Up.TMqmcA_TMqmcA-GFP-KmFRT-5	ctcatttttgtcgcgctggtcattgtcggcgcgggtgtcaaaatcgtagaatttaacaacaacatg agtaaagg
	Down.KmFRT_TMqmcA-GFP-KmFRT-3	Same sequence as Down.KmFRT_SPFHqmcA-GFP-KmFRT-3
For assembling the pZS*12TM^{pf3}-*gfp* plasmid	Up.pf3-GFP_pZS*12pf3-gfp-5	gtgagcggataacaagatacatgcaatccgtgattactg
	Down.pf3-GFP_pZS*12pf3-gfp-3	ctttactcatgttgttgttaaattcaaagaattg
	Up.GFP _pZS*12pf3-gfp-5	taacaacaacatgagtaaaggtgaagaac
	Down.GFP_pZS*12pf3-gfp-3	tctagactcagctaattaagtcatttgtagagttcatcc
	Up.linearized pZS*12 pZS*12pf3-gfp-5	ctacaaatgacttaattagctgagtctagag
	Down.linearized pZS*12pZS*12pf3-gfp-3	cggattgcatgtatcttgttatccgctc
For assembling the pZS*12TM^{pf3}-*gfp-aphAIII* plasmid	Up.KmFRT _pZS*12pf3-gfp-KmFRT-5	cgaaaggctcagtcgaacgacagaaagattttgggag
	Down.KmFRT_pZS*12pf3-gfp-KmFRT-3	cgaaaggcccagtcttcagggtttactcatatgaatatcc
	Up. linearized pZS*12_pZS*12pf3-gfp-KmFRT-5	ggatattcatatgagtaaaccctgaagactgggcctttcg
	Down. linearized pZS*12_pZS*12pf3-gfp-KmFRT-3	ctttctgtcgttcgactgagcctttcgttttatttg
For assembling the pZS*12TM^{pf3}-*qmcA-gfp-aphAIII* plasmid	Up. qmcA_pZS*12pf3-qmcA-gfp-KmFRT-5	tggatcaaagcgcaattctttatcgtaccgcagggctatc
	Down. qmcA_pZS*12pf3-qmcA-gfp-KmFRT-3	actcatgttgttgttaaattctggctgagtccgtttgttggc

	Up. linearized pZS*12_pZS*12pf3-gfp-Kmfrt-5	ggatattcatatgagtaaaccctgaagactgggcctttcg
	Down. linearized pZS*12_pZS*12pf3-gfp-Kmfrt-3	ggtacgataaagaattgcgctttgatcc
For assembling the pZS*12TM^{pf3}-$SPFH^{QmcA}$ -*gfp-aphAIII* plasmid	Up. SPFHqmcA_pZS*12pf3-SPFHqmcA-gfp-KmFRT-5	Same as Up. qmcA_pZS*12pf3-qmcA-gfp-KmFRT-5
	Down. SPFHqmcA_pZS*12pf3-SPFHqmcA-gfp-KmFRT-3	actcatgttgttgttaaattcaccttcggctttgaggatttcc
	Up. Linearised pZS*12_pZS*12pf3-SPFHqmcA-gfp-KmFRT-5	caaagccgaaggtgaatttaacaacaacatgagtaaagg
	Down. Linearised pZS*12_pZS*12pf3-SPFHqmcA-gfp-KmFRT-3	Same as Down. linearized pZS*12_pZS*12pf3-gfp-Kmfrt-3
For amplifying the DNA fragments to generate TM^{Pf3}-QmcA-GFP, TM^{Pf3}-$SPFH^{QmcA}$-GFP, and TM^{Pf3}-GFP strains	Up.Pf3_pf3-(QmcA)-GFP-KmFRT-5	caattttgctgattatggacggtacaacaggaggtttttccgatgcaatccgtgattactgatg
	Down.KmFRT_pf3-(QmcA)-GFP-KmFRT-3	Same sequence as Down.KmFRT_SPFHqmcA-GFP-KmFRT-3
For assembling the pUC18TM^{HflC}-*HflC-mCherry-aphAIII* plasmid	Up.hflC-mCherry_pUC18hflC-mCherry-KmFRT-5	gatttcttccgctacatgaagacgccgacttccgcaacgcgtggcggcggcggcagcatggtttccaagggcgaggag
	Down. hflC-mCherry_pUC18hflC-mCherry-KmFRT-3	caaaatctttctgtcgttatttgtacagctcatccatg
	Up.KmFRT_pUC18hflC-mCherry-KmFRT-5	cgacagaaagattttgggagcaaatgatgtgtgtaggc
	Down.KmFRT_pUC18hflC-mCherry-KmFRT-3	gaggatgcggtggctttattgacctgtaccgcagtcgttatatcagggtttactcatatgaatatc
	Up.linearized pUC18_ pUC18hflC-mCherry-KmFRT-5	caataaagccaccgcatcctcgaattcgtaatcatggtcatag
	Down.linearized pUC18_ pUC18hflC-mCherry-KmFRT-3	catgtagcggaagaaatcggatcctctagagtcgacctg
For amplifying the DNA fragment to generate TM^{HflC}-HflC-mCherry strain	Up.hflC_HflC-mCherry-KmFRT-5	Same as Up.hflC-mCherry_pUC18hflC-mCherry-5
	Down.KmFRT_HflC-mCherry-KmFRT-3	gaggatgcggtggctttattgacctgtaccgcagtcgttatatcagggtttactcatatgaatatc
For amplifying the DNA fragment to generate TM^{hflC}-$SPFH^{hflC}$-mCherry strain	Up.SPFHhflC_SPFHhflC-mCherry-CmFRT-5	gagcgtgaagcggtagcgcgtcgtcaccgttcacaaggtcaggaatttaacaacaacatggtttccaagg
	Down.CmFRT_SPFHhflC-mCherry-CmFRT-3	ggatgcggtggctttattgacctgtaccgcagtcgttatacatatgaatatcctccttagttcctattcc
For amplifying the DNA fragment to generate TM^{hflC}-mCherry strain	Up.TMhflC_TMhflC-mCherry-KmFRT-5	catcgtgctggtagtgctttacatgtctgtctttgtcgtcggcggcggcggcagcatg
	Down.KmFRT_TMhflC-mCherry-KmFRT-3	gaggatgcggtggctttattgacctgtaccgcagtcgttatatcagggtttactcatatgaatatc
	Up.cmi-pZS*12cmi-mcherry-5	gaaaggtaccatgaaagtgattagcatgaaatttatttttattc

For assembling the pZS*12*TM*^{cmi}*-*mCherry* plasmid	Down.cmi-pZS*12cmi-mCherry-3	tggaaaccatgttgttgttaaattcgcc
	Up.mCherry_pZS*12cmi-mCherry-5	taacaacaacatggtttccaagggcgag
	Down.mCherry_pZS*12cmi-mCherry-3	ctaattaagcttatttgtacagctcatccatgc
	Up.linearized pZS*12_pZS12cmi-mCherry-5	gtacaaataagcttaattagctgagtctagagg
	Down.linearized pZS*12_pZS12cmi-mCherry-3	tcactttcatggtacctttctcctctttaatg
For assembling the pZS*12*TM*^{cmi}*-*mCherry-cat* plasmid	Up.CmFRT_pZS*12cmi-mCherry-CmFRT-5	gctcagtcgagtgtaggctggagctgcttc
	Down. CmFRT_pZS*12cmi-mCherry-CmFRT-5	gcccagtcttcatatgaatatcctccttagttcctattcc
	Up.linearized pZS*12_ pZS*12cmi-mCherry-CmFRT-5	tattcatatgaagactgggcctttcgttttatc
	Down.linearized pZS*12_ pZS*12cmi-mCherry-CmFRT-3	cagcctacactcgactgagcctttcgttttatttg
For assembling the pZS*12*TM*^{cmi}*-*hflC-mCherry-cat* plasmid	Up.hflC_ pZS*12cmi-mCherry-CmFRT-5	agataaaggcgtcgtcaaagaaggtgagcgc
	Down.hflC_ pZS*12cmi-mCherry-CmFRT-3	tgttaaattcacgcgttgcggaagtcgg
	Up.linearized pZS*12_ pZS*12cmi-hflC-mCherry-CmFRT-5	cgcaacgcgtgaatttaacaacaacatggtttcc
	Down.linearized pZS*12_ pZS*12cmi-hflC-mCherry-CmFRT-3	ctttgacgacgcctttatcttcgctccaaaaaaac
For assembling the pZS*12*TM*^{cmi}*-*SPFH*^{HflC}*-mCherry-cat* plasmid	Up. SPFHhflC_ pZS*12cmi-SPFHhflC-mCherry-CmFRT-5	Same as Up.hflC_ pZS*12cmi-mCherry-CmFRT-5
	Down. SPFHhflC_ pZS*12cmi-SPFHhflC-mCherry-CmFRT-3	tgttaaattcctgaccttgtgaacggtg
	Up.linearized pZS*12_ pZS*12cmi-SPFHhflC-mCherry-CmFRT-5	acaaggtcaggaatttaacaacaacatggtttcc
	Down.linearized pZS*12_ pZS*12cmi-SPFHhflC-mCherry-CmFRT-5	Same as Down.linearized pZS*12_ pZS*12cmi-hflC-mCherry-CmFRT-3
For amplifying the DNA fragments to generate TM^{cmi}-HflC-mCherry, TM^{cmi}-SPFH^{HflC}-mCherry, TM^{cmi}-mCherry	Up.cmi_cmi-(HflC)-mCherry-CmFRT-5	ccaacgcgcagcgtaacgactaccagcgtcaggggaataacgatgaaagtgattagcatgaa
	Down.CmFRT_cmi-(HflC)-mCherry-CmFRT-3	ggatgcggtggctttattgacctgtaccgcagtcgttatacatatgaatatcctccttag
For amplifying the DNA fragment to generate AcrA-GFP strain	Up.acrA_AcrA-GFP-KmFRT-5	ccagcaagccgcaagcggtgctcagcctgaacagtccaagtctgaatttaacaacaacatgagtaaaggtgaagaac
	Down.KmFRT_AcrA-GFP-KmFRT-3	cgggcgatcgataaagaaattaggcatgtcttaacggctcctgtttaagtcagggtttactcatatgaatatcctcc

For assembling the pZS12**hflKC* plasmid	Up.hflKC_ pZS*12-HflKC-5	cattaaagaggagaaaggtaccatggcgtggaatcagcccggtaataacgg
	Down.hflKC_ pZS*12-HflKC -3	gatgcctctagactcagctaattaagcttttaacgcgttgcggaagtcggcg
	Up.linearized pZS*12_ pZS*12 -5	aagcttaattagctgagtctag
	Down.linearized pZS*12_ pZS*12-3	ggtacctttctcctctttaatgaattcgg

BIOLOG

Phenotype MicroArrays™

PM1 MicroPlate™ Carbon Sources

A1 Negative Control	A2 L-Arabinose	A3 N-Acetyl-D-Glucosamine	A4 D-Saccharic Acid	A5 Succinic Acid	A6 D-Galactose	A7 L-Aspartic Acid	A8 L-Proline	A9 D-Alanine	A10 D-Trehalose	A11 D-Mannose	A12 Dulcitol
B1 D-Serine	B2 D-Sorbitol	B3 Glycerol	B4 L-Fucose	B5 D-Glucuronic Acid	B6 D-Gluconic Acid	B7 D,L-α-Glycerol-Phosphate	B8 D-Xylose	B9 L-Lactic Acid	B10 Formic Acid	B11 D-Mannitol	B12 L-Glutamic Acid
C1 D-Glucose-6-Phosphate	C2 D-Galactonic Acid-γ-Lactone	C3 D,L-Malic Acid	C4 D-Ribose	C5 Tween 20	C6 L-Rhamnose	C7 D-Fructose	C8 Acetic Acid	C9 α-D-Glucose	C10 Maltose	C11 D-Melibiose	C12 Thymidine
D-1 L-Asparagine	D2 D-Aspartic Acid	D3 D-Glucosaminic Acid	D4 1,2-Propanediol	D5 Tween 40	D6 α-Keto-Glutaric Acid	D7 α-Keto-Butyric Acid	D8 α-Methyl-D-Galactoside	D9 α-D-Lactose	D10 Lactulose	D11 Sucrose	D12 Uridine
E1 L-Glutamine	E2 M-Tartaric Acid	E3 D-Glucose-1-Phosphate	E4 D-Fructose-6-Phosphate	E5 Tween 80	E6 α-Hydroxy Glutaric Acid-γ-Lactone	E7 α-Hydroxy Butyric Acid	E8 β-Methyl-D-Glucoside	E9 Adonitol	E10 Maltotriose	E11 2-Deoxy Adenosine	E12 Adenosine
F1 Glycyl-L-Aspartic Acid	F2 Citric Acid	F3 M-Inositol	F4 D-Threonine	F5 Fumaric Acid	F6 Bromo Succinic Acid	F7 Propionic Acid	F8 Mucic Acid	F9 Glycolic Acid	F10 Glyoxylic Acid	F11 D-Cellobiose	F12 Inosine
G1 Glycyl-L-Glutamic Acid	G2 Tricarballylic Acid	G3 L-Serine	G4 L-Threonine	G5 L-Alanine	G6 L-Alanyl-Glycine	G7 Acetoacetic Acid	G8 N-Acetyl-β-D-Mannosamine	G9 Mono Methyl Succinate	G10 Methyl Pyruvate	G11 D-Malic Acid	G12 L-Malic Acid
H1 Glycyl-L-Proline	H2 p-Hydroxy Phenyl Acetic Acid	H3 m-Hydroxy Phenyl Acetic Acid	H4 Tyramine	H5 D-Psicose	H6 L-Lyxose	H7 Glucuronamide	H8 Pyruvic Acid	H9 L-Galactonic Acid-γ-Lactone	H10 D-Galacturonic Acid	H11 Phenylethyl-amine	H12 2-Aminoethanol

PM2A MicroPlate™ Carbon Sources

A1 Negative Control	A2 Chondroitin Sulfate C	A3 α-Cyclodextrin	A4 β-Cyclodextrin	A5 γ-Cyclodextrin	A6 Dextrin	A7 Gelatin	A8 Glycogen	A9 Inulin	A10 Laminarin	A11 Mannan	A12 Pectin
B1 N-Acetyl-D-Galactosamine	B2 N-Acetyl-Neuraminic Acid	B3 β-D-Allose	B4 Amygdalin	B5 D-Arabinose	B6 D-Arabitol	B7 L-Arabitol	B8 Arbutin	B9 2-Deoxy-D-Ribose	B10 I-Erythritol	B11 D-Fucose	B12 3-0-β-D-Galacto-pyranosyl-D-Arabinose
C1 Gentiobiose	C2 L-Glucose	C3 Lactitol	C4 D-Melezitose	C5 Maltitol	C6 α-Methyl-D-Glucoside	C7 β-Methyl-D-Galactoside	C8 3-Methyl Glucose	C9 β-Methyl-D-Glucuronic Acid	C10 α-Methyl-D-Mannoside	C11 β-Methyl-D-Xyloside	C12 Palatinose
D1 D-Raffinose	D2 Salicin	D3 Sedoheptulosan	D4 L-Sorbose	D5 Stachyose	D6 D-Tagatose	D7 Turanose	D8 Xylitol	D9 N-Acetyl-D-Glucosaminitol	D10 γ-Amino Butyric Acid	D11 δ-Amino Valeric Acid	D12 Butyric Acid
E1 Capric Acid	E2 Caproic Acid	E3 Citraconic Acid	E4 Citramalic Acid	E5 D-Glucosamine	E6 2-Hydroxy Benzoic Acid	E7 4-Hydroxy Benzoic Acid	E8 β-Hydroxy Butyric Acid	E9 γ-Hydroxy Butyric Acid	E10 α-Keto Valeric Acid	E11 Itaconic Acid	E12 5-Keto-D-Gluconic Acid
F1 D-Lactic Acid Methyl Ester	F2 Malonic Acid	F3 Melibionic Acid	F4 Oxalic Acid	F5 Oxalomalic Acid	F6 Quinic Acid	F7 D-Ribono-1,4-Lactone	F8 Sebacic Acid	F9 Sorbic Acid	F10 Succinamic Acid	F11 D-Tartaric Acid	F12 L-Tartaric Acid
G1 Acetamide	G2 L-Alaninamide	G3 N-Acetyl-L-Glutamic Acid	G4 L-Arginine	G5 Glycine	G6 L-Histidine	G7 L-Homoserine	G8 Hydroxy-L-Proline	G9 L-Isoleucine	G10 L-Leucine	G11 L-Lysine	G12 L-Methionine
H1 L-Ornithine	H2 L-Phenylalanine	H3 L-Pyroglutamic Acid	H4 L-Valine	H5 D,L-Carnitine	H6 Sec-Butylamine	H7 D,L-Octopamine	H8 Putrescine	H9 Dihydroxy Acetone	H10 2,3-Butanediol	H11 2,3-Butanone	H12 3-Hydroxy 2-Butanone

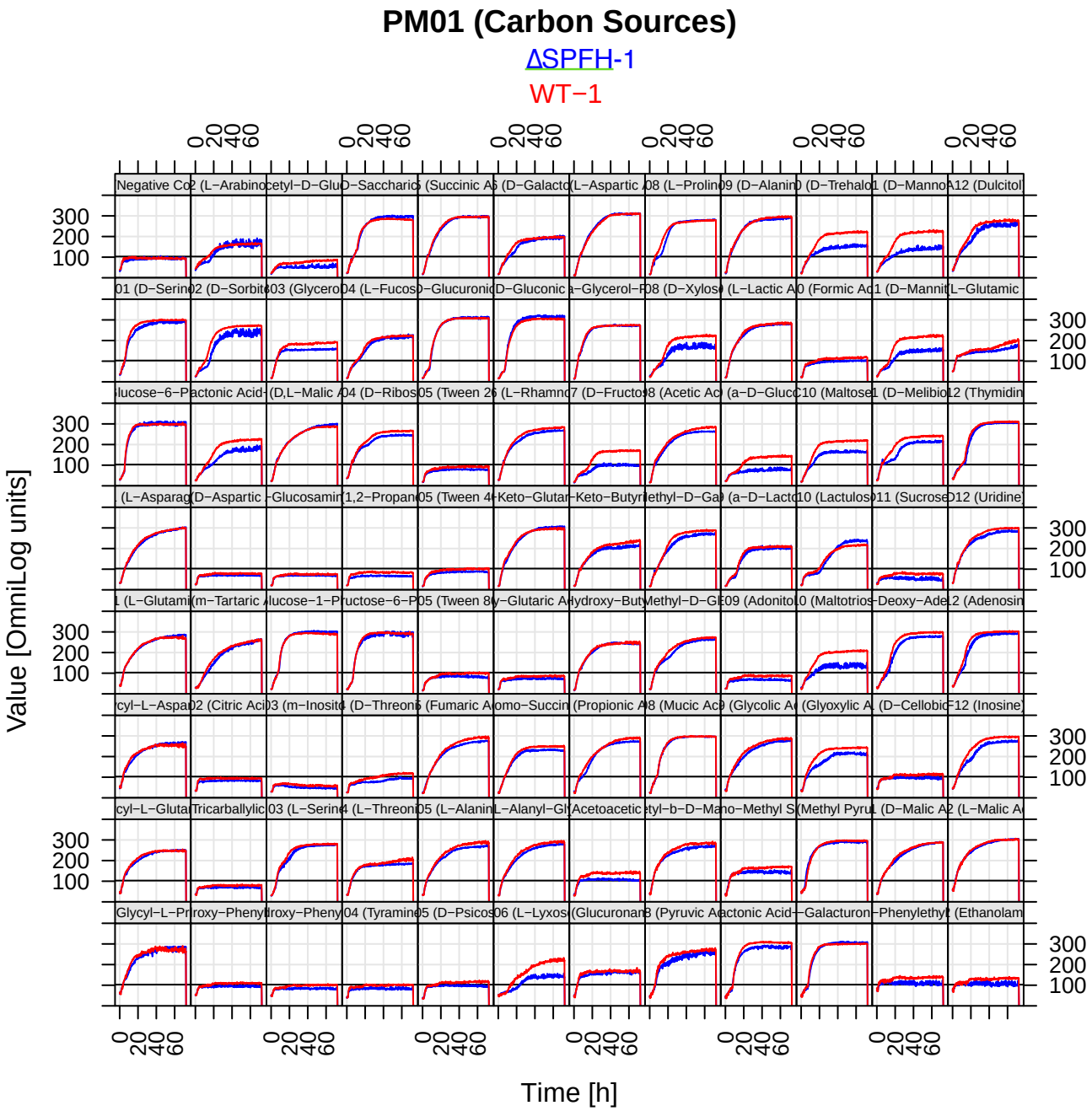
PM01 (Carbon Sources)
ΔSPFH-1
WT−1
Value [OmniLog units]
Time [h]

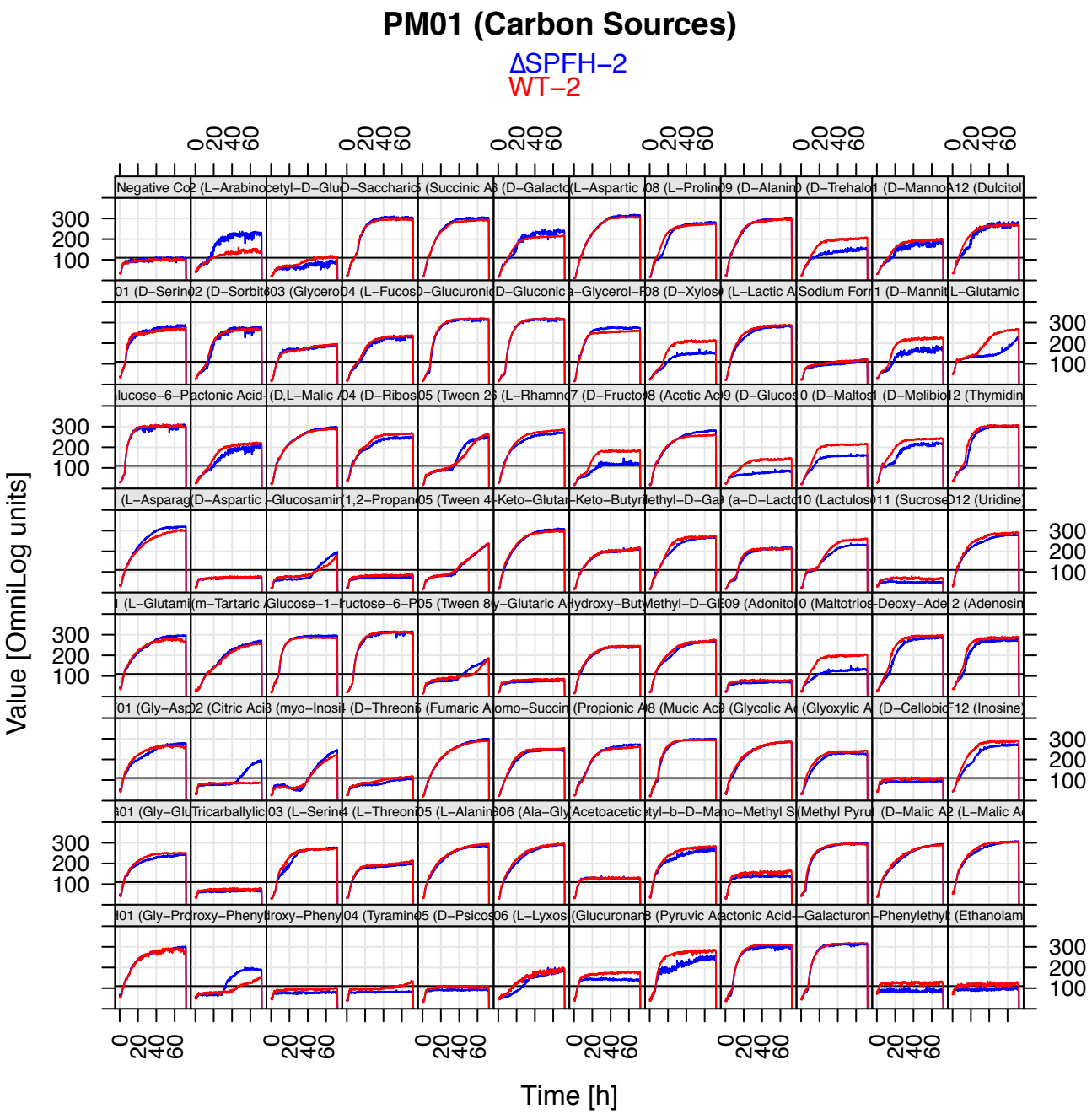
PM01 (Carbon Sources)
ΔSPFH−2
WT−2
Value [OmniLog units]
Time [h]

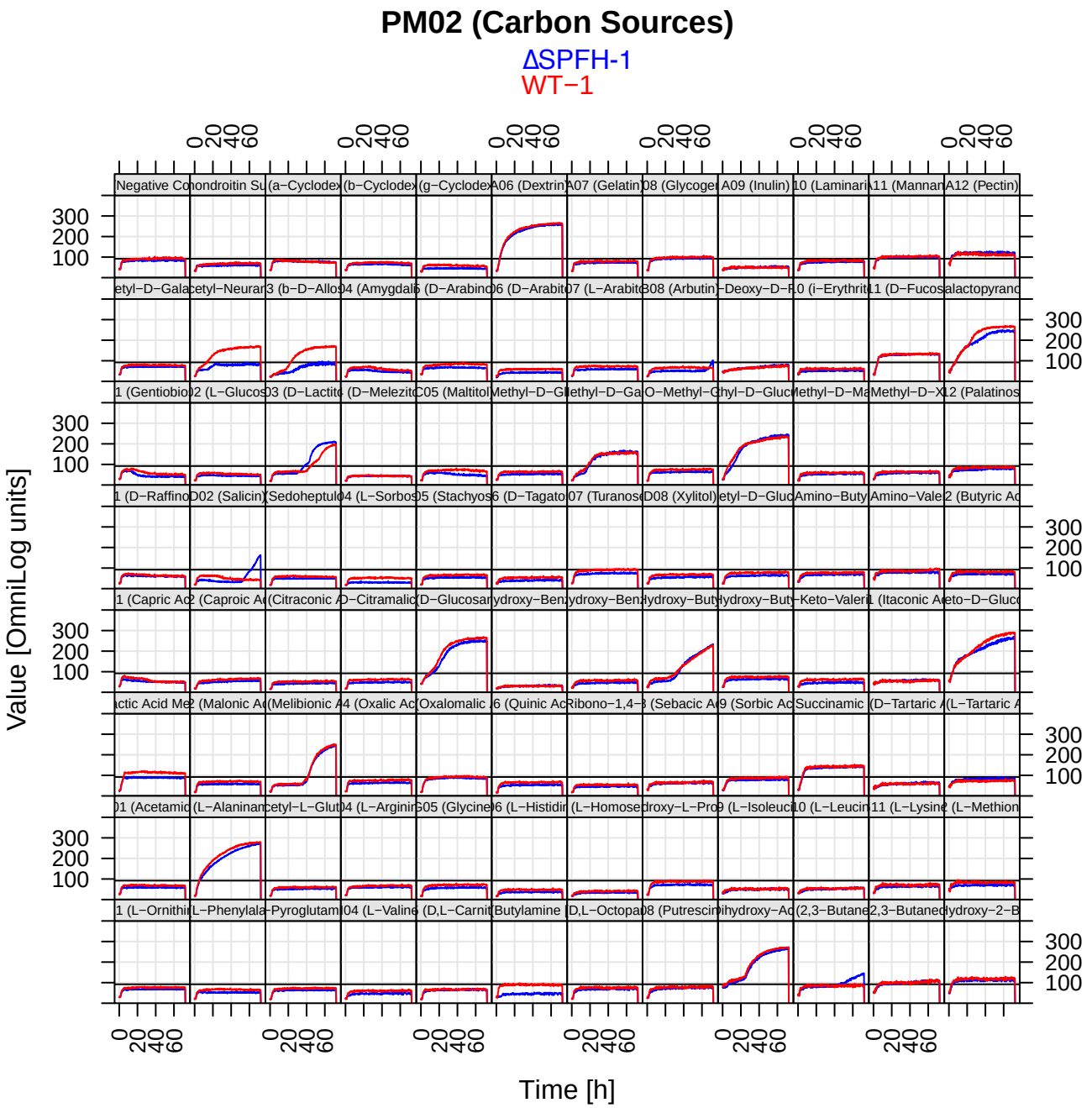
PM02 (Carbon Sources)
ΔSPFH-1
WT−1
Value [OmniLog units]
Time [h]
Negative Co
hondroitin Su
(a−Cyclodex
(b−Cyclodex
(g−Cyclodex
A06 (Dextrin)
A07 (Gelatin)
08 (Glycoger
A09 (Inulin)
10 (Laminari
11 (Mannan
A12 (Pectin)
etyl−D−Galac
etyl−Neurar
3 (b−D−Allos
04 (Amygdal
5 (D−Arabino
06 (D−Arabit
07 (L−Arabit
B08 (Arbutin
−Deoxy−D−R
10 (i−Erythrit
11 (D−Fucos
alactopyranc
1 (Gentiobio
02 (L−Glucos
03 (D−Lactito
(D−Melezito
C05 (Maltitol
Methyl−D−G
ethyl−D−Ga
O−Methyl−G
hyl−D−Gluc
ethyl−D−Ma
Methyl−D−X
12 (Palatinos
1 (D−Raffino
D02 (Salicin)
Sedoheptulo
04 (L−Sorbos
05 (Stachyos
6 (D−Tagato
07 (Turanos
D08 (Xylitol)
etyl−D−Gluc
Amino−Buty
Amino−Vale
2 (Butyric Ac
1 (Capric Ac
2 (Caproic A
(Citraconic A
D−Citramalic
(D−Glucosan
ydroxy−Ben
ydroxy−Ben
ydroxy−Buty
ydroxy−Buty
−Keto−Valeri
1 (Itaconic A
eto−D−Gluc
ctic Acid Me
2 (Malonic A
(Melibionic A
4 (Oxalic Ac
Oxalomalic
6 (Quinic Ac
Ribono−1,4−
(Sebacic A
9 (Sorbic Ac
Succinamic
(D−Tartaric A
(L−Tartaric A
01 (Acetamic
(L−Alaninan
etyl−L−Glut
04 (L−Arginin
S05 (Glycine
6 (L−Histidin
(L−Homosed
droxy−L−Pro
9 (L−Isoleuci
10 (L−Leucin
11 (L−Lysine
(L−Methion
1 (L−Ornithi
L−Phenylala
−Pyroglutam
04 (L−Valine
(D,L−Carnit
Butylamine
D,L−Octopa
08 (Putrescin
ihydroxy−Ac
(2,3−Butane
2,3−Butaned
ydroxy−2−B

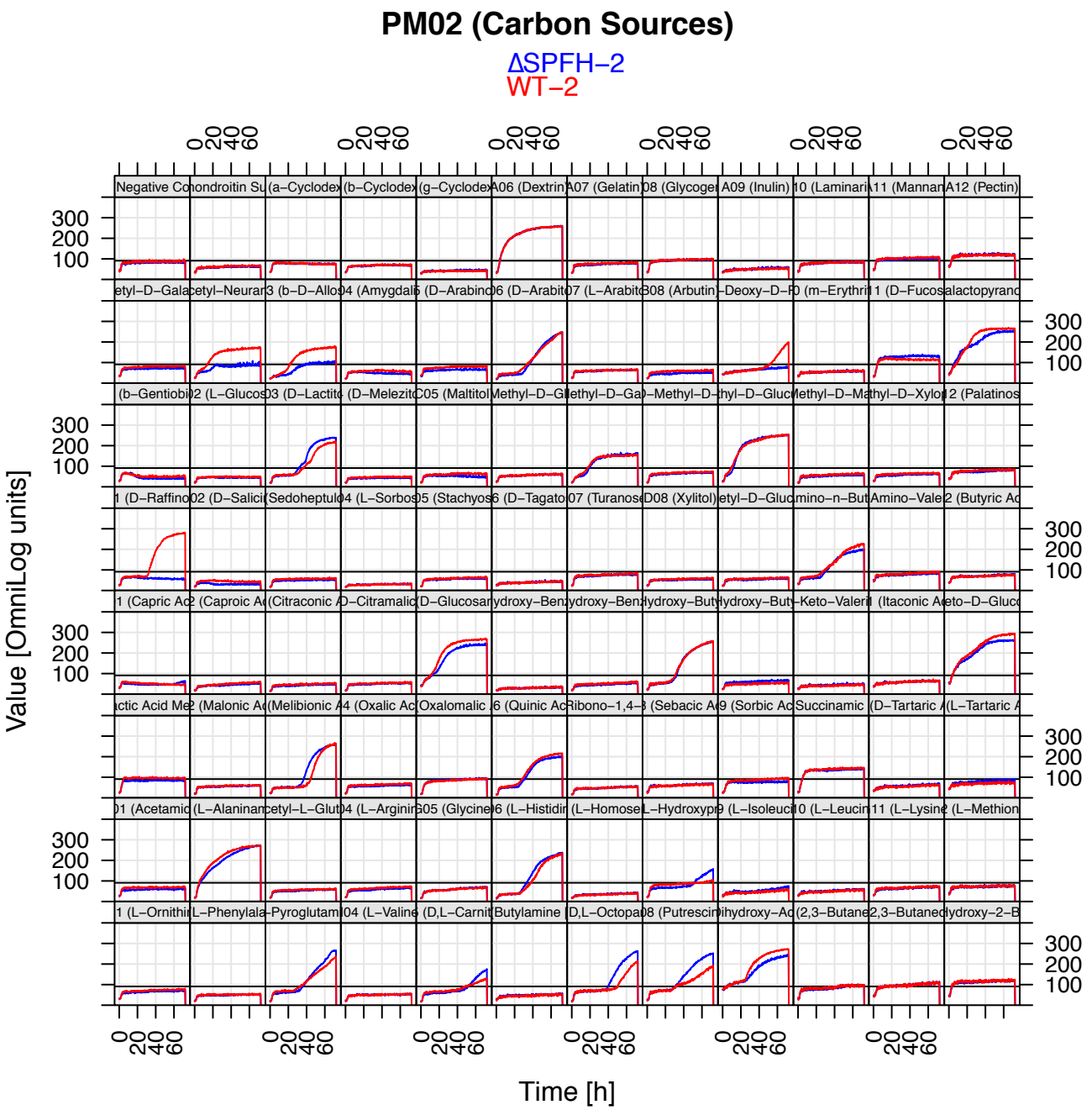
PM02 (Carbon Sources)
ΔSPFH−2
WT−2
Value [OmniLog units]
Time [h]
Negative Co
hondroitin Su
(a−Cyclodex
(b−Cyclodex
(g−Cyclodex
A06 (Dextrin)
A07 (Gelatin)
08 (Glycoger
A09 (Inulin)
10 (Laminari
11 (Mannan
A12 (Pectin)
etyl−D−Gala
cetyl−Neuran
3 (b−D−Allos
04 (Amygdal
5 (D−Arabino
06 (D−Arabit
07 (L−Arabit
B08 (Arbutin
−Deoxy−D−R
0 (m−Erythri
11 (D−Fucos
alactopyranc
(b−Gentiobi
02 (L−Glucos
03 (D−Lactito
(D−Melezito
C05 (Maltitol
Methyl−D−G
ethyl−D−Ga
−Methyl−D−
hyl−D−Gluc
ethyl−D−Ma
thyl−D−Xylo
2 (Palatinos
1 (D−Raffino
02 (D−Salici
Sedoheptulo
04 (L−Sorbos
05 (Stachyos
6 (D−Tagato
07 (Turanos
D08 (Xylitol)
etyl−D−Gluc
mino−n−But
Amino−Vale
2 (Butyric Ac
1 (Capric Ac
2 (Caproic Ac
(Citraconic A
D−Citramalic
(D−Glucosan
ydroxy−Ben
ydroxy−Ben
ydroxy−But
Hydroxy−But
−Keto−Valeri
1 (Itaconic Ac
eto−D−Gluc
ctic Acid Me
2 (Malonic Ac
(Melibionic A
4 (Oxalic Ac
Oxalomalic
6 (Quinic Ac
Ribono−1,4−
(Sebacic Ac
9 (Sorbic Ac
Succinamic
(D−Tartaric A
(L−Tartaric A
01 (Acetamic
(L−Alaninan
cetyl−L−Glut
04 (L−Arginin
G05 (Glycine
6 (L−Histidin
(L−Homose
L−Hydroxypr
9 (L−Isoleuci
10 (L−Leucin
11 (L−Lysine
(L−Methion
1 (L−Ornithin
L−Phenylala
−Pyroglutam
04 (L−Valine
(D,L−Carnit
Butylamine
D,L−Octopa
08 (Putrescin
ihydroxy−Ac
(2,3−Butane
2,3−Butaned
ydroxy−2−B

BIOLOG

Phenotype MicroArrays™

PM3B MicroPlate™ Nitrogen Sources

A1 Negative Control	A2 Ammonia	A3 Nitrite	A4 Nitrate	A5 Urea	A6 Biuret	A7 L-Alanine	A8 L-Arginine	A9 L-Asparagine	A10 L-Aspartic Acid	A11 L-Cysteine	A12 L-Glutamic Acid
B1 L-Glutamine	B2 Glycine	B3 L-Histidine	B4 L-Isoleucine	B5 L-Leucine	B6 L-Lysine	B7 L-Methionine	B8 L-Phenylalanine	B9 L-Proline	B10 L-Serine	B11 L-Threonine	B12 L-Tryptophan
C1 L-Tyrosine	C2 L-Valine	C3 D-Alanine	C4 D-Asparagine	C5 D-Aspartic Acid	C6 D-Glutamic Acid	C7 D-Lysine	C8 D-Serine	C9 D-Valine	C10 L-Citrulline	C11 L-Homoserine	C12 L-Ornithine
D-1 N-Acetyl-D,L-Glutamic Acid	D2 N-Phthaloyl-L-Glutamic Acid	D3 L-Pyroglutamic Acid	D4 Hydroxylamine	D5 Methylamine	D6 N-Amylamine	D7 N-Butylamine	D8 Ethylamine	D9 Ethanolamine	D10 Ethylenediamine	D11 Putrescine	D12 Agmatine
E1 Histamine	E2 β-Phenylethyl-amine	E3 Tyramine	E4 Acetamide	E5 Formamide	E6 Glucuronamide	E7 D,L-Lactamide	E8 D-Glucosamine	E9 D-Galactosamine	E10 D-Mannosamine	E11 N-Acetyl-D-Glucosamine	E12 N-Acetyl-D-Galactosamine
F1 N-Acetyl-D-Mannosamine	F2 Adenine	F3 Adenosine	F4 Cytidine	F5 Cytosine	F6 Guanine	F7 Guanosine	F8 Thymine	F9 Thymidine	F10 Uracil	F11 Uridine	F12 Inosine
G1 Xanthine	G2 Xanthosine	G3 Uric Acid	G4 Alloxan	G5 Allantoin	G6 Parabanic Acid	G7 D,L-α-Amino-N-Butyric Acid	G8 γ-Amino-N-Butyric Acid	G9 ε-Amino-N-Caproic Acid	G10 D,L-α-Amino-Caprylic Acid	G11 δ-Amino-N-Valeric Acid	G12 α-Amino-N-Valeric Acid
H1 Ala-Asp	H2 Ala-Gln	H3 Ala-Glu	H4 Ala-Gly	H5 Ala-His	H6 Ala-Leu	H7 Ala-Thr	H8 Gly-Asn	H9 Gly-Gln	H10 Gly-Glu	H11 Gly-Met	H12 Met-Ala

PM4A MicroPlate™ Phosphorus and Sulfur Sources

A1 Negative Control	A2 Phosphate	A3 Pyrophosphate	A4 Trimeta-phosphate	A5 Tripoly-phosphate	A6 Triethyl Phosphate	A7 Hypophosphite	A8 Adenosine- 2'-monophosphate	A9 Adenosine- 3'-monophosphate	A10 Adenosine- 5'-monophosphate	A11 Adenosine- 2',3'-cyclic monophosphate	A12 Adenosine- 3',5'-cyclic monophosphate
B1 Thiophosphate	B2 Dithiophosphate	B3 D,L-α-Glycerol Phosphate	B4 β-Glycerol Phosphate	B5 Carbamyl Phosphate	B6 D-2-Phospho-Glyceric Acid	B7 D-3-Phospho-Glyceric Acid	B8 Guanosine- 2'-monophosphate	B9 Guanosine- 3'-monophosphate	B10 Guanosine- 5'-monophosphate	B11 Guanosine- 2',3'-cyclic monophosphate	B12 Guanosine- 3',5'-cyclic monophosphate
C1 Phosphoenol Pyruvate	C2 Phospho-Glycolic Acid	C3 D-Glucose-1-Phosphate	C4 D-Glucose-6-Phosphate	C5 2-Deoxy-D-Glucose 6-Phosphate	C6 D-Glucosamine-6-Phosphate	C7 6-Phospho-Gluconic Acid	C8 Cytidine- 2'-monophosphate	C9 Cytidine- 3'-monophosphate	C10 Cytidine- 5'-monophosphate	C11 Cytidine- 2',3'-cyclic monophosphate	C12 Cytidine- 3',5'-cyclic monophosphate
D1 D-Mannose-1-Phosphate	D2 D-Mannose-6-Phosphate	D3 Cysteamine-S-Phosphate	D4 Phospho-L-Arginine	D5 O-Phospho-D-Serine	D6 O-Phospho-L-Serine	D7 O-Phospho-L-Threonine	D8 Uridine- 2'-monophosphate	D9 Uridine- 3'-monophosphate	D10 Uridine- 5'-monophosphate	D11 Uridine- 2',3'-cyclic monophosphate	D12 Uridine- 3',5'-cyclic monophosphate
E1 O-Phospho-D-Tyrosine	E2 O-Phospho-L-Tyrosine	E3 Phosphocreatine	E4 Phosphoryl Choline	E5 O-Phosphoryl-Ethanolamine	E6 Phosphono Acetic Acid	E7 2-Aminoethyl Phosphonic Acid	E8 Methylene Diphosphonic Acid	E9 Thymidine- 3'-monophosphate	E10 Thymidine- 5'-monophosphate	E11 Inositol Hexaphosphate	E12 Thymidine 3',5'- cyclic monophosphate
F1 Negative Control	F2 Sulfate	F3 Thiosulfate	F4 Tetrathionate	F5 Thiophosphate	F6 Dithiophosphate	F7 L-Cysteine	F8 D-Cysteine	F9 L-Cysteinyl-Glycine	F10 L-Cysteic Acid	F11 Cysteamine	F12 L-Cysteine Sulfinic Acid
G1 N-Acetyl-L-Cysteine	G2 S-Methyl-L-Cysteine	G3 Cystathionine	G4 Lanthionine	G5 Glutathione	G6 D,L-Ethionine	G7 L-Methionine	G8 D-Methionine	G9 Glycyl-L-Methionine	G10 N-Acetyl-D,L-Methionine	G11 L- Methionine Sulfoxide	G12 L-Methionine Sulfone
H1 L-Djenkolic Acid	H2 Thiourea	H3 1-Thio-β-D-Glucose	H4 D,L-Lipoamide	H5 Taurocholic Acid	H6 Taurine	H7 Hypotaurine	H8 p-Amino Benzene Sulfonic Acid	H9 Butane Sulfonic Acid	H10 2-Hydroxyethane Sulfonic Acid	H11 Methane Sulfonic Acid	H12 Tetramethylene Sulfone

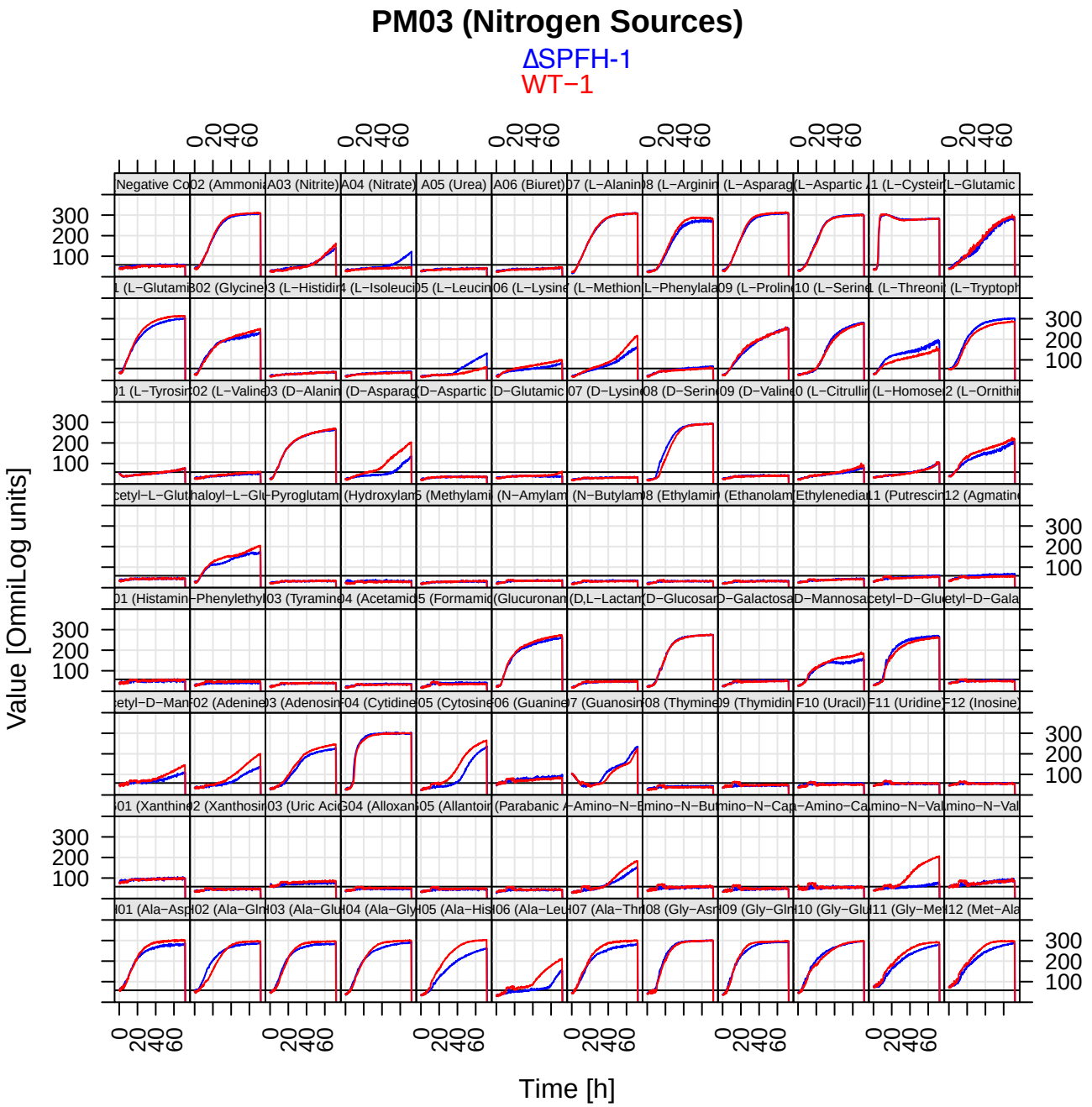
PM03 (Nitrogen Sources)
ΔSPFH-1
WT−1
Value [OmniLog units]
Time [h]
Negative Co
A02 (Ammonia)
A03 (Nitrite)
A04 (Nitrate)
A05 (Urea)
A06 (Biuret)
A07 (L−Alanin
A08 (L−Arginin
(L−Asparag
(L−Aspartic
A11 (L−Cystein
L−Glutamic
(L−Glutami
B02 (Glycine)
B03 (L−Histidin
B04 (L−Isoleuci
B05 (L−Leucin
B06 (L−Lysine
(L−Methion
L−Phenylala
B09 (L−Prolin
B10 (L−Serine
B11 (L−Threoni
(L−Tryptoph
01 (L−Tyrosin
02 (L−Valine)
03 (D−Alanin
(D−Asparag
(D−Aspartic
D−Glutamic
C07 (D−Lysin
C08 (D−Serin
C09 (D−Valine
C10 (L−Citrullin
(L−Homose
C12 (L−Ornithi
cetyl−L−Glut
haloyl−L−Glu
Pyroglutam
(Hydroxylan
D05 (Methylami
(N−Amylam
(N−Butylam
D08 (Ethylamin
(Ethanolam
Ethylenedia
D11 (Putrescin
D12 (Agmatin
01 (Histamin
−Phenylethyl
03 (Tyramine
04 (Acetamid
05 (Formamid
(Glucuronam
(D,L−Lactam
(D−Glucosar
D−Galactosa
D−Mannosa
cetyl−D−Glu
etyl−D−Gala
cetyl−D−Man
02 (Adenine)
03 (Adenosin
04 (Cytidine
05 (Cytosine
06 (Guanine)
07 (Guanosin
08 (Thymine)
09 (Thymidin
F10 (Uracil)
F11 (Uridine)
F12 (Inosine)
01 (Xanthine
02 (Xanthosin
03 (Uric Acid
G04 (Alloxan
05 (Allantoin
(Parabanic A
−Amino−N−E
mino−N−Bu
mino−N−Cap
−Amino−Ca
mino−N−Val
mino−N−Val
01 (Ala−Asp
02 (Ala−Gln
03 (Ala−Glu
04 (Ala−Gly
05 (Ala−His
06 (Ala−Leu
07 (Ala−Thr
08 (Gly−Asn
09 (Gly−Gln
10 (Gly−Glu
11 (Gly−Met
12 (Met−Ala
0
20
40
60
100
200
300

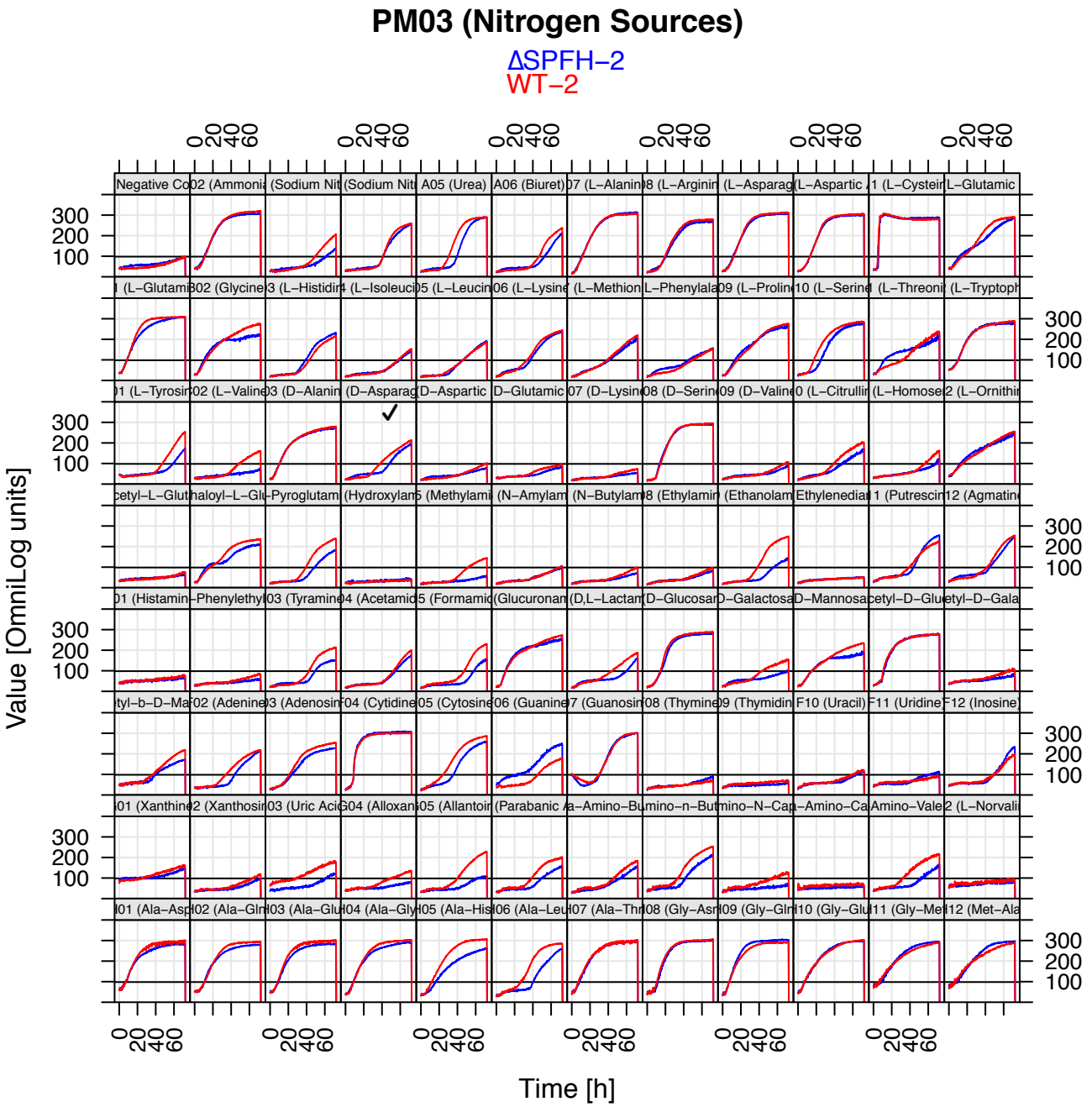
PM03 (Nitrogen Sources)
ΔSPFH−2
WT−2
Value [OmniLog units]
Time [h]
Negative Co
A05 (Urea)
A06 (Biuret)
L−Glutamic
(D−Asparag
Pyroglutam
Phenylethyl
Adenine
Adenosin
Cytidine
Cytosine
Guanine
Guanosin
Thymine
Thymidin
F10 (Uracil)
F11 (Uridine)
F12 (Inosine)
Xanthine
Xanthosin
Uric Acid
Alloxan
Allantoin
Ala−Asp
Ala−Gln
Ala−Glu
Ala−Gly
Ala−His
Ala−Leu
Ala−Thr
Gly−Asn
Gly−Gln
Gly−Glu
Gly−Met
Met−Ala

BIOLOG

Phenotype MicroArrays™

PM9 MicroPlate™ Osmolytes

A1 NaCl 1%	A2 NaCl 2%	A3 NaCl 3%	A4 NaCl 4%	A5 NaCl 5%	A6 NaCl 5.5%	A7 NaCl 6%	A8 NaCl 6.5%	A9 NaCl 7%	A10 NaCl 8%	A11 NaCl 9%	A12 NaCl 10%
B1 NaCl 6%	B2 NaCl 6% + Betaine	B3 NaCl 6% + N-N Dimethyl glycine	B4 NaCl 6% + Sarcosine	B5 NaCl 6% + Dimethyl sulphonyl propionate	B6 NaCl 6% + MOPS	B7 NaCl 6% + Ectoine	B8 NaCl 6% + Choline	B9 NaCl 6% + Phosphoryl choline	B10 NaCl 6% + Creatine	B11 NaCl 6% + Creatinine	B12 NaCl 6% + L- Carnitine
C1 NaCl 6% + KCl	C2 NaCl 6% + L-proline	C3 NaCl 6% + N-Acethyl L-glutamine	C4 NaC1 6% + β-Glutamic acid	C5 NaC1 6% + γ–Amino -n-butyric acid	C6 NaC1 6% + Glutathione	C7 NaCl 6% + Glycerol	C8 NaC1 6% + Trehalose	C9 NaC1 6% + Trimethylamine -N-oxide	C10 NaC1 6% + Trimethylamine	C11 NaCl 6% + Octopine	C12 NaC1 6% + Trigonelline
D-1 Potassium chloride 3%	D2 Potassium chloride 4%	D3 Potassium chloride 5%	D4 Potassium chloride 6%	D5 Sodium sulfate 2%	D6 Sodium sulfate 3%	D7 Sodium sulfate 4%	D8 Sodium sulfate 5%	D9 Ethylene glycol 5%	D10 Ethylene glycol 10%	D11 Ethylene glycol 15%	D12 Ethylene glycol 20%
E1 Sodium formate 1%	E2 Sodium formate 2%	E3 Sodium formate 3%	E4 Sodium formate 4%	E5 Sodium formate 5%	E6 Sodium formate 6%	E7 Urea 2%	E8 Urea 3%	E9 Urea 4%	E10 Urea 5%	E11 Urea 6%	E12 Urea 7%
F1 Sodium Lactate 1%	F2 Sodium Lactate 2%	F3 Sodium Lactate 3%	F4 Sodium Lactate 4%	F5 Sodium Lactate 5%	F6 Sodium Lactate 6%	F7 Sodium Lactate 7%	F8 Sodium Lactate 8%	F9 Sodium Lactate 9%	F10 Sodium Lactate 10%	F11 Sodium Lactate 11%	F12 Sodium Lactate 12%
G1 Sodium Phosphate pH 7 20mM	G2 Sodium Phosphate pH 7 50mM	G3 Sodium Phosphate pH 7 100mM	G4 Sodium Phosphate pH 7 200mM	G5 Sodium Benzoate pH 5.2 20mM	G6 Sodium Benzoate pH 5.2 50mM	G7 Sodium Benzoate pH5.2 100mM	G8 Sodium Benzoate pH 5.2 200mM	G9 Ammonium sulfate pH8 10mM	G10 Ammonium sulfate pH 8 20mM	G11 Ammonium sulfate pH 8 50mM	G12 Ammonium sulfate pH8 100mM
H1 Sodium Nitrate 10mM	H2 Sodium Nitrate 20mM	H3 Sodium Nitrate 40mM	H4 Sodium Nitrate 60mM	H5 Sodium Nitrate 80mM	H6 Sodium Nitrate 100mM	H7 Sodium Nitrite 10mM	H8 Sodium Nitrite 20mM	H9 Sodium Nitrite 40mM	H10 Sodium Nitrite 60mM	H11 Sodium Nitrite 80mM	H12 Sodium Nitrite 100mM

PM10 MicroPlate™ pH

A1 pH 3.5	A2 pH 4	A3 pH 4.5	A4 pH 5	A5 pH 5.5	A6 pH 6	A7 pH 7	A8 pH 8	A9 pH 8.5	A10 pH 9	A11 pH 9.5	A12 pH 10
B1 pH 4.5	B2 pH 4.5 + L-Alanine	B3 pH 4.5 + L-Arginine	B4 pH 4.5 + L-Asparagine	B5 pH 4.5 + L-Aspartic Acid	B6 pH 4.5 + L-Glutamic Acid	B7 pH 4.5 + L-Glutamine	B8 pH 4.5 + Glycine	B9 pH 4.5 + L-Histidine	B10 pH 4.5 + L-Isoleucine	B11 pH 4.5 + L-Leucine	B12 pH 4.5 + L-Lysine
C1 pH 4.5 + L-Methionine	C2 pH 4.5 + L-Phenylalanine	C3 pH 4.5 + L-Proline	C4 pH 4.5 + L-Serine	C5 pH 4.5 + L-Threonine	C6 pH 4.5 + L-Tryptophan	C7 pH 4.5 + L-Tyrosine	C8 pH 4.5 + L-Valine	C9 pH 4.5 + Hydroxy-L-Proline	C10 pH 4.5 + L-Ornithine	C11 pH 4.5 + L-Homoarginine	C12 pH 4.5 + L-Homoserine
D-1 pH 4.5 + Anthranilic acid	D2 pH 4.5 + L-Norleucine	D3 pH 4.5 + L-Norvaline	D4 pH 4.5 + α- Amino-N-butyric acid	D5 pH 4.5 + p-Aminobenzoate	D6 pH 4.5 + L-Cysteic acid	D7 pH 4.5 + D-Lysine	D8 pH 4.5 + 5-Hydroxy Lysine	D9 pH 4.5 + 5-Hydroxy Tryptophan	D10 pH 4.5 + D,L-Diamino pimelic acid	D11 pH 4.5 + Trimethyl amine-N-oxide	D12 pH 4.5 + Urea
E1 pH 9.5	E2 pH 9.5 + L-Alanine	E3 pH 9.5 + L-Arginine	E4 pH 9.5 + L-Asparagine	E5 pH 9.5 + L-Aspartic Acid	E6 pH 9.5 + L-Glutamic Acid	E7 pH 9.5 + L-Glutamine	E8 pH 9.5 + Glycine	E9 pH 9.5 + L-Histidine	E10 pH 9.5 + L-Isoleucine	E11 pH 9.5 + L-Leucine	E12 pH 9.5 + L-Lysine
F1 pH 9.5 + L-Methionine	F2 pH 9.5 + L-Phenylalanine	F3 pH 9.5 + L-Proline	F4 pH 9.5 + L-Serine	F5 pH 9.5 + L-Threonine	F6 pH 9.5 + L-Tryptophan	F7 pH 9.5 + L-Tyrosine	F8 pH 9.5 + L-Valine	F9 pH 9.5 + Hydroxy-L-Proline	F10 pH 9.5 + L-Ornithine	F11 pH 9.5 + L-Homoarginine	F12 pH 9.5 + L-Homoserine
G1 pH 9.5 + Anthranilic acid	G2 pH 9.5 + L-Norleucine	G3 pH 9.5 + L-Norvaline	G4 pH 9.5 + Agmatine	G5 pH 9.5 + Cadaverine	G6 pH 9.5 + Putrescine	G7 pH 9.5 + Histamine	G8 pH 9.5 + Phenylethylamine	G9 pH 9.5 + Tyramine	G10 pH 9.5 + Creatine	G11 pH 9.5 + Trimethyl amine-N-oxide	G12 pH 9.5 + Urea
H1 X-Caprylate	H2 X–α-D-Glucoside	H3 X-β-D-Glucoside	H4 X-α-D-Galactoside	H5 X-β-D-Galactoside	H6 X-α- D-Glucuronide	H7 X-β- D-Glucuronide	H8 X-β-D-Glucosaminide	H9 X-β-D-Galactosaminide	H10 X-α-D-Mannoside	H11 X-PO4	H12 X-SO4

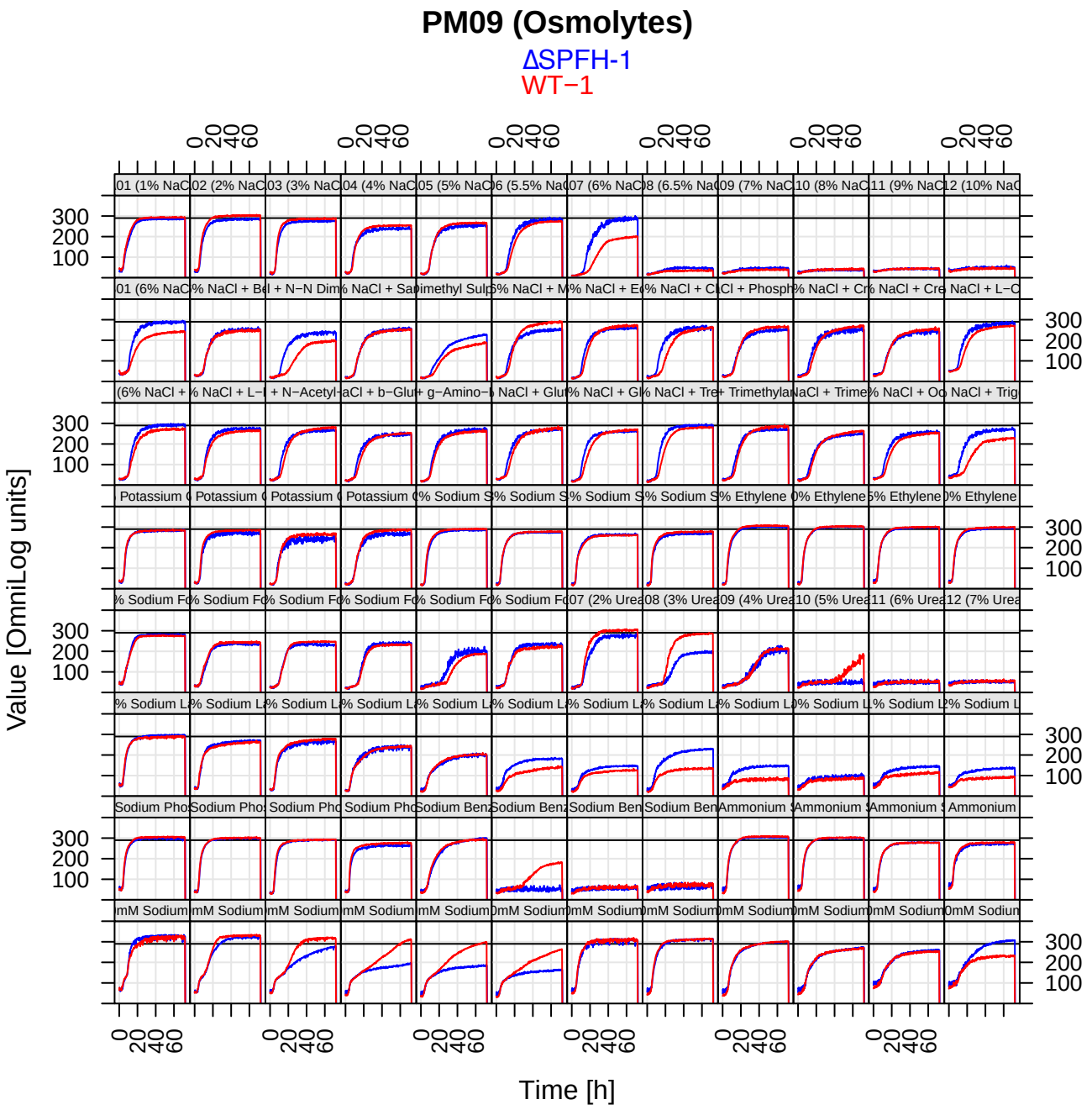
PM09 (Osmolytes)
ΔSPFH-1
WT−1
Value [OmniLog units]
Time [h]

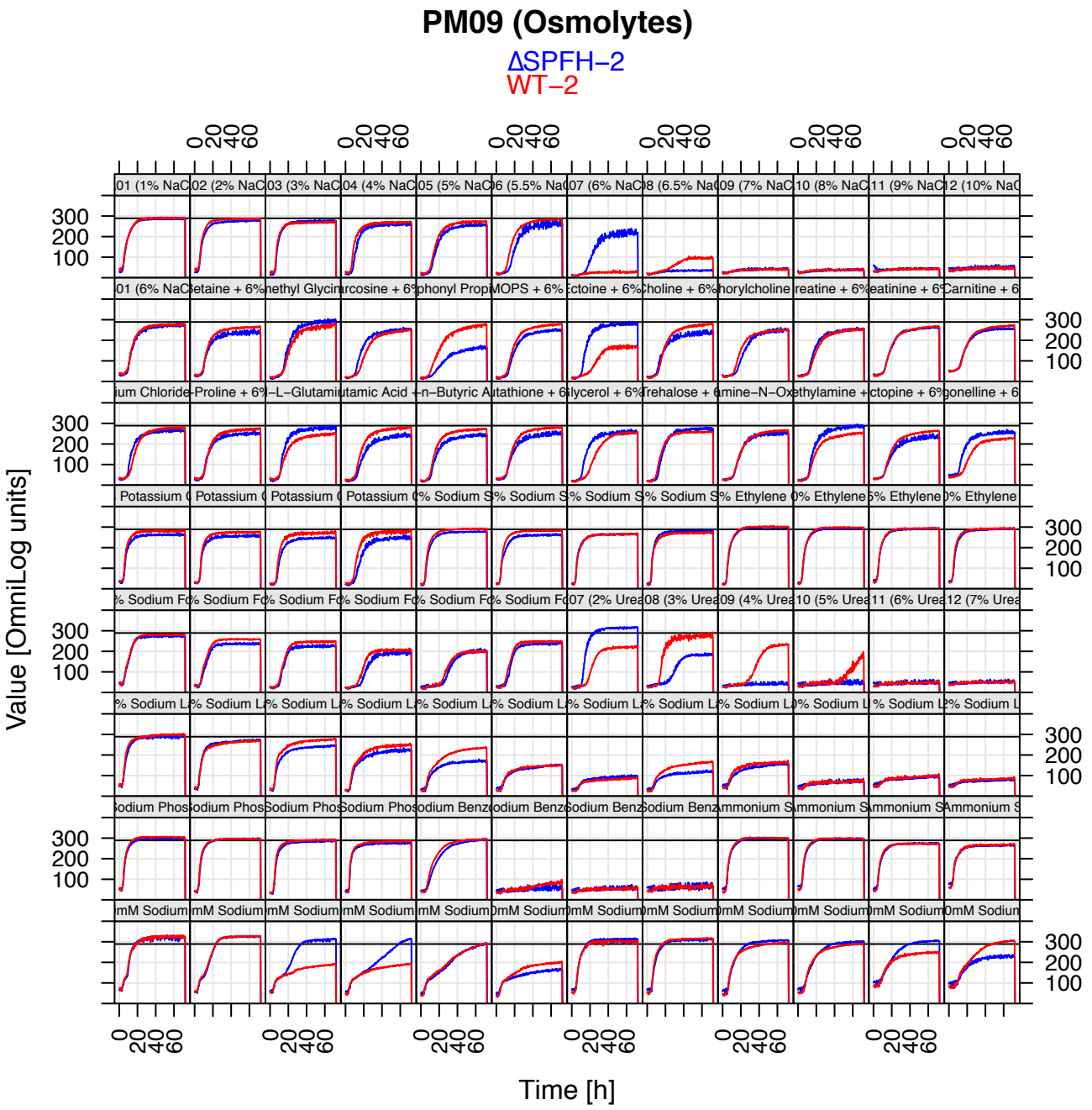
PM09 (Osmolytes)
ΔSPFH−2
WT−2
Value [OmniLog units]
Time [h]

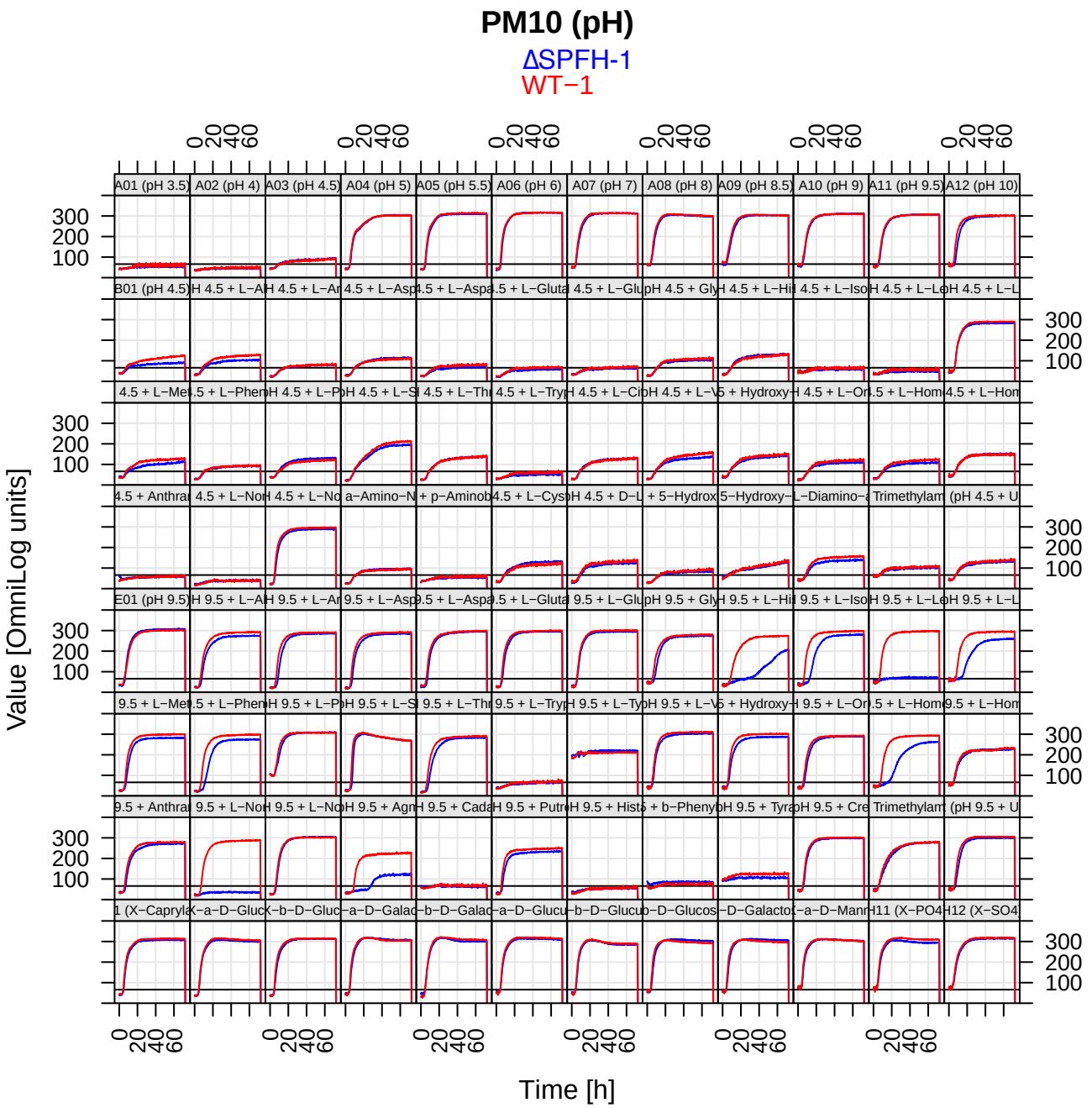
PM10 (pH)
ΔSPFH-1
WT−1
A01 (pH 3.5)
A02 (pH 4)
A03 (pH 4.5)
A04 (pH 5)
A05 (pH 5.5)
A06 (pH 6)
A07 (pH 7)
A08 (pH 8)
A09 (pH 8.5)
A10 (pH 9)
A11 (pH 9.5)
A12 (pH 10)
B01 (pH 4.5)
H 4.5 + L−A
H 4.5 + L−Ar
4.5 + L−Asp
4.5 + L−Aspa
.5 + L−Gluta
4.5 + L−Glu
pH 4.5 + Gly
H 4.5 + L−Hi
4.5 + L−Iso
H 4.5 + L−Le
H 4.5 + L−L
4.5 + L−Met
.5 + L−Phen
H 4.5 + L−Pr
H 4.5 + L−Se
4.5 + L−Thr
4.5 + L−Try
H 4.5 + L−Tr
H 4.5 + L−V
5 + Hydroxy−
H 4.5 + L−Or
.5 + L−Hom
4.5 + L−Hon
4.5 + Anthra
4.5 + L−No
H 4.5 + L−No
a−Amino−N
+ p−Aminob
4.5 + L−Cys
H 4.5 + D−L
+ 5−Hydrox
5−Hydroxy−
L−Diamino−a
Trimethylam
(pH 4.5 + U
E01 (pH 9.5)
H 9.5 + L−A
H 9.5 + L−Ar
9.5 + L−Asp
9.5 + L−Aspa
.5 + L−Gluta
9.5 + L−Glu
pH 9.5 + Gly
H 9.5 + L−Hi
9.5 + L−Iso
H 9.5 + L−Le
H 9.5 + L−L
9.5 + L−Met
.5 + L−Phen
H 9.5 + L−Pr
H 9.5 + L−Se
9.5 + L−Thr
9.5 + L−Try
H 9.5 + L−Ty
H 9.5 + L−V
5 + Hydroxy−
H 9.5 + L−Or
.5 + L−Hom
9.5 + L−Hon
9.5 + Anthra
9.5 + L−No
H 9.5 + L−No
H 9.5 + Agm
H 9.5 + Cada
H 9.5 + Putr
H 9.5 + Hist
ŏ + b−Phenyl
H 9.5 + Tyra
H 9.5 + Cre
Trimethylam
(pH 9.5 + U
1 (X−Capryla
X−a−D−Gluc
X−b−D−Gluc
−a−D−Galac
−b−D−Galac
−a−D−Glucu
−b−D−Glucu
o−D−Glucos
−D−Galacto
−a−D−Manr
H11 (X−PO4
H12 (X−SO4
Value [OmniLog units]
Time [h]

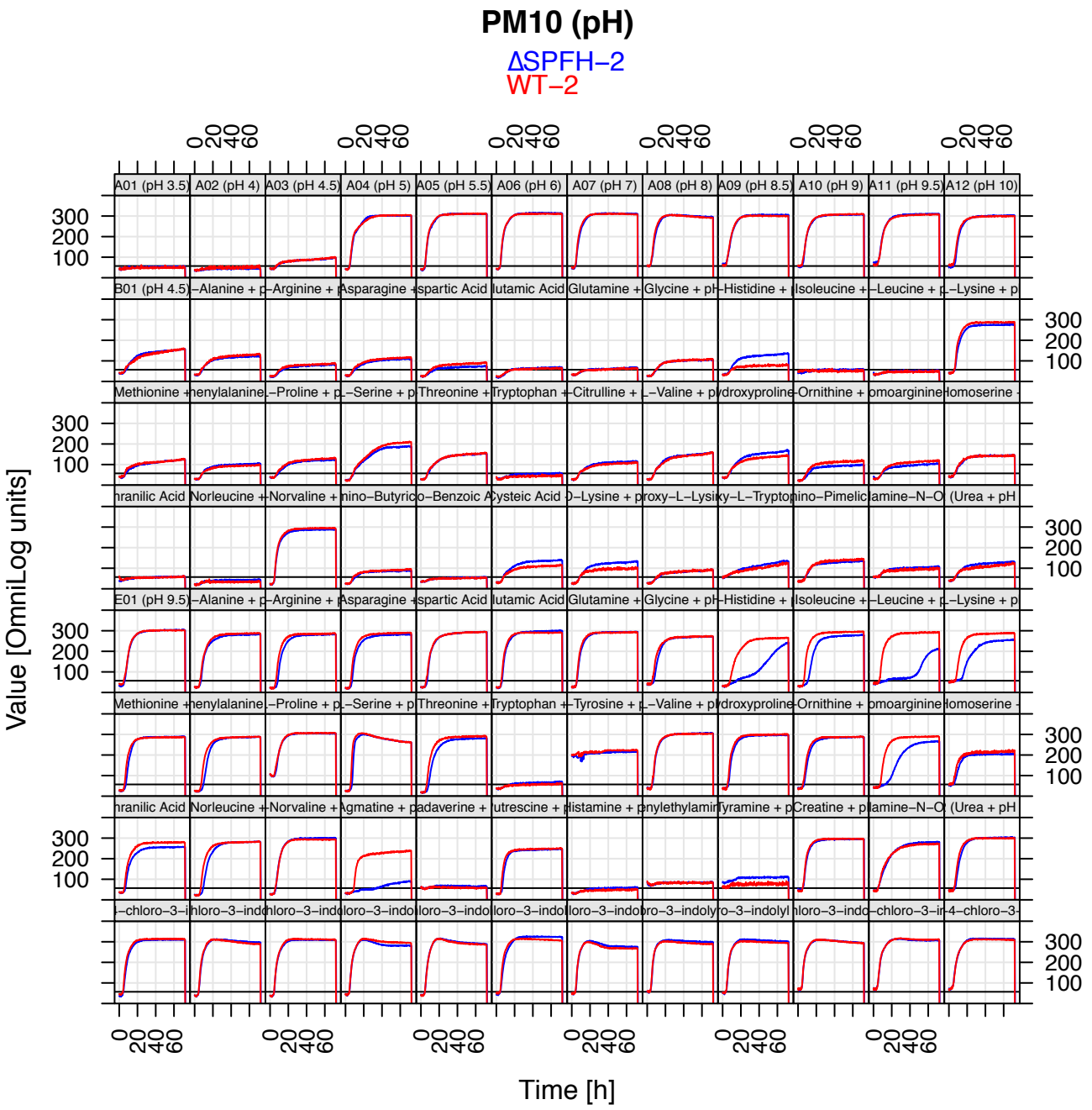
PM10 (pH)
ΔSPFH−2
WT−2
A01 (pH 3.5)
A02 (pH 4)
A03 (pH 4.5)
A04 (pH 5)
A05 (pH 5.5)
A06 (pH 6)
A07 (pH 7)
A08 (pH 8)
A09 (pH 8.5)
A10 (pH 9)
A11 (pH 9.5)
A12 (pH 10)
B01 (pH 4.5)
E01 (pH 9.5)
Value [OmniLog units]
Time [h]

PM11C MicroPlate™

A1 Amikacin 1	A2 Amikacin 2	A3 Amikacin 3	A4 Amikacin 4	A5 Chlortetracycline 1	A6 Chlortetracycline 2	A7 Chlortetracycline 3	A8 Chlortetracycline 4	A9 Lincomycin 1	A10 Lincomycin 2	A11 Lincomycin 3	A12 Lincomycin 4
B1 Amoxicillin 1	B2 Amoxicillin 2	B3 Amoxicillin 3	B4 Amoxicillin 4	B5 Cloxacillin 1	B6 Cloxacillin 2	B7 Cloxacillin 3	B8 Cloxacillin 4	B9 Lomefloxacin 1	B10 Lomefloxacin 2	B11 Lomefloxacin 3	B12 Lomefloxacin 4
C1 Bleomycin 1	C2 Bleomycin 2	C3 Bleomycin 3	C4 Bleomycin 4	C5 Colistin 1	C6 Colistin 2	C7 Colistin 3	C8 Colistin 4	C9 Minocycline 1	C10 Minocycline 2	C11 Minocycline 3	C12 Minocycline 4
D1 Capreomycin 1	D2 Capreomycin 2	D3 Capreomycin 3	D4 Capreomycin 4	D5 Demeclocycline 1	D6 Demeclocycline 2	D7 Demeclocycline 3	D8 Demeclocycline 4	D9 Nafcillin 1	D10 Nafcillin 2	D11 Nafcillin 3	D12 Nafcillin 4
E1 Cefazolin 1	E2 Cefazolin 2	E3 Cefazolin 3	E4 Cefazolin 4	E5 Enoxacin 1	E6 Enoxacin 2	E7 Enoxacin 3	E8 Enoxacin 4	E9 Nalidixic acid 1	E10 Nalidixic acid 2	E11 Nalidixic acid 3	E12 Nalidixic acid 4
F1 Chloramphenicol 1	F2 Chloramphenicol 2	F3 Chloramphenicol 3	F4 Chloramphenicol 4	F5 Erythromycin 1	F6 Erythromycin 2	F7 Erythromycin 3	F8 Erythromycin 4	F9 Neomycin 1	F10 Neomycin 2	F11 Neomycin 3	F12 Neomycin 4
G1 Ceftriaxone 1	G2 Ceftriaxone 2	G3 Ceftriaxone 3	G4 Ceftriaxone 4	G5 Gentamicin 1	G6 Gentamicin 2	G7 Gentamicin 3	G8 Gentamicin 4	G9 Potassium tellurite 1	G10 Potassium tellurite 2	G11 Potassium tellurite 3	G12 Potassium tellurite 4
H1 Cephalothin 1	H2 Cephalothin 2	H3 Cephalothin 3	H4 Cephalothin 4	H5 Kanamycin 1	H6 Kanamycin 2	H7 Kanamycin 3	H8 Kanamycin 4	H9 Ofloxacin 1	H10 Ofloxacin 2	H11 Ofloxacin 3	H12 Ofloxacin 4

PM12B MicroPlate™

A1 Penicillin G 1	A2 Penicillin G 2	A3 Penicillin G 3	A4 Penicillin G 4	A5 Tetracycline 1	A6 Tetracycline 2	A7 Tetracycline 3	A8 Tetracycline 4	A9 Carbenicillin 1	A10 Carbenicillin 2	A11 Carbenicillin 3	A12 Carbenicillin 4
B1 Oxacillin 1	B2 Oxacillin 2	B3 Oxacillin 3	B4 Oxacillin 4	B5 Penimepicycline 1	B6 Penimepicycline 2	B7 Penimepicycline 3	B8 Penimepicycline 4	B9 Polymyxin B 1	B10 Polymyxin B 2	B11 Polymyxin B 3	B12 Polymyxin B 4
C1 Paromomycin 1	C2 Paromomycin 2	C3 Paromomycin 3	C4 Paromomycin 4	C5 Vancomycin 1	C6 Vancomycin 2	C7 Vancomycin 3	C8 Vancomycin 4	C9 D,L-Serine hydroxamate 1	C10 D,L-Serine hydroxamate 2	C11 D,L-Serine hydroxamate 3	C12 D,L-Serine hydroxamate 4
D1 Sisomicin 1	D2 Sisomicin 2	D3 Sisomicin 3	D4 Sisomicin 4	D5 Sulfamethazine 1	D6 Sulfamethazine 2	D7 Sulfamethazine 3	D8 Sulfamethazine 4	D9 Novobiocin 1	D10 Novobiocin 2	D11 Novobiocin 3	D12 Novobiocin 4
E1 2,4-Diamino-6,7-diisopropyl-pteridine 1	E2 2,4-Diamino-6,7-diisopropyl-pteridine 2	E3 2,4-Diamino-6,7-diisopropyl-pteridine 3	E4 2,4-Diamino-6,7-diisopropyl-pteridine 4	E5 Sulfadiazine 1	E6 Sulfadiazine 2	E7 Sulfadiazine 3	E8 Sulfadiazine 4	E9 Benzethonium chloride 1	E10 Benzethonium chloride 2	E11 Benzethonium chloride 3	E12 Benzethonium chloride 4
F1 Tobramycin 1	F2 Tobramycin 2	F3 Tobramycin 3	F4 Tobramycin 4	F5 Sulfathiazole 1	F6 Sulfathiazole 2	F7 Sulfathiazole 3	F8 Sulfathiazole 4	F9 5-Fluoroorotic acid 1	F10 5-Fluoroorotic acid 2	F11 5-Fluoroorotic acid 3	F12 5-Fluoroorotic acid 4
G1 Spectinomycin 1	G2 Spectinomycin 2	G3 Spectinomycin 3	G4 Spectinomycin 4	G5 Sulfa-methoxazole 1	G6 Sulfa-methoxazole 2	G7 Sulfa-methoxazole 3	G8 Sulfa-methoxazole 4	G9 L-Aspartic-β-hydroxamate 1	G10 L-Aspartic-β-hydroxamate 2	G11 L-Aspartic-β-hydroxamate 3	G12 L-Aspartic-β-hydroxamate 4
H1 Spiramycin 1	H2 Spiramycin 2	H3 Spiramycin 3	H4 Spiramycin 4	H5 Rifampicin 1	H6 Rifampicin 2	H7 Rifampicin 3	H8 Rifampicin 4	H9 Dodecyltrimethyl ammonium bromide 1	H10 Dodecyltrimethyl ammonium bromide 2	H11 Dodecyltrimethyl ammonium bromide 3	H12 Dodecyltrimethyl ammonium bromide 4

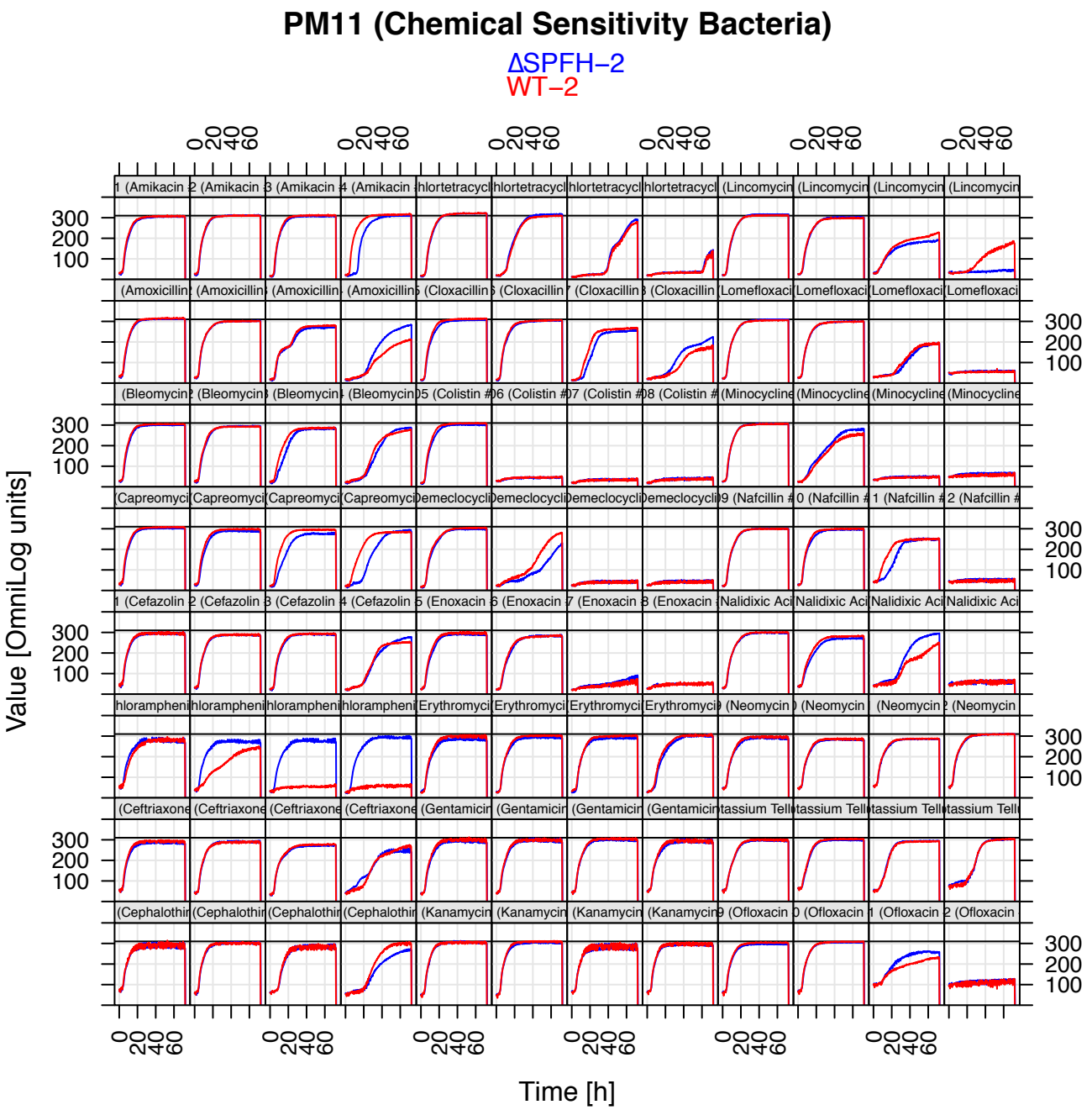
PM11 (Chemical Sensitivity Bacteria)
ΔSPFH−2
WT−2
Value [OmniLog units]
Time [h]

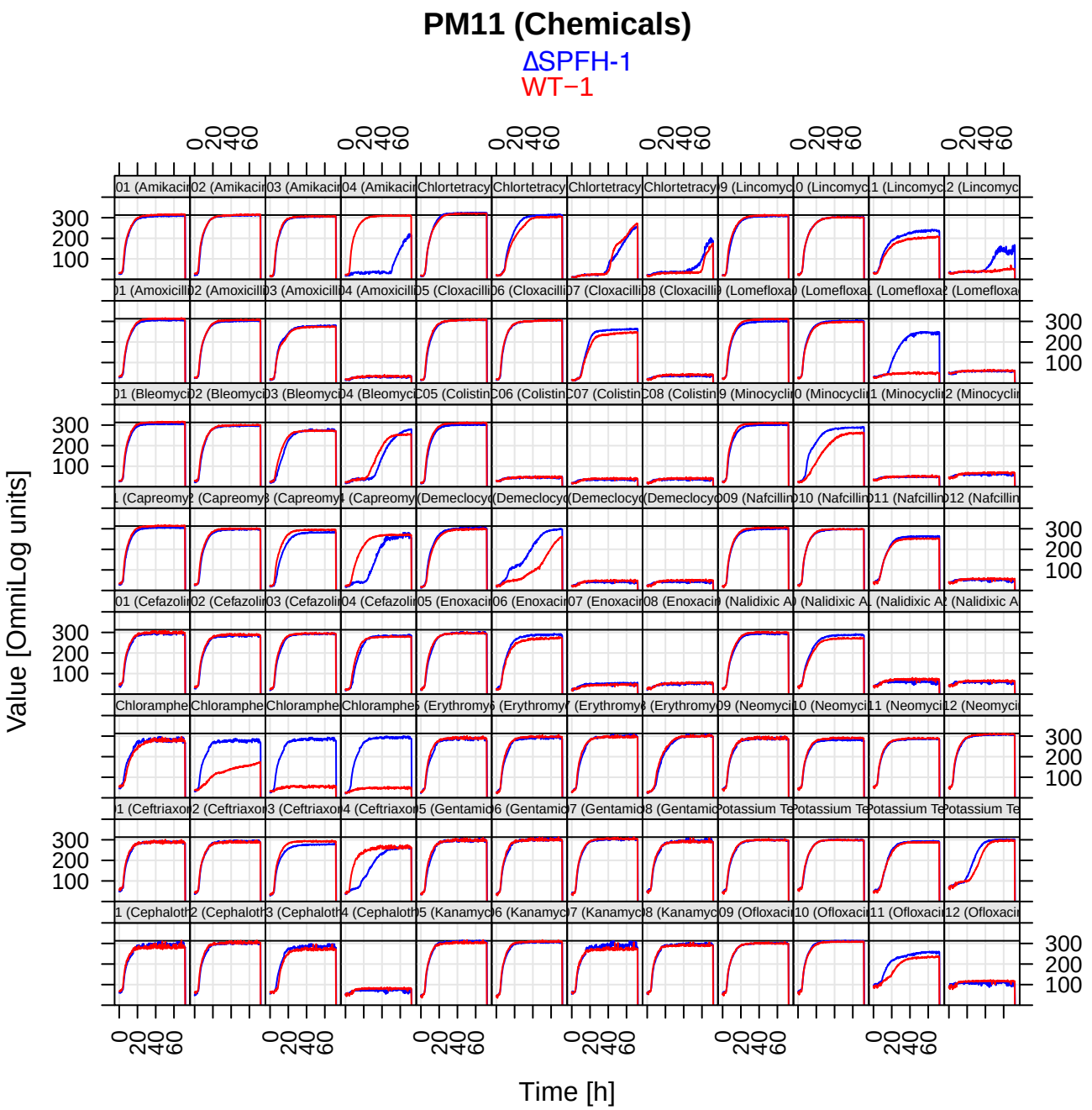
PM11 (Chemicals)
ΔSPFH-1
WT−1
Value [OmniLog units]
Time [h]

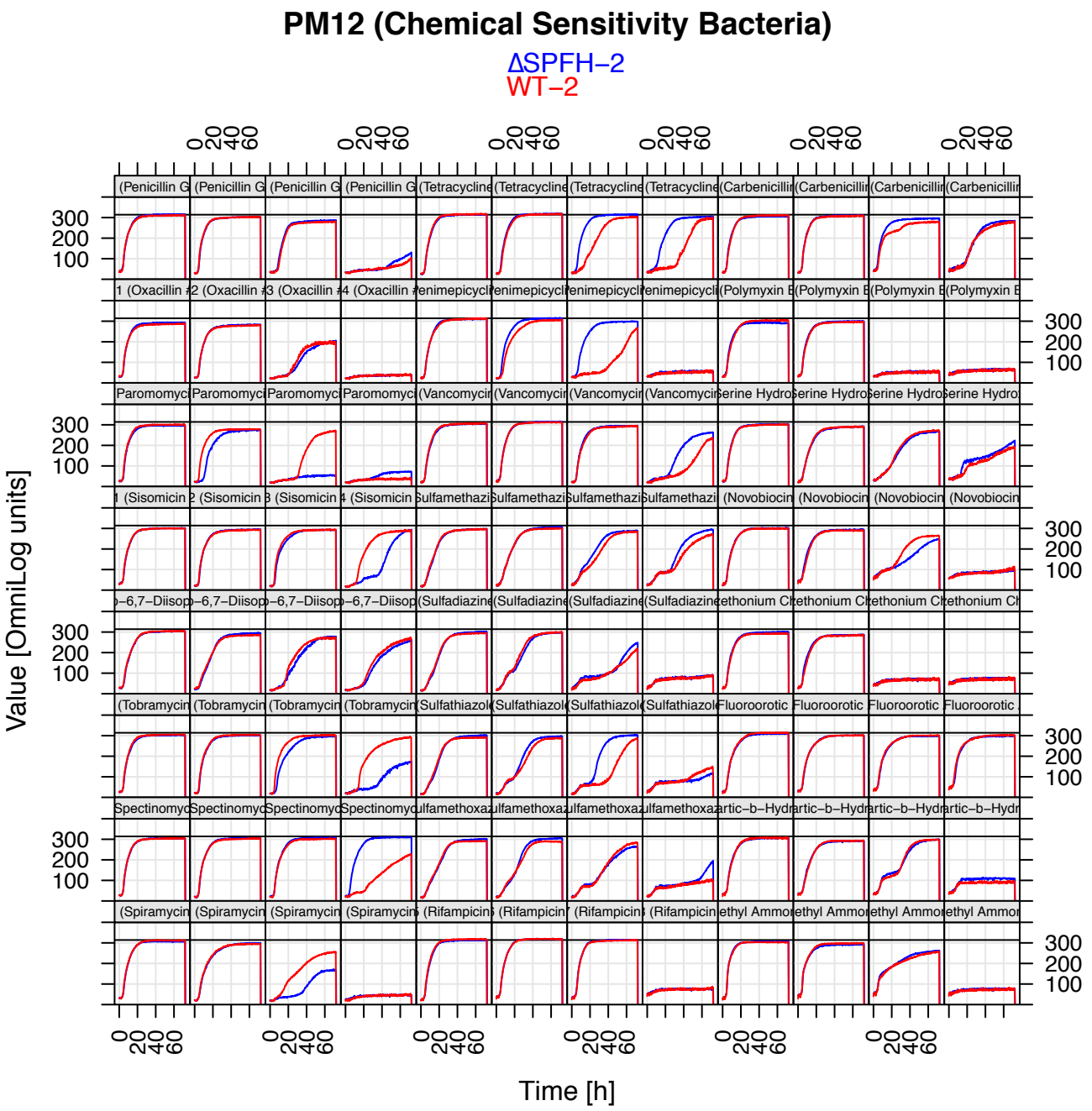
PM12 (Chemical Sensitivity Bacteria)
ΔSPFH−2
WT−2
Value [OmniLog units]
Time [h]
0
20
40
60
100
200
300
(Penicillin G
(Penicillin G
(Penicillin G
(Penicillin G
(Tetracycline
(Tetracycline
(Tetracycline
(Tetracycline
(Carbenicillin
(Carbenicillin
(Carbenicillin
(Carbenicillin
1 (Oxacillin #2 (Oxacillin #3 (Oxacillin #4 (Oxacillin #
enimepicycli
enimepicycli
enimepicycli
enimepicycli
(Polymyxin B
(Polymyxin B
(Polymyxin B
(Polymyxin B
Paromomycı
Paromomycı
Paromomycı
Paromomycı
(Vancomycin
(Vancomycin
(Vancomycin
(Vancomycin
Serine Hydro
Serine Hydro
Serine Hydro
Serine Hydro
1 (Sisomicin 2 (Sisomicin 3 (Sisomicin 4 (Sisomicin
Sulfamethazi
Sulfamethazi
Sulfamethazi
Sulfamethazi
(Novobiocin
(Novobiocin
(Novobiocin
(Novobiocin
–6,7–Diisop
–6,7–Diisop
–6,7–Diisop
–6,7–Diisop
(Sulfadiazine
(Sulfadiazine
(Sulfadiazine
(Sulfadiazine
ethonium Cl
ethonium Cl
ethonium Cl
ethonium Cl
(Tobramycin
(Tobramycin
(Tobramycin
(Tobramycin
(Sulfathiazol
(Sulfathiazol
(Sulfathiazol
(Sulfathiazol
Fluoroorotic
Fluoroorotic
Fluoroorotic
Fluoroorotic
Spectinomyc
Spectinomyc
Spectinomyc
Spectinomyc
ulfamethoxaz
ulfamethoxaz
ulfamethoxaz
ulfamethoxaz
artic–b–Hydr
artic–b–Hydr
artic–b–Hydr
artic–b–Hydr
(Spiramycin
(Spiramycin
(Spiramycin
(Spiramycin
(Rifampicin
(Rifampicin
(Rifampicin
(Rifampicin
ethyl Ammo
ethyl Ammo
ethyl Ammo
ethyl Ammo

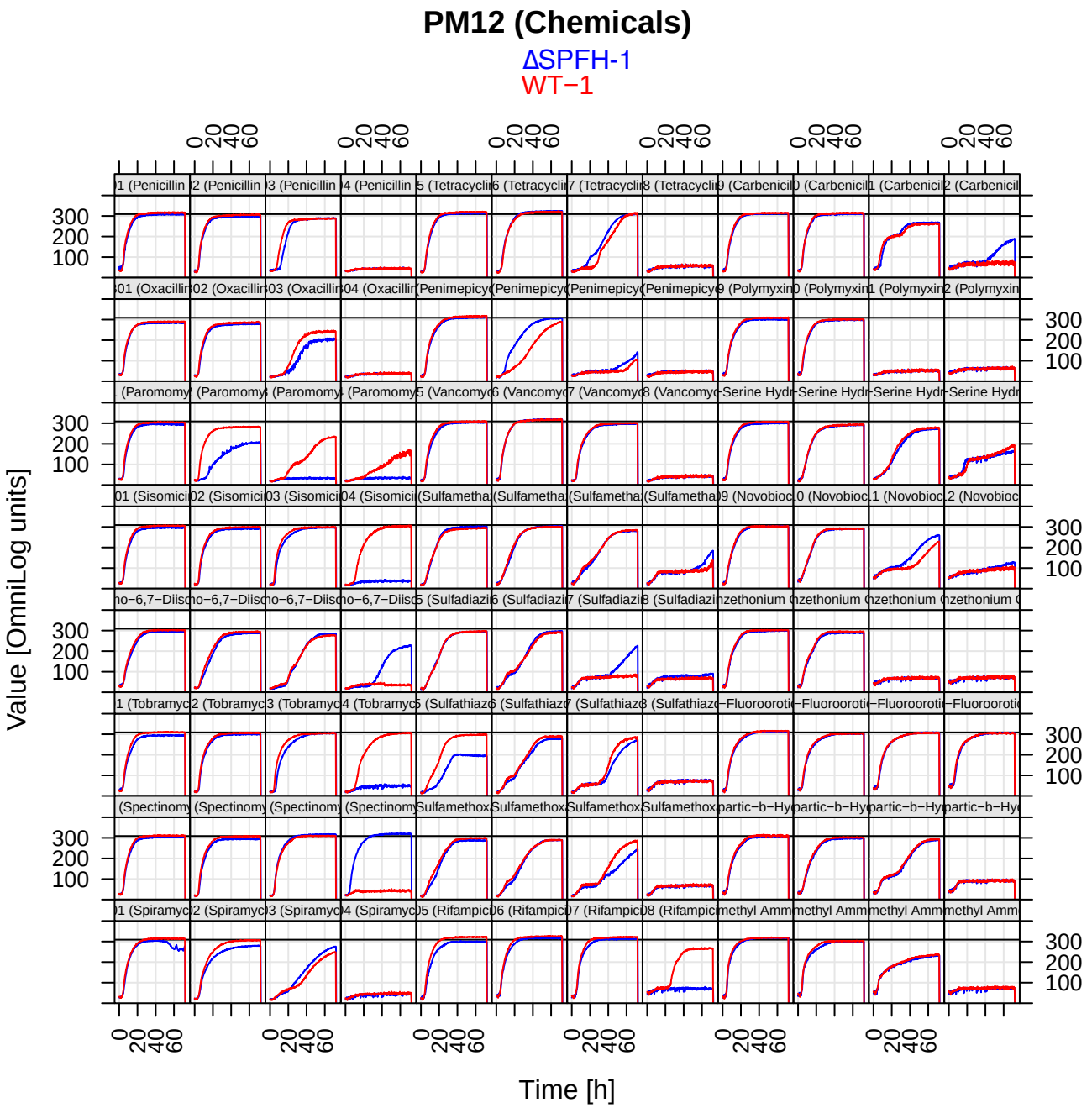
PM12 (Chemicals)
ΔSPFH-1
WT−1
Value [OmniLog units]
Time [h]
0
20
40
60
100
200
300

PM13B MicroPlate™

A1 Ampicillin 1	A2 Ampicillin 2	A3 Ampicillin 3	A4 Ampicillin 4	A5 Dequalinium chloride 1	A6 Dequalinium chloride 2	A7 Dequalinium chloride 3	A8 Dequalinium chloride 4	A9 Nickel chloride 1	A10 Nickel chloride 2	A11 Nickel chloride 3	A12 Nickel chloride 4
B1 Azlocillin 1	B2 Azlocillin 2	B3 Azlocillin 3	B4 Azlocillin 4	B5 2, 2'-Dipyridyl 1	B6 2, 2'-Dipyridyl 2	B7 2, 2'-Dipyridyl 3	B8 2, 2'-Dipyridyl 4	B9 Oxolinic acid 1	B10 Oxolinic acid 2	B11 Oxolinic acid 3	B12 Oxolinic acid 4
C1 6-Mercapto-purine 1	C2 6-Mercapto-purine 2	C3 6-Mercapto-purine 3	C4 6-Mercapto-purine 4	C5 Doxycycline 1	C6 Doxycycline 2	C7 Doxycycline 3	C8 Doxycycline 4	C9 Potassium chromate 1	C10 Potassium chromate 2	C11 Potassium chromate 3	C12 Potassium chromate 4
D1 Cefuroxime 1	D2 Cefuroxime 2	D3 Cefuroxime 3	D4 Cefuroxime 4	D5 5-Fluorouracil 1	D6 5-Fluorouracil 2	D7 5-Fluorouracil 3	D8 5-Fluorouracil 4	D9 Rolitetracycline 1	D10 Rolitetracycline 2	D11 Rolitetracycline 3	D12 Rolitetracycline 4
E1 Cytosine-1-beta-D-arabino-furanoside 1	E2 Cytosine-1-beta-D-arabino-furanoside 2	E3 Cytosine-1-beta-D-arabino-furanoside 3	E4 Cytosine-1-beta-D-arabino-furanoside 4	E5 Geneticin (G418) 1	E6 Geneticin (G418) 2	E7 Geneticin (G418) 3	E8 Geneticin (G418) 4	E9 Ruthenium red 1	E10 Ruthenium red 2	E11 Ruthenium red 3	E12 Ruthenium red 4
F1 Cesium chloride 1	F2 Cesium chloride 2	F3 Cesium chloride 3	F4 Cesium chloride 4	F5 Glycine 1	F6 Glycine 2	F7 Glycine 3	F8 Glycine 4	F9 Thallium (I) acetate 1	F10 Thallium (I) acetate 2	F11 Thallium (I) acetate 3	F12 Thallium (I) acetate 4
G1 Cobalt chloride 1	G2 Cobalt chloride 2	G3 Cobalt chloride 3	G4 Cobalt chloride 4	G5 Manganese chloride 1	G6 Manganese chloride 2	G7 Manganese chloride 3	G8 Manganese chloride 4	G9 Trifluoperazine 1	G10 Trifluoperazine 2	G11 Trifluoperazine 3	G12 Trifluoperazine 4
H1 Cupric chloride 1	H2 Cupric chloride 2	H3 Cupric chloride 3	H4 Cupric chloride 4	H5 Moxalactam 1	H6 Moxalactam 2	H7 Moxalactam 3	H8 Moxalactam 4	H9 Tylosin 1	H10 Tylosin 2	H11 Tylosin 3	H12 Tylosin 4

PM14A MicroPlate™

A1 Acriflavine 1	A2 Acriflavine 2	A3 Acriflavine 3	A4 Acriflavine 4	A5 Furaltadone 1	A6 Furaltadone 2	A7 Furaltadone 3	A8 Furaltadone 4	A9 Sanguinarine 1	A10 Sanguinarine 2	A11 Sanguinarine 3	A12 Sanguinarine 4
B1 9-Aminoacridine 1	B2 9-Aminoacridine 2	B3 9-Aminoacridine 3	B4 9-Aminoacridine 4	B5 Fusaric acid 1	B6 Fusaric acid 2	B7 Fusaric acid 3	B8 Fusaric acid 4	B9 Sodium arsenate 1	B10 Sodium arsenate 2	B11 Sodium arsenate 3	B12 Sodium arsenate 4
C1 Boric Acid 1	C2 Boric Acid 2	C3 Boric Acid 3	C4 Boric Acid 4	C5 1-Hydroxy-pyridine -2-thione 1	C6 1-Hydroxy-pyridine -2-thione 2	C7 1-Hydroxy-pyridine -2-thione 3	C8 1-Hydroxy-pyridine -2-thione 4	C9 Sodium cyanate 1	C10 Sodium cyanate 2	C11 Sodium cyanate 3	C12 Sodium cyanate 4
D1 Cadmium chloride 1	D2 Cadmium chloride 2	D3 Cadmium chloride 3	D4 Cadmium chloride 4	D5 Iodoacetate 1	D6 Iodoacetate 2	D7 Iodoacetate 3	D8 Iodoacetate 4	D9 Sodium dichromate 1	D10 Sodium dichromate 2	D11 Sodium dichromate 3	D12 Sodium dichromate 4
E1 Cefoxitin 1	E2 Cefoxitin 2	E3 Cefoxitin 3	E4 Cefoxitin 4	E5 Nitrofurantoin 1	E6 Nitrofurantoin 2	E7 Nitrofurantoin 3	E8 Nitrofurantoin 4	E9 Sodium metaborate 1	E10 Sodium metaborate 2	E11 Sodium metaborate 3	E12 Sodium metaborate 4
F1 Chloramphenicol 1	F2 Chloramphenicol 2	F3 Chloramphenicol 3	F4 Chloramphenicol 4	F5 Piperacillin 1	F6 Piperacillin 2	F7 Piperacillin 3	F8 Piperacillin 4	F9 Sodium metavanadate 1	F10 Sodium metavanadate 2	F11 Sodium metavanadate 3	F12 Sodium metavanadate 4
G1 Chelerythrine 1	G2 Chelerythrine 2	G3 Chelerythrine 3	G4 Chelerythrine 4	G5 Carbenicillin 1	G6 Carbenicillin 2	G7 Carbenicillin 3	G8 Carbenicillin 4	G9 Sodium nitrite 1	G10 Sodium nitrite 2	G11 Sodium nitrite 3	G12 Sodium nitrite 4
H1 EGTA 1	H2 EGTA 2	H3 EGTA 3	H4 EGTA 4	H5 Promethazine 1	H6 Promethazine 2	H7 Promethazine 3	H8 Promethazine 4	H9 Sodium orthovanadate 1	H10 Sodium orthovanadate 2	H11 Sodium orthovanadate 3	H12 Sodium orthovanadate 4

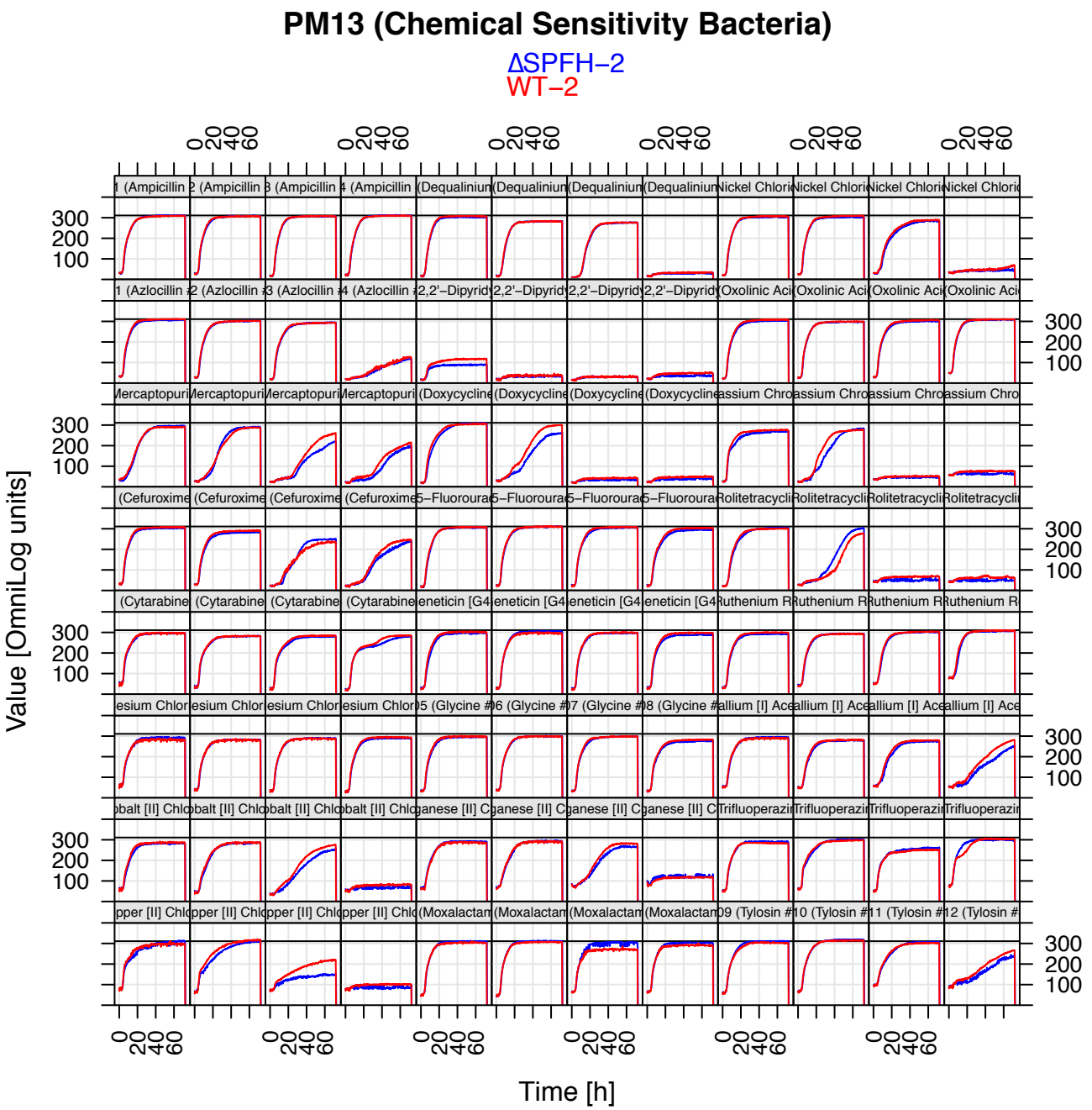
PM13 (Chemical Sensitivity Bacteria)
ΔSPFH−2
WT−2
Value [OmniLog units]
Time [h]

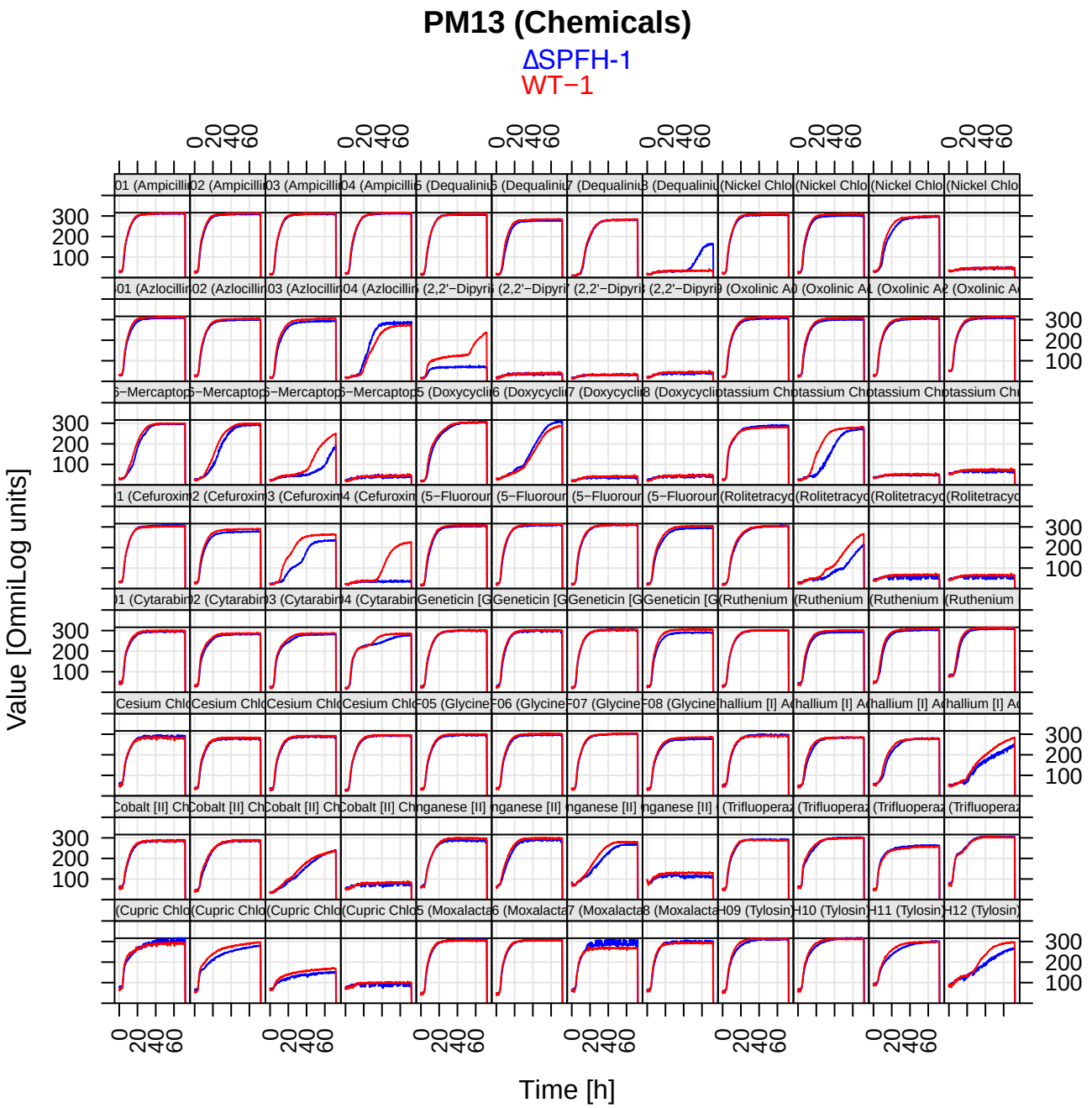
PM13 (Chemicals)
ΔSPFH-1
WT−1
Value [OmniLog units]
Time [h]

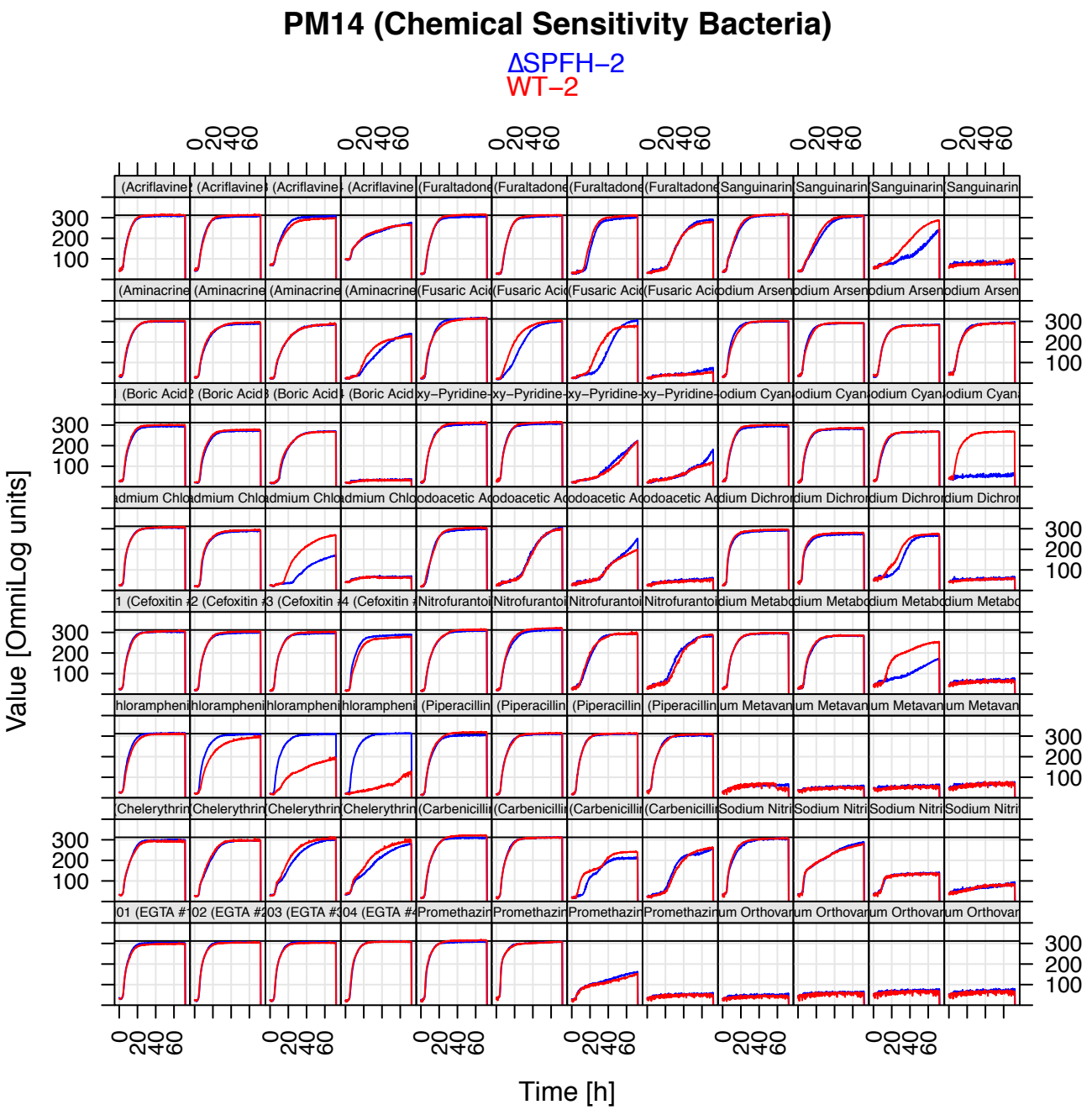
PM14 (Chemical Sensitivity Bacteria)
ΔSPFH−2
WT−2
Value [OmniLog units]
Time [h]

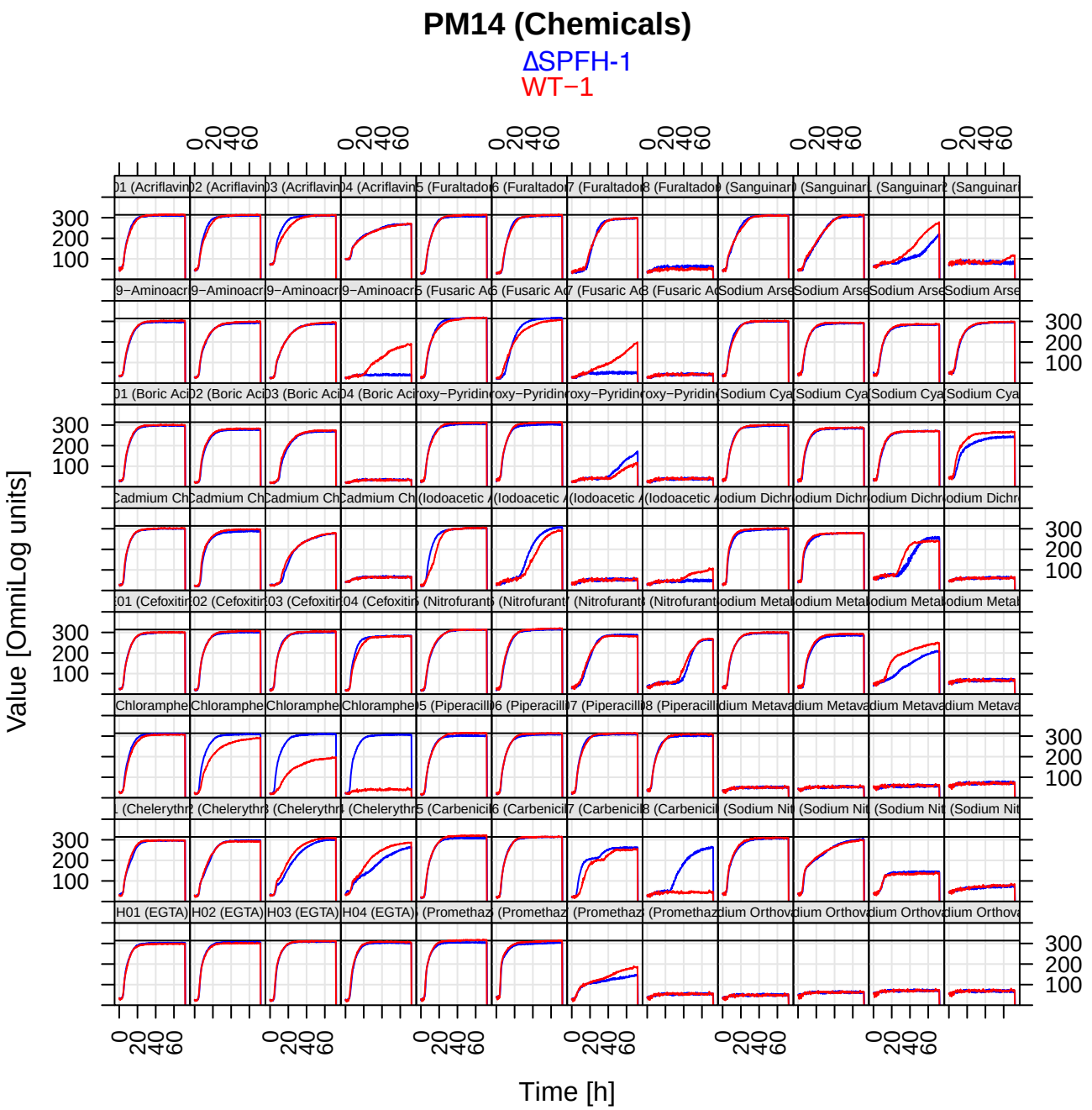
PM14 (Chemicals)
ΔSPFH-1
WT−1
Value [OmniLog units]
Time [h]

PM15B MicroPlate™

A1 Procaine 1	A2 Procaine 2	A3 Procaine 3	A4 Procaine 4	A5 Guanidine hydrochloride 1	A6 Guanidine hydrochloride 2	A7 Guanidine hydrochloride 3	A8 Guanidine hydrochloride 4	A9 Cefmetazole 1	A10 Cefmetazole 2	A11 Cefmetazole 3	A12 Cefmetazole 4
B1 D-Cycloserine 1	B2 D-Cycloserine 2	B3 D-Cycloserine 3	B4 D-Cycloserine 4	B5 EDTA 1	B6 EDTA 2	B7 EDTA 3	B8 EDTA 4	B9 5,7-Dichloro- 8-hydroxy-quinaldine 1	B10 5,7-Dichloro- 8-hydroxy-quinaldine 2	B11 5,7-Dichloro- 8-hydroxy-quinaldine 3	B12 5,7-Dichloro- 8-hydroxy-quinaldine 4
C1 5,7-Dichloro-8-hydroxyquinoline 1	C2 5,7-Dichloro-8-hydroxyquinoline 2	C3 5,7-Dichloro-8-hydroxyquinoline 3	C4 5,7-Dichloro-8-hydroxyquinoline 4	C5 Fusidic acid 1	C6 Fusidic acid 2	C7 Fusidic acid 3	C8 Fusidic acid 4	C9 1,10-Phenanthroline 1	C10 1,10-Phenanthroline 2	C11 1,10-Phenanthroline 3	C12 1,10-Phenanthroline 4
D1 Phleomycin 1	D2 Phleomycin 2	D3 Phleomycin 3	D4 Phleomycin 4	D5 Domiphen bromide 1	D6 Domiphen bromide 2	D7 Domiphen bromide 3	D8 Domiphen bromide 4	D9 Nordihydroguaia retic acid 1	D10 Nordihydroguaia retic acid 2	D11 Nordihydroguaia retic acid 3	D12 Nordihydroguaia retic acid 4
E1 Alexidine 1	E2 Alexidine 2	E3 Alexidine 3	E4 Alexidine 4	E5 5-Nitro-2-furaldehyde semicarbazone 1	E6 5-Nitro-2-furaldehyde semicarbazone 2	E7 5-Nitro-2-furaldehyde semicarbazone 3	E8 5-Nitro-2-furaldehyde semicarbazone 4	E9 Methyl viologen 1	E10 Methyl viologen 2	E11 Methyl viologen 3	E12 Methyl viologen 4
F1 3, 4-Dimethoxy-benzyl alcohol 1	F2 3, 4-Dimethoxy-benzyl alcohol 2	F3 3, 4-Dimethoxy-benzyl alcohol 3	F4 3, 4-Dimethoxy-benzyl alcohol 4	F5 Oleandomycin 1	F6 Oleandomycin 2	F7 Oleandomycin 3	F8 Oleandomycin 4	F9 Puromycin 1	F10 Puromycin 2	F11 Puromycin 3	F12 Puromycin 4
G1 CCCP 1	G2 CCCP 2	G3 CCCP 3	G4 CCCP 4	G5 Sodium azide 1	G6 Sodium azide 2	G7 Sodium azide 3	G8 Sodium azide 4	G9 Menadione 1	G10 Menadione 2	G11 Menadione 3	G12 Menadione 4
H1 2-Nitroimidazole 1	H2 2-Nitroimidazole 2	H3 2-Nitroimidazole 3	H4 2-Nitroimidazole 4	H5 Hydroxyurea 1	H6 Hydroxyurea 2	H7 Hydroxyurea 3	H8 Hydroxyurea 4	H9 Zinc chloride 1	H10 Zinc chloride 2	H11 Zinc chloride 3	H12 Zinc chloride 4

PM16A MicroPlate™

A1 Cefotaxime 1	A2 Cefotaxime 2	A3 Cefotaxime 3	A4 Cefotaxime 4	A5 Phosphomycin 1	A6 Phosphomycin 2	A7 Phosphomycin 3	A8 Phosphomycin 4	A9 5-Chloro-7-iodo-8-hydroxy-quinoline 1	A10 5-Chloro-7-iodo-8-hydroxy-quinoline 2	A11 5-Chloro-7-iodo-8-hydroxy-quinoline 3	A12 5-Chloro-7-iodo-8-hydroxy-quinoline 4
B1 Norfloxacin 1	B2 Norfloxacin 2	B3 Norfloxacin 3	B4 Norfloxacin 4	B5 Sulfanilamide 1	B6 Sulfanilamide 2	B7 Sulfanilamide 3	B8 Sulfanilamide 4	B9 Trimethoprim 1	B10 Trimethoprim 2	B11 Trimethoprim 3	B12 Trimethoprim 4
C1 Dichlofluanid 1	C2 Dichlofluanid 2	C3 Dichlofluanid 3	C4 Dichlofluanid 4	C5 Protamine sulfate 1	C6 Protamine sulfate 2	C7 Protamine sulfate 3	C8 Protamine sulfate 4	C9 Cetylpyridinium chloride 1	C10 Cetylpyridinium chloride 2	C11 Cetylpyridinium chloride 3	C12 Cetylpyridinium chloride 4
D1 1-Chloro -2,4-dinitrobenzene 1	D2 1-Chloro -2,4-dinitrobenzene 2	D3 1-Chloro -2,4-dinitrobenzene 3	D4 1-Chloro -2,4-dinitrobenzene 4	D5 Diamide 1	D6 Diamide 2	D7 Diamide 3	D8 Diamide 4	D9 Cinoxacin 1	D10 Cinoxacin 2	D11 Cinoxacin 3	D12 Cinoxacin 4
E1 Streptomycin 1	E2 Streptomycin 2	E3 Streptomycin 3	E4 Streptomycin 4	E5 5-Azacytidine 1	E6 5-Azacytidine 2	E7 5-Azacytidine 3	E8 5-Azacytidine 4	E9 Rifamycin SV 1	E10 Rifamycin SV 2	E11 Rifamycin SV 3	E12 Rifamycin SV 4
F1 Potassium tellurite 1	F2 Potassium tellurite 2	F3 Potassium tellurite 3	F4 Potassium tellurite 4	F5 Sodium selenite 1	F6 Sodium selenite 2	F7 Sodium selenite 3	F8 Sodium selenite 4	F9 Aluminum sulfate 1	F10 Aluminum sulfate 2	F11 Aluminum sulfate 3	F12 Aluminum sulfate 4
G1 Chromium chloride 1	G2 Chromium chloride 2	G3 Chromium chloride 3	G4 Chromium chloride 4	G5 Ferric chloride 1	G6 Ferric chloride 2	G7 Ferric chloride 3	G8 Ferric chloride 4	G9 L-Glutamic-g-hydroxamate 1	G10 L-Glutamic-g-hydroxamate 2	G11 L-Glutamic-g-hydroxamate 3	G12 L-Glutamic-g-hydroxamate 4
H1 Glycine hydroxamate 1	H2 Glycine hydroxamate 2	H3 Glycine hydroxamate 3	H4 Glycine hydroxamate 4	H5 Chloroxylenol 1	H6 Chloroxylenol 2	H7 Chloroxylenol 3	H8 Chloroxylenol 4	H9 Sorbic acid 1	H10 Sorbic acid 2	H11 Sorbic acid 3	H12 Sorbic acid 4

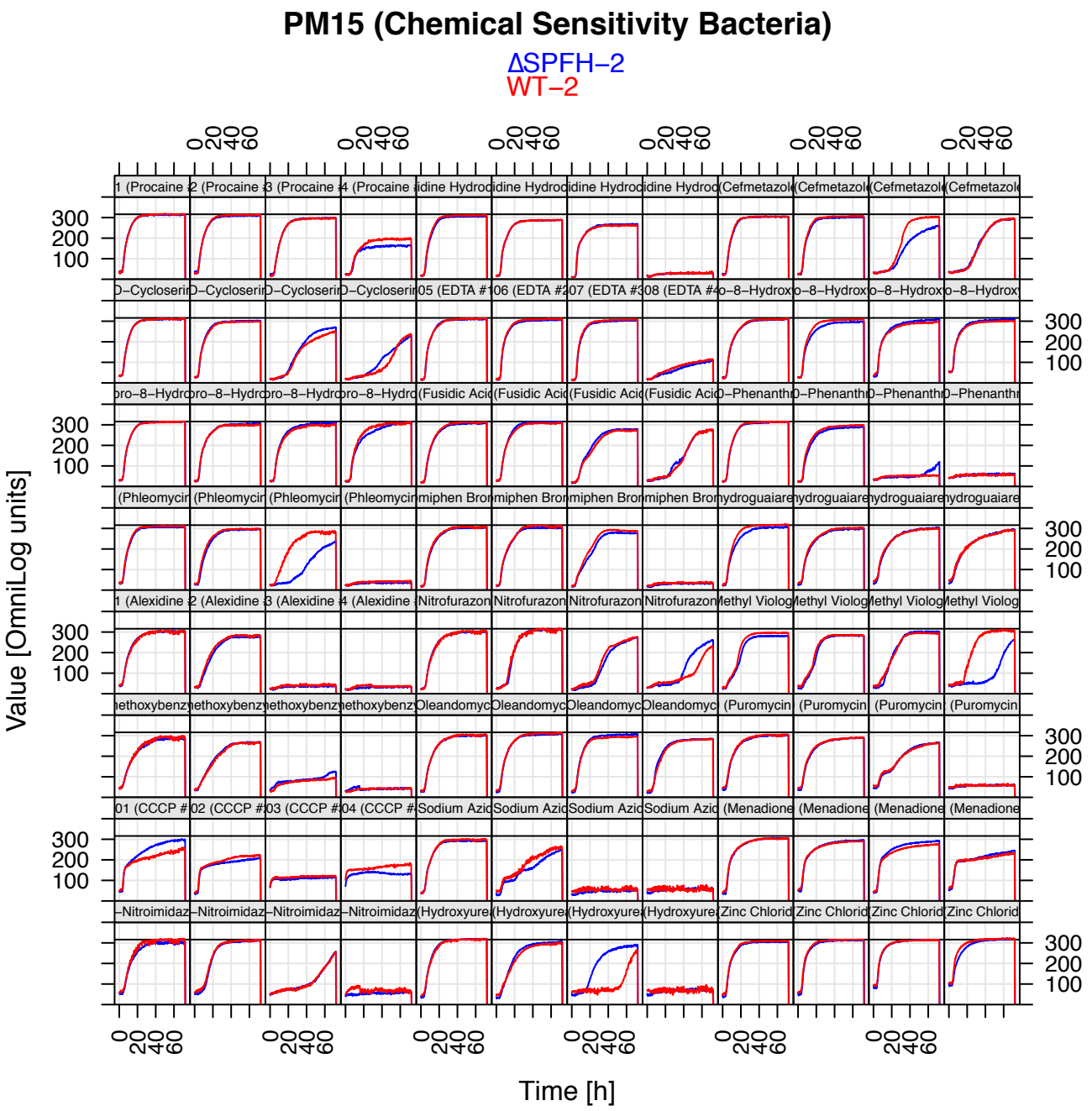
PM15 (Chemical Sensitivity Bacteria)
ΔSPFH−2
WT−2
Value [OmniLog units]
Time [h]

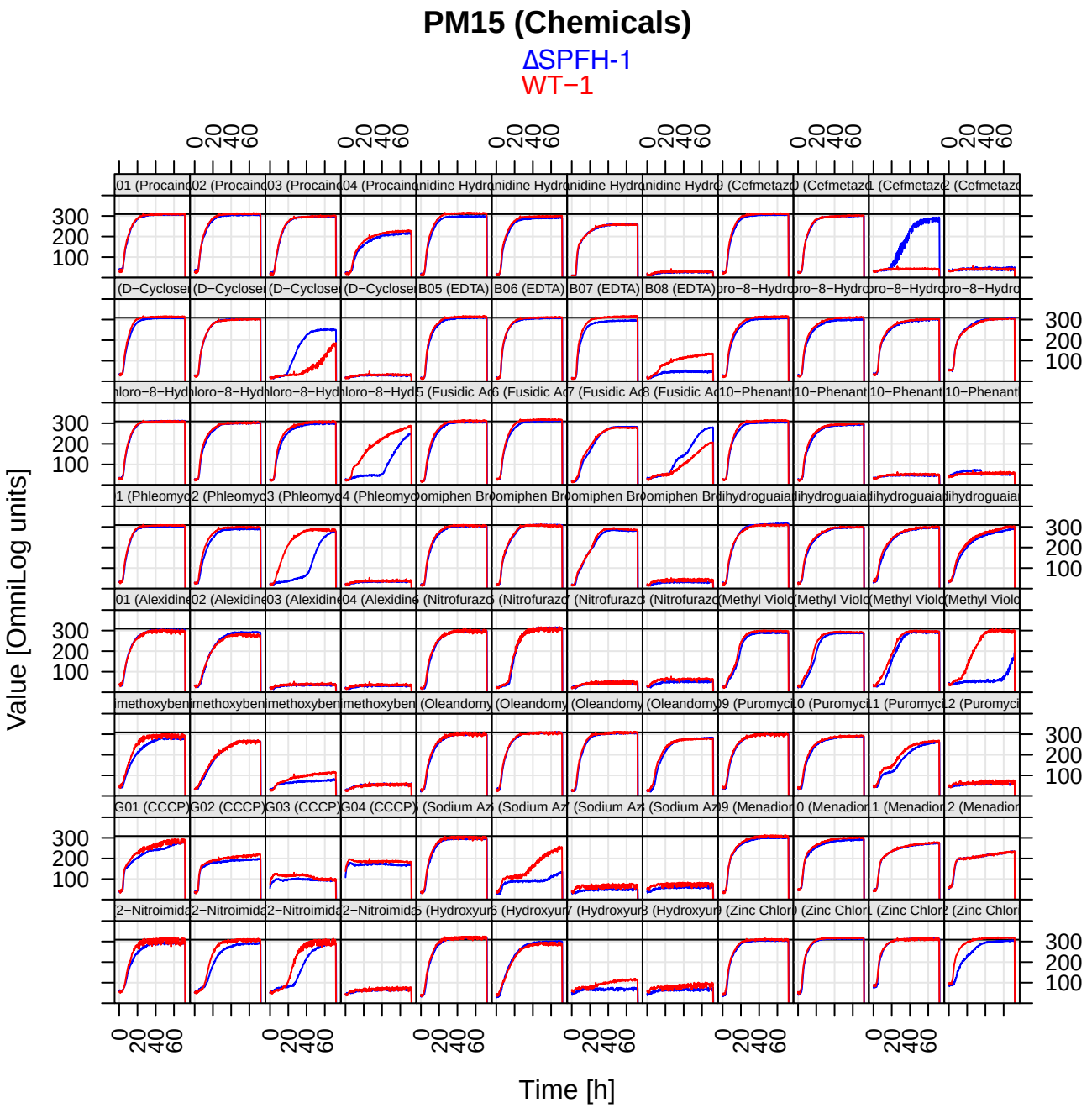
PM15 (Chemicals)
ΔSPFH-1
WT−1
Value [OmniLog units]
Time [h]

PM16 (Chemical Sensitivity Bacteria)

ΔSPFH–2
WT–2

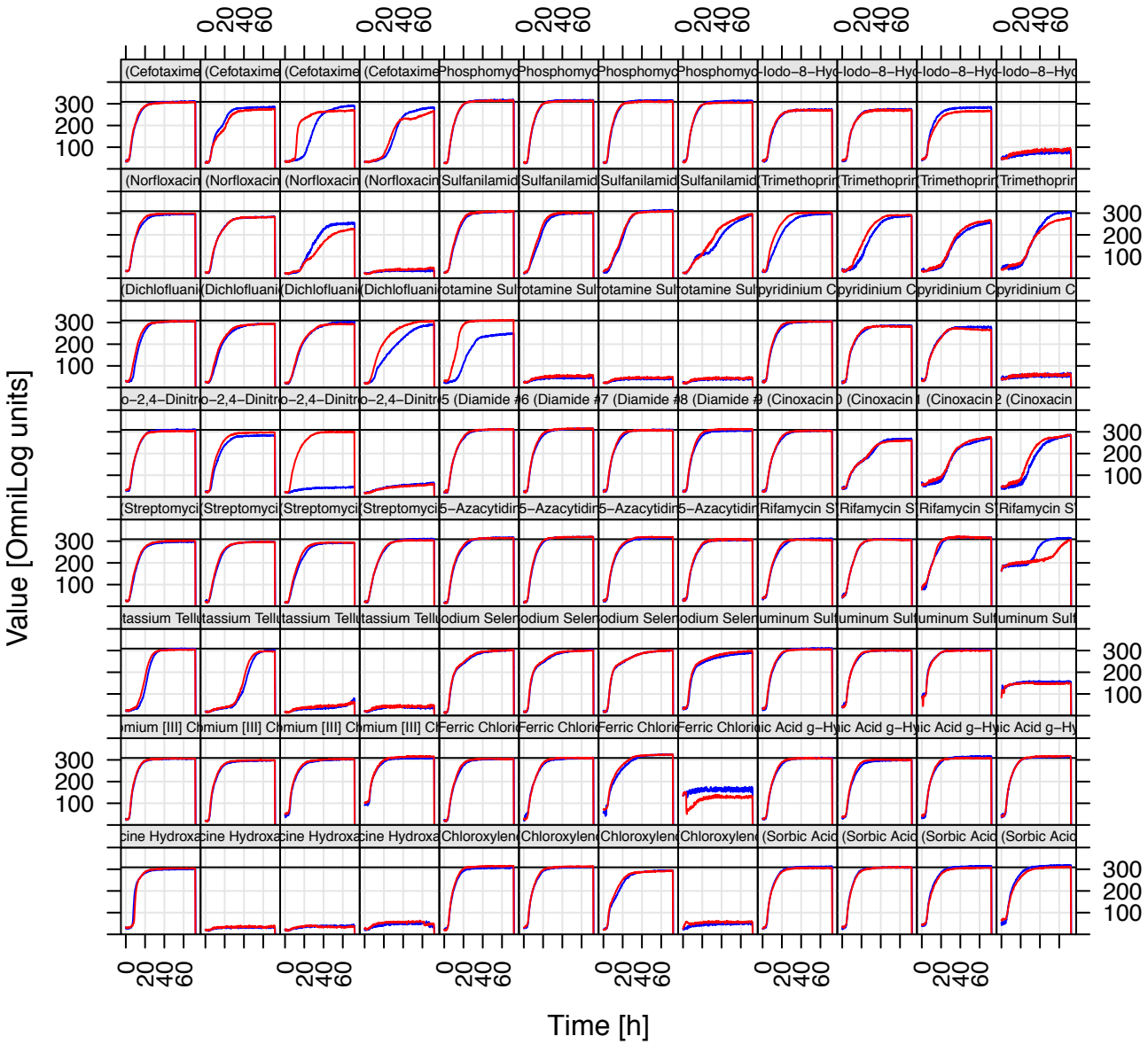

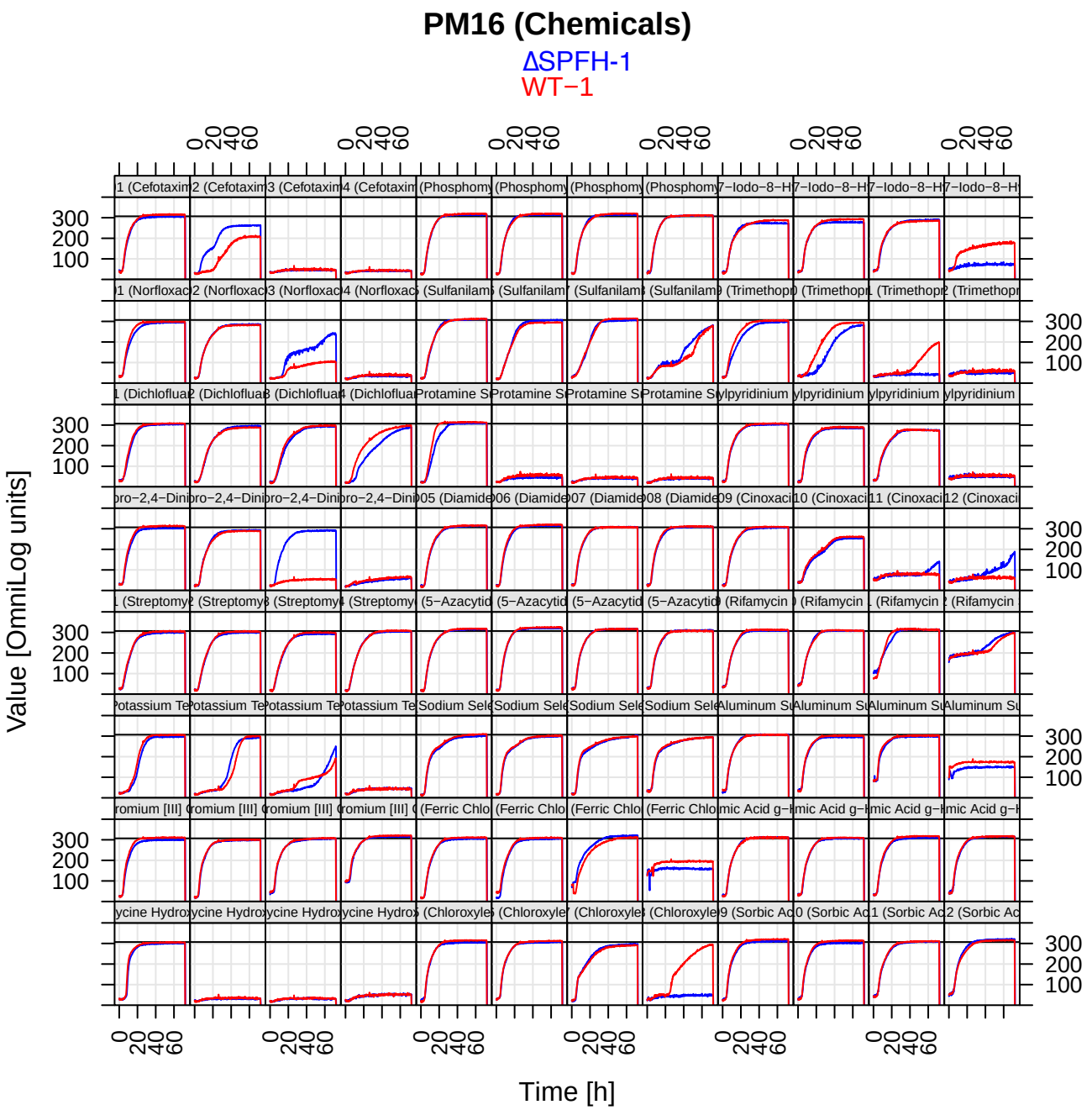
PM16 (Chemicals)
ΔSPFH-1
WT−1
Value [OmniLog units]
Time [h]

PM17A MicroPlate™

A1 D-Serine 1	A2 D-Serine 2	A3 D-Serine 3	A4 D-Serine 4	A5 β-Chloro-L-alanine hydrochloride 1	A6 β-Chloro-L-alanine hydrochloride 2	A7 β-Chloro-L-alanine hydrochloride 3	A8 β-Chloro-L-alanine hydrochloride 4	A9 Thiosalicylic acid 1	A10 Thiosalicylic acid 2	A11 Thiosalicylic acid 3	A12 Thiosalicylic acid 4
B1 Sodium salicylate 1	B2 Sodium salicylate 2	B3 Sodium salicylate 3	B4 Sodium salicylate 4	B5 Hygromycin B 1	B6 Hygromycin B 2	B7 Hygromycin B 3	B8 Hygromycin B 4	B9 Ethionamide 1	B10 Ethionamide 2	B11 Ethionamide 3	B12 Ethionamide 4
C1 4-Aminopyridine 1	C2 4-Aminopyridine 2	C3 4-Aminopyridine 3	C4 4-Aminopyridine 4	C5 Sulfachloro-pyridazine 1	C6 Sulfachloro-pyridazine 2	C7 Sulfachloro-pyridazine 3	C8 Sulfachloro-pyridazine 4	C9 Sulfamono-methoxine 1	C10 Sulfamono-methoxine 2	C11 Sulfamono-methoxine 3	C12 Sulfamono-methoxine 4
D1 Oxycarboxin 1	D2 Oxycarboxin 2	D3 Oxycarboxin 3	D4 Oxycarboxin 4	D5 3-Amino-1,2,4-triazole 1	D6 3-Amino-1,2,4-triazole 2	D7 3-Amino-1,2,4-triazole 3	D8 3-Amino-1,2,4-triazole 4	D9 Chlorpromazine 1	D10 Chlorpromazine 2	D11 Chlorpromazine 3	D12 Chlorpromazine 4
E1 Niaproof 1	E2 Niaproof 2	E3 Niaproof 3	E4 Niaproof 4	E5 Compound 48/80 1	E6 Compound 48/80 2	E7 Compound 48/80 3	E8 Compound 48/80 4	E9 Sodium tungstate 1	E10 Sodium tungstate 2	E11 Sodium tungstate 3	E12 Sodium tungstate 4
F1 Lithium chloride 1	F2 Lithium chloride 2	F3 Lithium chloride 3	F4 Lithium chloride 4	F5 DL-Methionine hydroxamate 1	F6 DL-Methionine hydroxamate 2	F7 DL-Methionine hydroxamate 3	F8 DL-Methionine hydroxamate 4	F9 Tannic acid 1	F10 Tannic acid 2	F11 Tannic acid 3	F12 Tannic acid 4
G1 Chlorambucil 1	G2 Chlorambucil 2	G3 Chlorambucil 3	G4 Chlorambucil 4	G5 Cefamandole nafate 1	G6 Cefamandole nafate 2	G7 Cefamandole nafate 3	G8 Cefamandole nafate 4	G9 Cefoperazone 1	G10 Cefoperazone 2	G11 Cefoperazone 3	G12 Cefoperazone 4
H1 Cefsulodin 1	H2 Cefsulodin 2	H3 Cefsulodin 3	H4 Cefsulodin 4	H5 Caffeine 1	H6 Caffeine 2	H7 Caffeine 3	H8 Caffeine 4	H9 Phenylarsine oxide 1	H10 Phenylarsine oxide 2	H11 Phenylarsine oxide 3	H12 Phenylarsine oxide 4

PM18C MicroPlate™

A1 Ketoprofen 1	A2 Ketoprofen 2	A3 Ketoprofen 3	A4 Ketoprofen 4	A5 Sodium pyrophosphate decahydrate 1	A6 Sodium pyrophosphate decahydrate 2	A7 Sodium pyrophosphate decahydrate 3	A8 Sodium pyrophosphate decahydrate 4	A9 Thiamphenicol 1	A10 Thiamphenicol 2	A11 Thiamphenicol 3	A12 Thiamphenicol 4
B1 Trifluorothymidine 1	B2 Trifluorothymidine 2	B3 Trifluorothymidine 3	B4 Trifluorothymidine 4	B5 Pipemidic Acid 1	B6 Pipemidic Acid 2	B7 Pipemidic Acid 3	B8 Pipemidic Acid 4	B9 Azathioprine 1	B10 Azathioprine 2	B11 Azathioprine 3	B12 Azathioprine 4
C1 Poly-L-lysine 1	C2 Poly-L-lysine 2	C3 Poly-L-lysine 3	C4 Poly-L-lysine 4	C5 Sulfisoxazole 1	C6 Sulfisoxazole 2	C7 Sulfisoxazole 3	C8 Sulfisoxazole 4	C9 Pentachloro-phenol 1	C10 Pentachloro-phenol 2	C11 Pentachloro-phenol 3	C12 Pentachloro-phenol 4
D1 Sodium m-arsenite 1	D2 Sodium m-arsenite 2	D3 Sodium m-arsenite 3	D4 Sodium m-arsenite 4	D5 Sodium bromate 1	D6 Sodium bromate 2	D7 Sodium bromate 3	D8 Sodium bromate 4	D9 Lidocane 1	D10 Lidocane 2	D11 Lidocane 3	D12 Lidocane 4
E1 Sodium metasilicate 1	E2 Sodium metasilicate 2	E3 Sodium metasilicate 3	E4 Sodium metasilicate 4	E5 Sodium m-periodate 1	E6 Sodium m-periodate 2	E7 Sodium m-periodate 3	E8 Sodium m-periodate 4	E9 Antimony (III) chloride 1	E10 Antimony (III) chloride 2	E11 Antimony (III) chloride 3	E12 Antimony (III) chloride 4
F1 Semicarbazide 1	F2 Semicarbazide 2	F3 Semicarbazide 3	F4 Semicarbazide 4	F5 Tinidazole 1	F6 Tinidazole 2	F7 Tinidazole 3	F8 Tinidazole 4	F9 Aztreonam 1	F10 Aztreonam 2	F11 Aztreonam 3	F12 Aztreonam 4
G1 Triclosan 1	G2 Triclosan 2	G3 Triclosan 3	G4 Triclosan 4	G5 3,5-Diamino-1,2,4-triazole (Guanazole) 1	G6 3,5-Diamino-1,2,4-triazole (Guanazole) 2	G7 3,5-Diamino-1,2,4-triazole (Guanazole) 3	G8 3,5-Diamino-1,2,4-triazole (Guanazole) 4	G9 Myricetin 1	G10 Myricetin 2	G11 Myricetin 3	G12 Myricetin 4
H1 5-fluoro-5'-deoxyuridine 1	H2 5-fluoro-5'-deoxyuridine 2	H3 5-fluoro-5'-deoxyuridine 3	H4 5-fluoro-5'-deoxyuridine 4	H5 2-Phenylphenol 1	H6 2-Phenylphenol 2	H7 2-Phenylphenol 3	H8 2-Phenylphenol 4	H9 Plumbagin 1	H10 Plumbagin 2	H11 Plumbagin 3	H12 Plumbagin 4

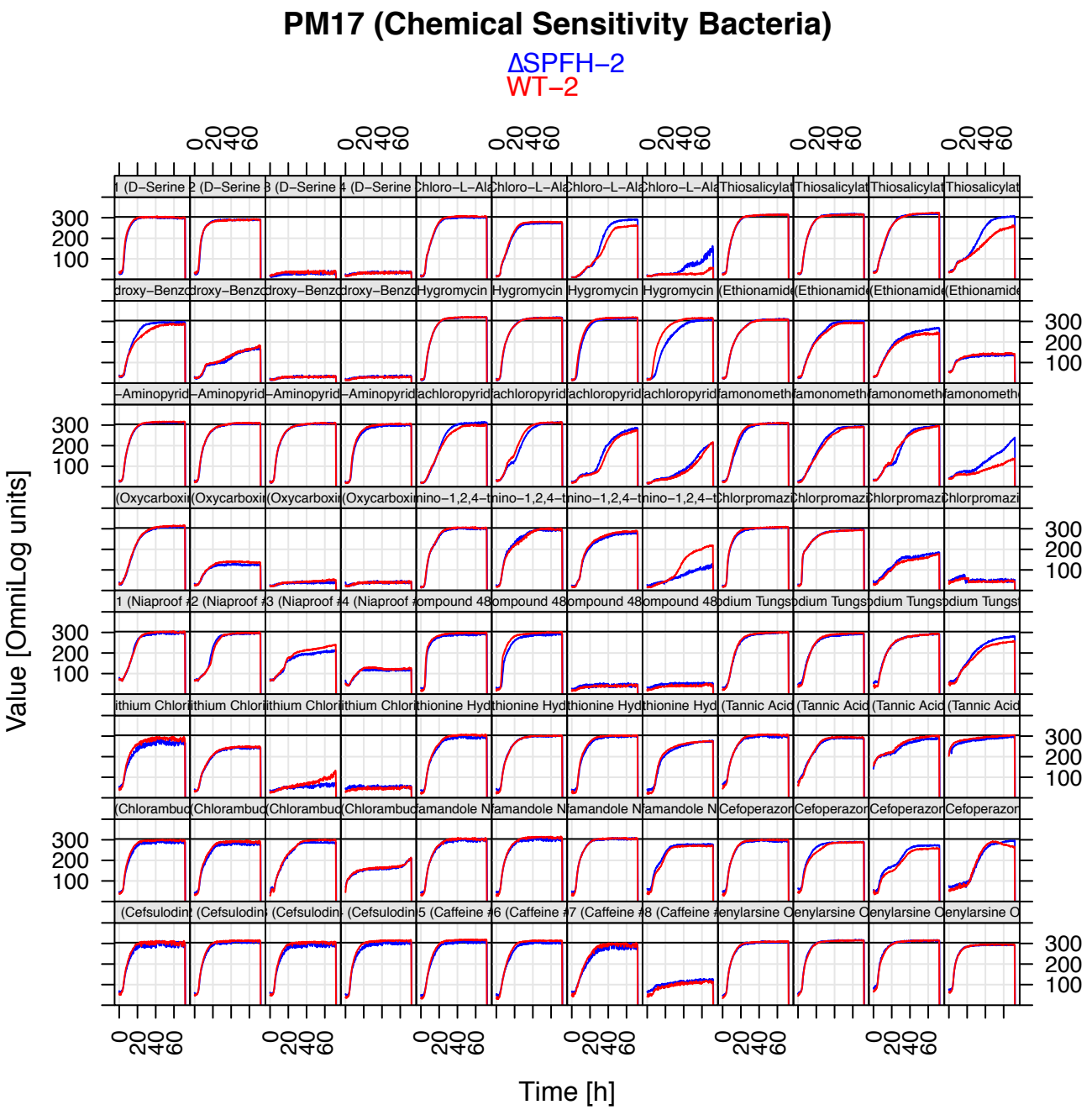
PM17 (Chemical Sensitivity Bacteria)
ΔSPFH−2
WT−2
Value [OmniLog units]
Time [h]

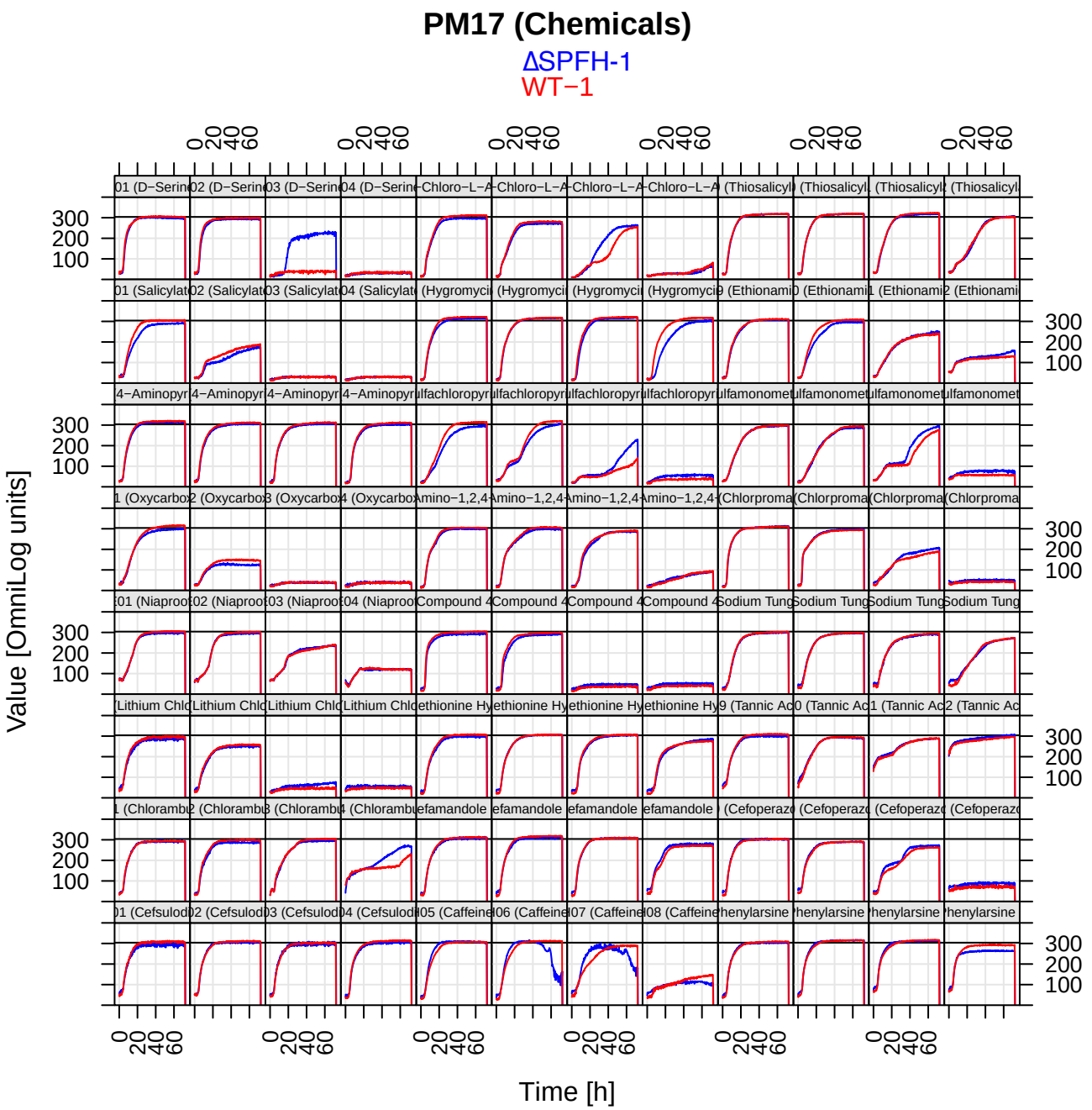
PM17 (Chemicals)
ΔSPFH-1
WT−1
Value [OmniLog units]
Time [h]

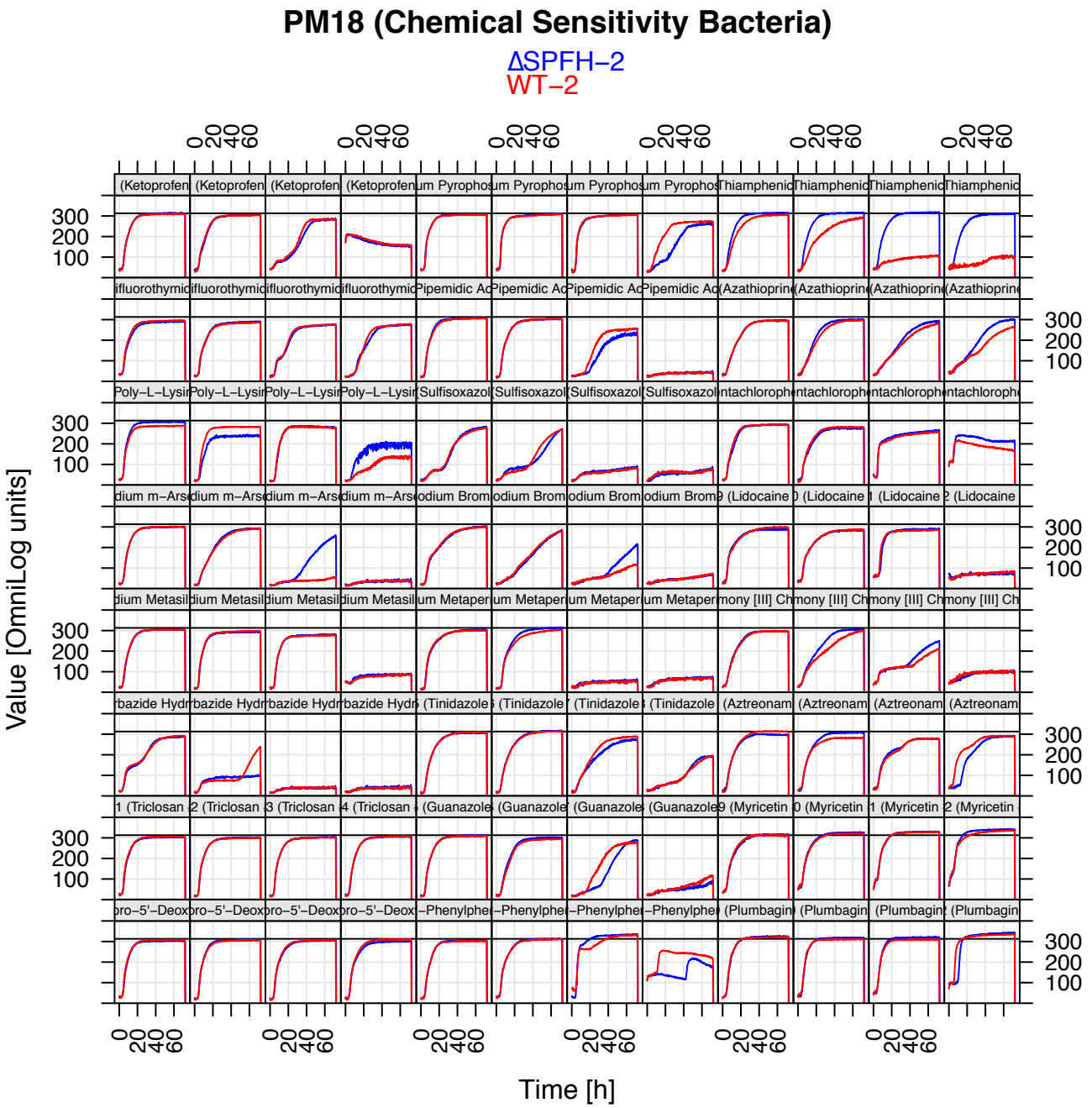
PM18 (Chemical Sensitivity Bacteria)
ΔSPFH–2
WT–2
Value [OmniLog units]
Time [h]
(Ketoprofen
um Pyrophos
Thiamphenic
ifluorothymic
Pipemidic Ac
(Azathioprin
Poly–L–Lysin
Sulfisoxazol
ntachlorophen
dium m–Ars
odium Brom
(Lidocaine
dium Metasil
um Metaper
mony [III] Ch
bazide Hydr
(Tinidazole
(Aztreonam
(Triclosan
(Guanazole
(Myricetin
ro–5'–Deox
–Phenylpher
(Plumbagin
0
20
40
60
100
200
300

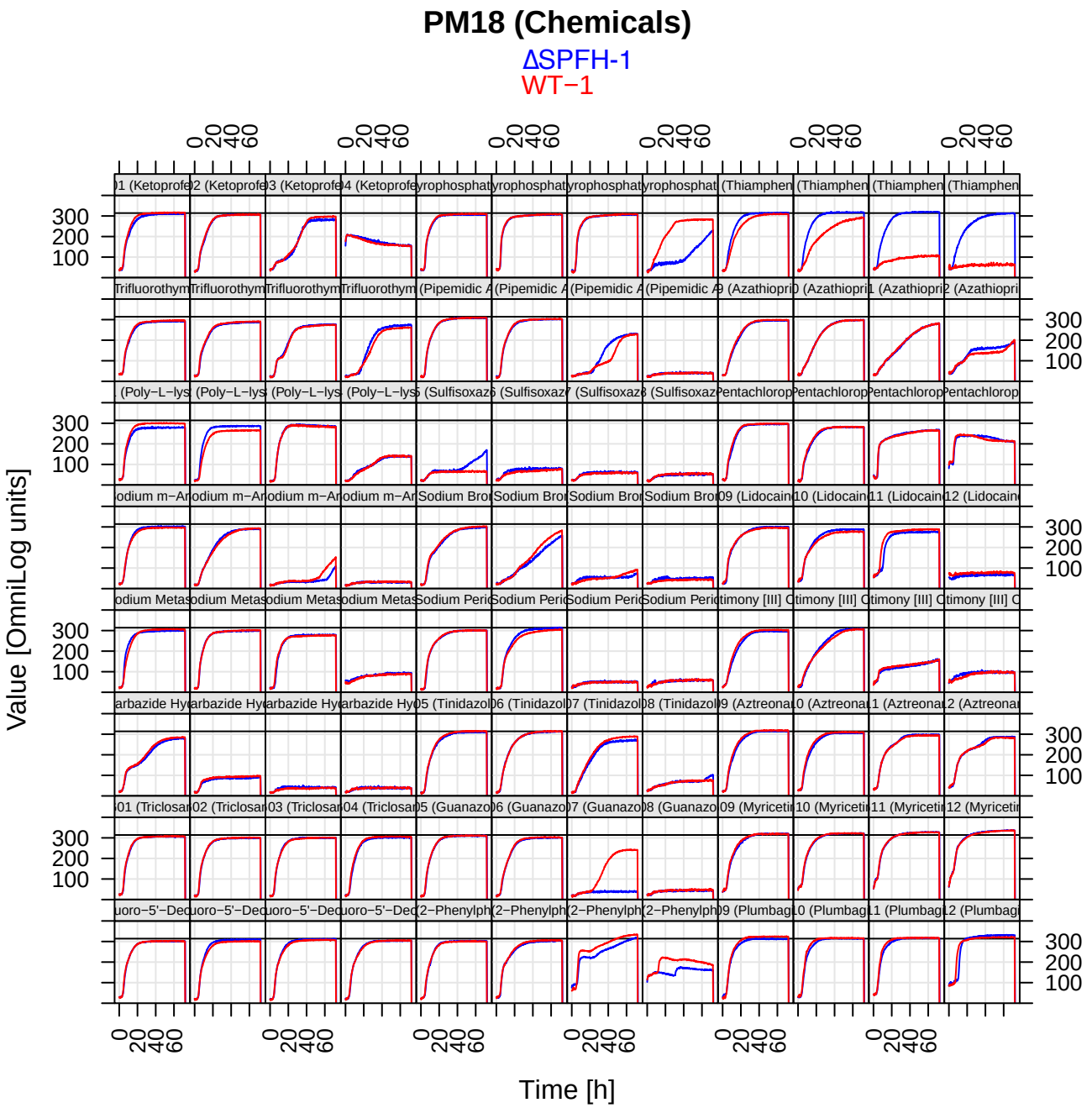
PM18 (Chemicals)
ΔSPFH-1
WT−1
Value [OmniLog units]
Time [h]

PM19 MicroPlate™

A1 Josamycin 1	A2 Josamycin 2	A3 Josamycin 3	A4 Josamycin 4	A5 Gallic acid 1	A6 Gallic acid 2	A7 Gallic acid 3	A8 Gallic acid 4	A9 Coumarin 1	A10 Coumarin 2	A11 Coumarin 3	A12 Coumarin 4
B1 Methyltrioctyl-ammonium chloride 1	B2 Methyltrioctyl-ammonium chloride 2	B3 Methyltrioctyl-ammonium chloride 3	B4 Methyltrioctyl-ammonium chloride 4	B5 Harmane 1	B6 Harmane 2	B7 Harmane 3	B8 Harmane 4	B9 2,4-Dintrophenol 1	B10 2,4-Dintrophenol 2	B11 2,4-Dintrophenol 3	B12 2,4-Dintrophenol 4
C1 Chlorhexidine 1	C2 Chlorhexidine 2	C3 Chlorhexidine 3	C4 Chlorhexidine 4	C5 Umbelliferone 1	C6 Umbelliferone 2	C7 Umbelliferone 3	C8 Umbelliferone 4	C9 Cinnamic acid 1	C10 Cinnamic acid 2	C11 Cinnamic acid 3	C12 Cinnamic acid 4
D1 Disulphiram 1	D2 Disulphiram 2	D3 Disulphiram 3	D4 Disulphiram 4	D5 Iodonitro Tetrazolium Violet 1	D6 Iodonitro Tetrazolium Violet 2	D7 Iodonitro Tetrazolium Violet 3	D8 Iodonitro Tetrazolium Violet 4	D9 Phenyl- methyl-sulfonyl-fluoride (PMSF) 1	D10 Phenyl- methyl-sulfonyl-fluoride (PMSF) 2	D11 Phenyl- methyl-sulfonyl-fluoride (PMSF) 3	D12 Phenyl- methyl-sulfonyl-fluoride (PMSF) 4
E1 FCCP 1	E2 FCCP 2	E3 FCCP 3	E4 FCCP 4	E5 D,L-Thioctic Acid 1	E6 D,L-Thioctic Acid 2	E7 D,L-Thioctic Acid 3	E8 D,L-Thioctic Acid 4	E9 Lawsone 1	E10 Lawsone 2	E11 Lawsone 3	E12 Lawsone 4
F1 Phenethicillin 1	F2 Phenethicillin 2	F3 Phenethicillin 3	F4 Phenethicillin 4	F5 Blasticidin S 1	F6 Blasticidin S 2	F7 Blasticidin S 3	F8 Blasticidin S 4	F9 Sodium caprylate 1	F10 Sodium caprylate 2	F11 Sodium caprylate 3	F12 Sodium caprylate 4
G1 Lauryl sulfobetaine 1	G2 Lauryl sulfobetaine 2	G3 Lauryl sulfobetaine 3	G4 Lauryl sulfobetaine 4	G5 Dihydro-streptomycin 1	G6 Dihydro-streptomycin 2	G7 Dihydro-streptomycin 3	G8 Dihydro-streptomycin 4	G9 Hydroxylamine 1	G10 Hydroxylamine 2	G11 Hydroxylamine 3	G12 Hydroxylamine 4
H1 Hexammine cobalt (III) chloride 1	H2 Hexammine cobalt (III) chloride 2	H3 Hexammine cobalt (III) chloride 3	H4 Hexammine cobalt (III) chloride 4	H5 Thioglycerol 1	H6 Thioglycerol 2	H7 Thioglycerol 3	H8 Thioglycerol 4	H9 Polymyxin B 1	H10 Polymyxin B 2	H11 Polymyxin B 3	H12 Polymyxin B 4

PM20B MicroPlate™

A1 Amitriptyline 1	A2 Amitriptyline 2	A3 Amitriptyline 3	A4 Amitriptyline 4	A5 Apramycin 1	A6 Apramycin 2	A7 Apramycin 3	A8 Apramycin 4	A9 Benserazide 1	A10 Benserazide 2	A11 Benserazide 3	A12 Benserazide 4
B1 Orphenadrine 1	B2 Orphenadrine 2	B3 Orphenadrine 3	B4 Orphenadrine 4	B5 D,L-Propranolol 1	B6 D,L-Propranolol 2	B7 D,L-Propranolol 3	B8 D,L-Propranolol 4	B9 Tetrazolium violet 1	B10 Tetrazolium violet 2	B11 Tetrazolium violet 3	B12 Tetrazolium violet 4
C1 Thioridazine 1	C2 Thioridazine 2	C3 Thioridazine 3	C4 Thioridazine 4	C5 Atropine 1	C6 Atropine 2	C7 Atropine 3	C8 Atropine 4	C9 Ornidazole 1	C10 Ornidazole 2	C11 Ornidazole 3	C12 Ornidazole 4
D1 Proflavine 1	D2 Proflavine 2	D3 Proflavine 3	D4 Proflavine 4	D5 Ciprofloxacin 1	D6 Ciprofloxacin 2	D7 Ciprofloxacin 3	D8 Ciprofloxacin 4	D9 18-Crown-6 ether 1	D10 18-Crown-6 ether 2	D11 18-Crown-6 ether 3	D12 18-Crown-6 ether 4
E1 Crystal violet 1	E2 Crystal violet 2	E3 Crystal violet 3	E4 Crystal violet 4	E5 Dodine 1	E6 Dodine 2	E7 Dodine 3	E8 Dodine 4	E9 Hexa-chlorophene 1	E10 Hexa-chlorophene 2	E11 Hexa-chlorophene 3	E12 Hexa-chlorophene 4
F1 4-Hydroxy-coumarin 1	F2 4-Hydroxy-coumarin 2	F3 4-Hydroxy-coumarin 3	F4 4-Hydroxy-coumarin 4	F5 Oxytetracycline 1	F6 Oxytetracycline 2	F7 Oxytetracycline 3	F8 Oxytetracycline 4	F9 Pridinol 1	F10 Pridinol 2	F11 Pridinol 3	F12 Pridinol 4
G1 Captan 1	G2 Captan 2	G3 Captan 3	G4 Captan 4	G5 3,5-Dinitro-benzene 1	G6 3,5-Dinitro-benzene 2	G7 3,5-Dinitro-benzene 3	G8 3,5-Dinitro-benzene 4	G9 8-Hydroxy-quinoline 1	G10 8-Hydroxy-quinoline 2	G11 8-Hydroxy-quinoline 3	G12 8-Hydroxy-quinoline 4
H1 Patulin 1	H2 Patulin 2	H3 Patulin 3	H4 Patulin 4	H5 Tolylfluanid 1	H6 Tolylfluanid 2	H7 Tolylfluanid 3	H8 Tolylfluanid 4	H9 Troleandomycin 1	H10 Troleandomycin 2	H11 Troleandomycin 3	H12 Troleandomycin 4

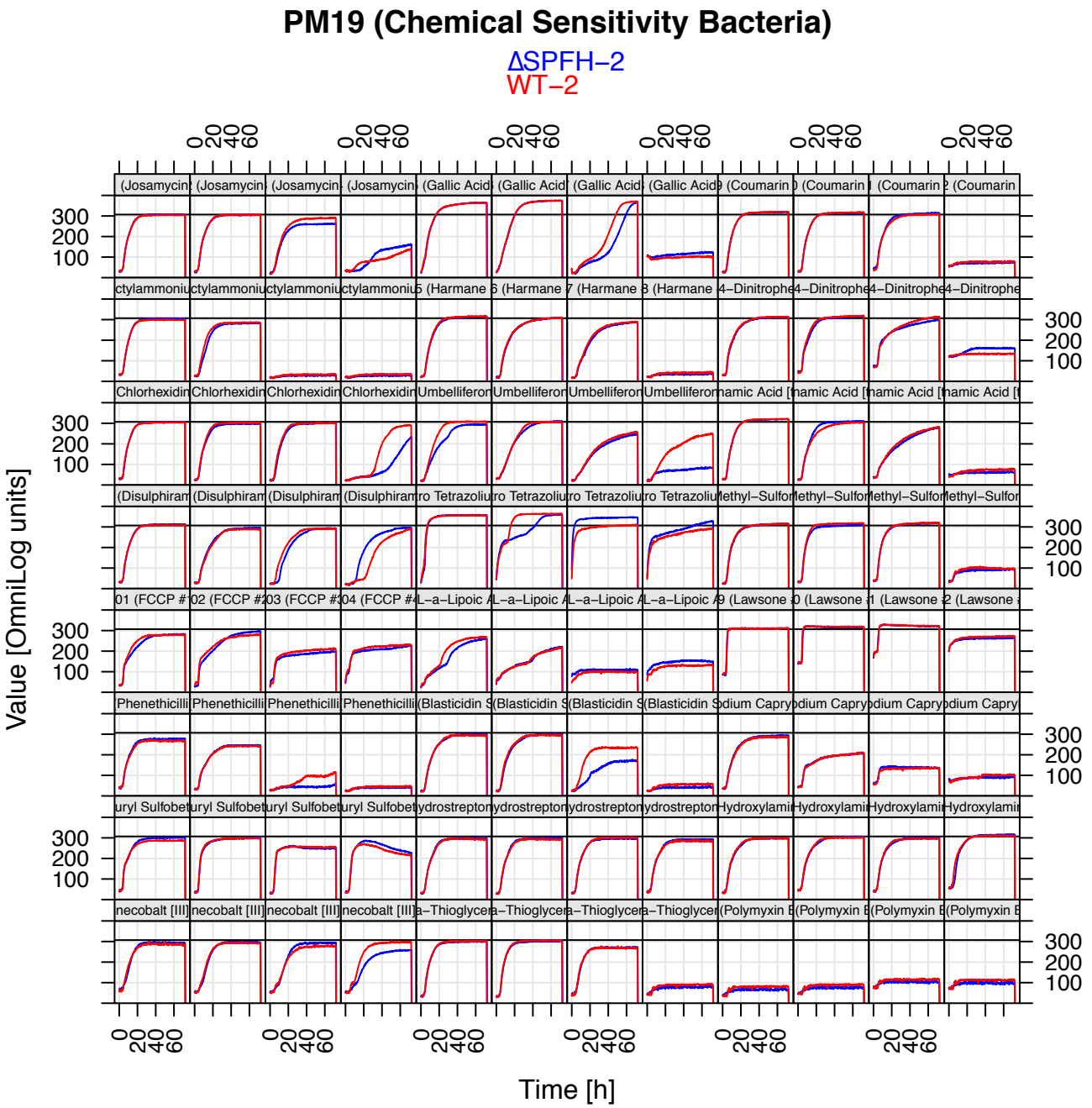
PM19 (Chemical Sensitivity Bacteria)
ΔSPFH−2
WT−2
Value [OmniLog units]
Time [h]

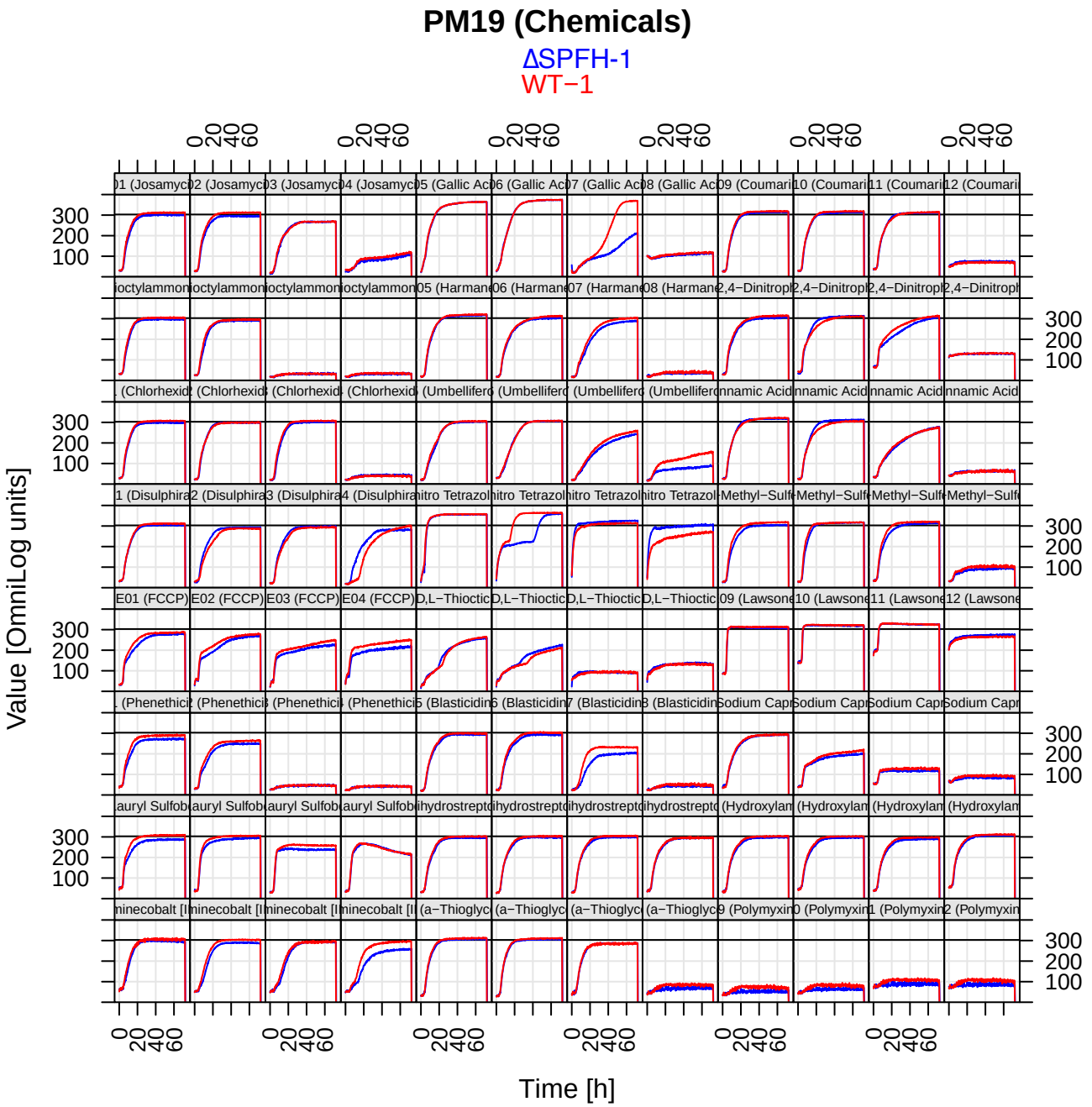
PM19 (Chemicals)
ΔSPFH-1
WT−1
Value [OmniLog units]
Time [h]

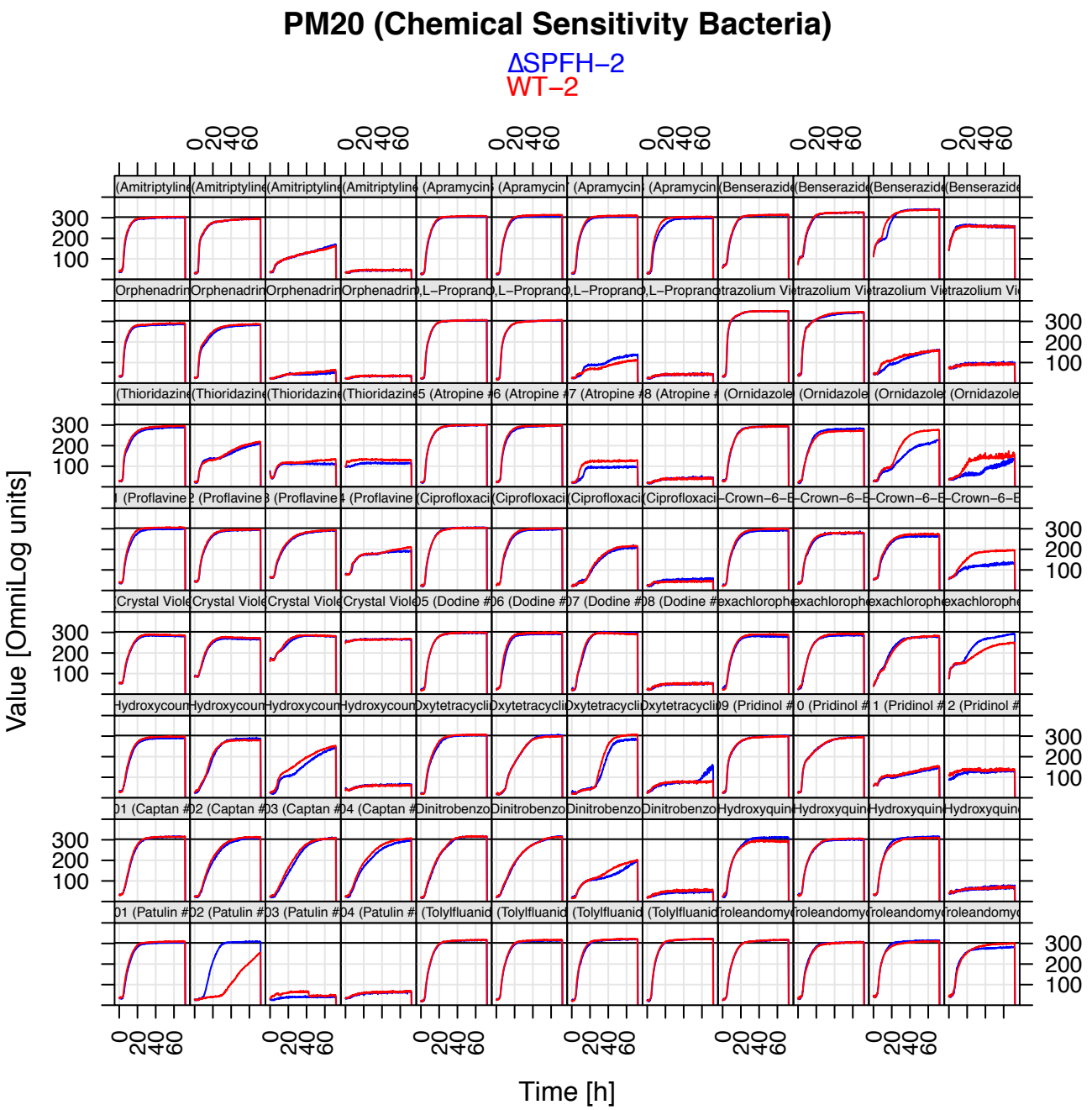
PM20 (Chemical Sensitivity Bacteria)
ΔSPFH−2
WT−2
Value [OmniLog units]
Time [h]

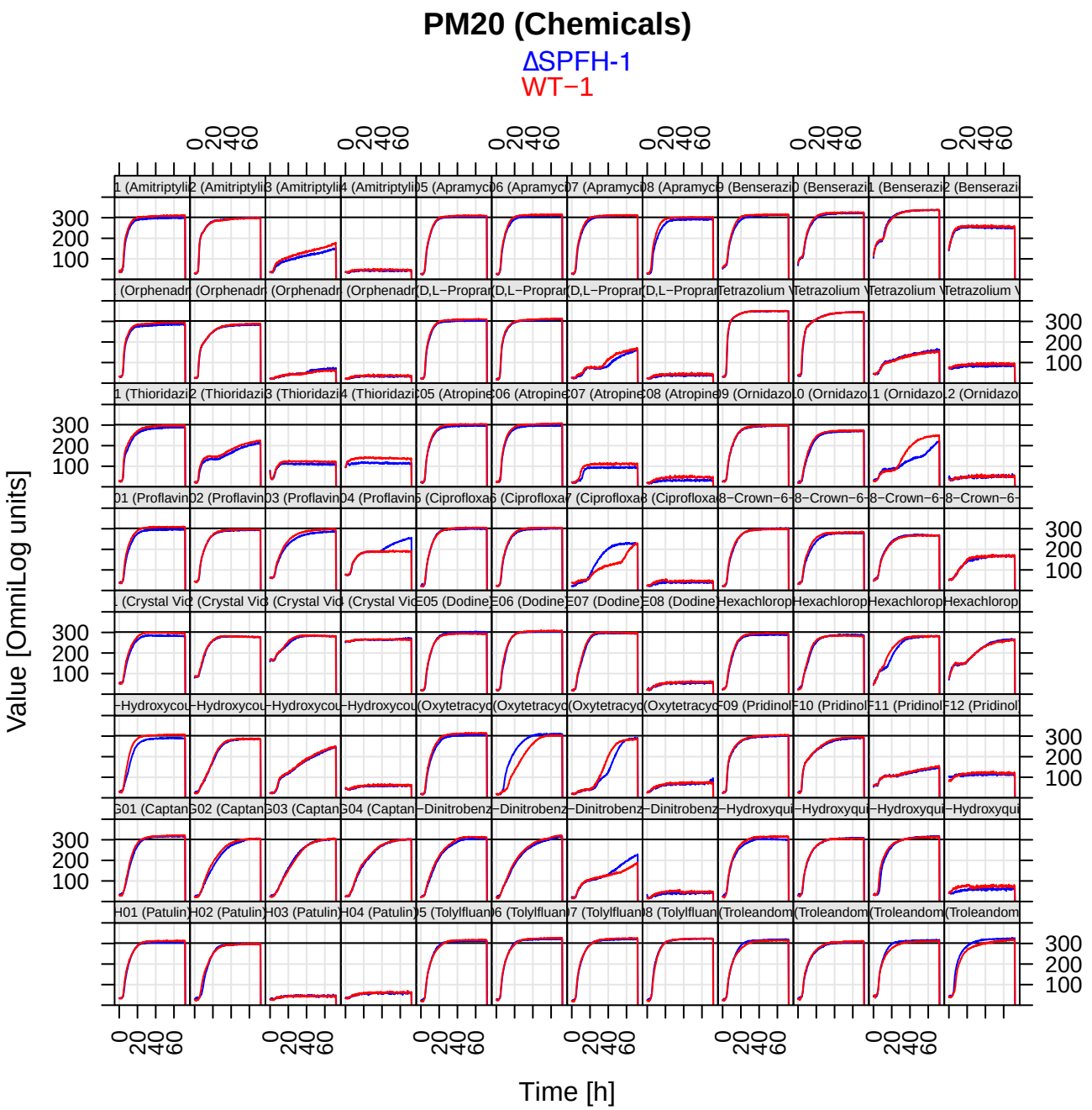
PM20 (Chemicals)
ΔSPFH-1
WT−1
Value [OmniLog units]
Time [h]